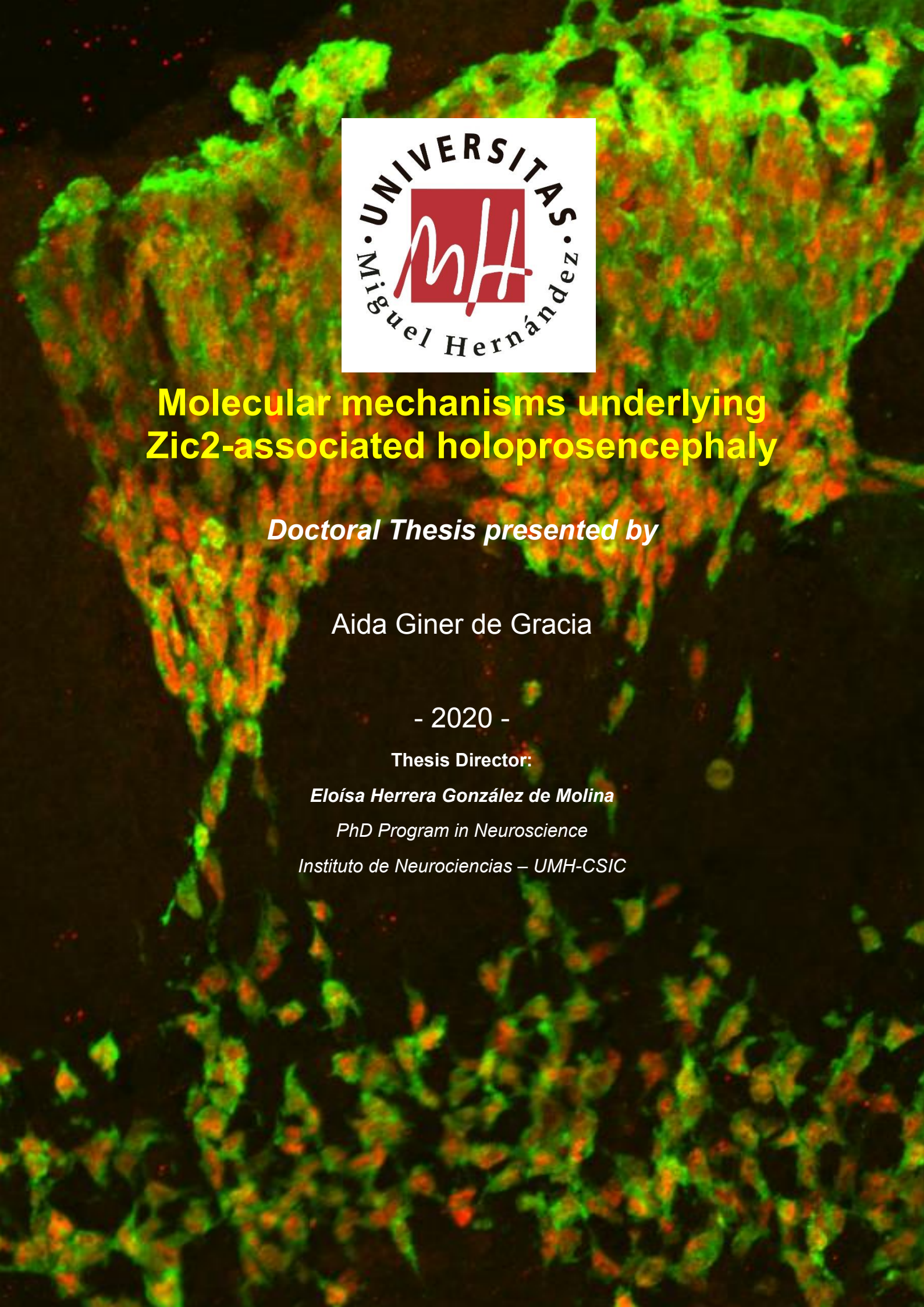

Molecular mechanisms underlying Zic2-associated holoprosencephaly

Doctoral Thesis presented by

Aida Giner de Gracia

- 2020 -

Thesis Director:

Eloísa Herrera González de Molina

PhD Program in Neuroscience

Instituto de Neurociencias – UMH-CSIC

Molecular mechanisms underlying Zic2-associated holoprosencephaly

Doctoral Thesis presented by

Aida Giner de Gracia

- 2020 -

Thesis Director:

Eloísa Herrera González de Molina

PhD Program in Neuroscience

Instituto de Neurociencias – UMH-CSIC

Sant Joan d'Alacant, March 2020

A quien corresponda,

La tesis doctoral titulada *"Molecular mechanisms underlying Zic2-associated holoprosencephaly"* ha sido desarrollada por mí misma, Aida Giner de Gracia. Esta tesis se presenta en formato convencional y presenta como índices de calidad la presentación del trabajo en 3 congresos internacionales (Póster en el congreso SENC2017, con el título "Nrp2 as a Zic2 effector during neural crest cells migration"; póster en el congreso AXON2019 con el título "Zic2 regulates Draxin to promote Neural Crest cells delamination" y un póster en el congreso EDBC 2019 con el título "Deregulation of the Wnt and TGF-β signaling pathways underlies Zic2-associated holoprosencephaly") además de la organización del congreso ENCODS 2017. La tesis está basada en estudios experimentales llevados a cabo en el Instituto de Neurociencias de Alicante en el programa de doctorado de Neurociencias de la Universidad Miguel Hernández.

Atentamente,

Firmado por
Aida Giner,

Aida Giner de Gracia

Sant Joan d'Alacant, Marzo 2020

D. Eloísa Herrera González de Molina, Investigadora Científica del CSIC

AUTORIZO la presentación de la Tesis Doctoral titulada "Molecular mechanisms underlying Zic2-associated holoprosencephaly" realizada por D/Dª Aida Giner de Gracia, bajo mi inmediata dirección y supervisión como directora de su Tesis Doctoral en el Instituto de Neurociencias (UMH-CSIC) y que presenta para la obtención del grado de Doctor por la Universidad Miguel Hernández.

Y para que conste, a los efectos oportunos, firmo el presente certificado.

Firmado por ELOISA HERRERA GONZALEZ DE MOLINA - NIF:24252485C el día 29/06/2020 con un certificado emitido por ACCVCA-120

Dra Eloísa Herrera González de Molina:

D. Miguel Valdeolmillos López, Catedrático y Coordinador del programa de doctorado en Neurociencias del Instituto de Neurociencias de Alicante, centro mixto de la Universidad Miguel Hernández (UMH) y de la Agencia Estatal Consejo Superior de Investigaciones Científicas (CSIC),

CERTIFICO:

Que la Tesis Doctoral titulada "Molecular mechanisms underlying Zic2-associated holoprosencephaly" ha sido realizada por Dª. Aida Giner de Gracia, bajo la dirección de Dª Eloísa Herrera González de Molina como directora, y doy mi conformidad para que sea presentada a la Comisión de Doctorado de la Universidad Miguel Hernández.

Y para que conste, a los efectos oportunos, firmo el presente certificado.

MIGUEL ANGEL|VALDEOLMILLOS|LOPEZ

Firmado digitalmente por MIGUEL ANGEL|VALDEOLMILLOS|LOPEZ
Fecha: 2020.06.29 13:15:48 +02'00'

Dr. Miguel Valdeolmillos López

E-mail :
miguel.valdeolmillos@umh.es
www.in.umh.es

Tel: +34 965 919540
Fax: +34 965 919549

Av Ramón y Cajal s/n
CAMPUS DE SANT JOAN
03550 SANT JOAN D'ALACANT– ESPAÑA

ACKNOWLEDGEMENTS / AGRADECIMIENTOS

Como empezar... al final esta parece que es la parte de la tesis que más cuesta de escribir...

En primer lugar, quiero darle las gracias a Eloísa por darme la oportunidad de realizar la tesis en su laboratorio, de formarme como investigadora, de aprender muchísimo. Porque cuando de repente, después de dos años en el INA, de altibajos, de no saber si podía tener una beca, de si podía hacer de verdad el doctorado, ella me dio esa oportunidad, gracias.

A la gente del laboratorio, por tantos momentos, conversaciones de viernes y por aguantar mis chistes malos (malísimos):

Maca, eh Macarena ayyy...aún recuerdo cuando estábamos en el 013, y nos quedábamos las últimas y me dabas mil consejos, no sólo de cosas del laboratorio, sino de la vida en general. Como bien dice Luís, siempre tienes tu propia opinión de cosas del lab y de todo, con tu vocecita, tan graciosa. Pero siempre eres tan buena y sabes ver el lado bueno de las cosas, ¡aunque seas tan negativa y crítica para tus resultados! Que la inmuno de OAZ se ve feílla.... que está foto está un poco así... y luego va y tus fotos salen en exposiciones!! Estos años contigo han sido geniales, aunque no te lo diga he echado de menos sentarme a tu lado como en el lab 013, aunque me distraía con nuestras conversaciones, jejeje. ¡¡Creo que no hay palabras suficientes...gracias!!

Dianitaa, recuerdo cuando nos conocimos en el lab de Bea, como era la última en llegar me caían a mí todas las broncas, y te tenía un miedo...y aún un poco pero menos, jajaja. Gracias por todos los momentos, conversaciones, por contarnos las penas, no sólo como compañeras sino como amigas, tu llegada al laboratorio de Elo y conocerte mejor para mí se convirtió en una alegría. Nuestro viaje a Madrid, genial... que bien lo pasamos, ¡y por muchos más así! Siempre digo cuando lea la tesis...¡así que ya sabes!

Cruz, Crucecita... gracias por enseñarte prácticamente todo lo que sé del lab, y por todos los momentos de risas, de tus ideas ingeniosas y graciosas. Además,

has sido en quien más he confiado para hablar de mi proyecto, en parte porque está relacionado con el tuyo, pero en parte también porque, aunque seas un poco desastrillo (lo raro es que sepas donde tienes el móvil, las llaves o el coche jajaja), tienes mucha experiencia pensando hipótesis, experimentos y eres una persona muy inteligente. Gracias por todo vecina de bancada :P y a tu maridito Hugo por haber sido parte de muchos de mis clonajes.

Rocío, recuerdo cuando llegaste al lab, empezamos a llevarnos muy bien, hicimos buen grupete, junto con Ana. Pasé un cumpleaños genial en las fiestas de moros y cristianos. Luego sé que hemos tenido nuestros más y nuestros menos y es que somos muy diferentes, pero creo que estos últimos meses hemos lidiado con nuestras diferencias y hemos crecido personalmente. Gracias por las risas, las fiestas, por confiar en mí para contarme tus cosas, por los miércoles tontos, por todo.

Al resto de gente del lab: Vero, Marta, Augusto, Iván, Yaiza, Bea, Mayte, Luís gracias también por todos los momentos del lab, las conversaciones de viernes y por hacer amena mi tesis en el laboratorio.

No me olvido también de la gente que ha pasado por el laboratorio...

Blanquita...para mí has sido todo un apoyo en esta tesis, aunque sólo hayamos coincidido unos meses, recuerdo que siempre me traías alegría. Ha sido genial compartir contigo ese último tiempo que estuviste acabando experimentos y escribiendo la tesis y también poder seguir el contacto ¡incluso poder habernos visto por tu tierra granaína! ¡Muchas gracias de parte de tu minibeca!

Gerald, a ti también muchas gracias, hemos compartido muchos cafés, cervezas, charlas... y también cosas científicas! Somos los electroporadores oficiales de pollitos, jejeje.

Santi, de los chicos más frikis que he conocido (tenía que decirlo). Siempre con tus datos curiosos, frikadas, etc, que animaban el laboratorio. ¡La verdad es que en estos últimos meses de mi tesis has faltado tú! Te he echado de menos, tanto en el lab, como en el fútbol, que éramos los pobres cojitos lesionados, jaja aún tengo las cicatrices de aquel día en el campo de Benimagrell y recuerdo que tardamos casi una hora en ir al INA y volver de lo cojos que íbamos, y se

pensaban que nos habíamos ido a algún lado jajaja. Espero poder llamarte doctor pronto y poder seguir en contacto, sobre todo. ¡¡Muchas gracias por todos los momentos contigo!!

Ahora viene la gente del INA de fuera del lab:

El primero de todos, como no... ¡mi Álvaro! En año y poco que hemos coincidido te has convertido en mi mejor amigo, y es que sin ti no habría sido lo mismo este último año de tesis. Te llaman en tu lab el buffer del laboratorio y creo que también eres mi buffer, siempre escuchándome, siempre intentando que vea el otro lado de las cosas, siempre animándome. Si algún día no podía ir a tomar café porque me coincidía con experimento ahí estabas tú preguntándome: ¿cómo estás, vas muy liada con experimentos? Y es que te agradezco tanto que no sé ni cómo expresarlo, ya sabes que hasta lloré el día que nos despedíamos que te ibas para tus tierras zamoranas, ¡mozo! ¡A ver si es verdad que coincidimos de postdoc o a dónde quiera que vayamos!

¡Óscar! ¡¡Aunque seamos tan diferentes, gracias por soportarme!! Jajaja con mis ñoñerías y tú ¡cómo no! tan del norte... Gracias por escuchar mis historias de mis guerreros (espero que sólo Álvaro y tu entendáis esta parte de los agradecimientos, a ver si algún día finiquito la lista, sería buena señal ;) Gracias por escucharme, por tus bromas, tus memes, etc. y espero que me des un abrazo bien grande cuando sea doctora, que eso sí que no te lo perdono ;P

También al resto de gente de IPO lab, por compartir tantos ratos en el comedor, jeje y alguna cenita que otra. Gracias chicos.

Kike, señor Velasco, te rellenaría una página entera de agradecimientos. Me alegro tanto de haber coincidido contigo, que ojalá te hubiera conocido antes. Hace gracia que fuera por el roco y la escalada que nos conociéramos y no por el INA en sí. Me acuerdo cuando me apunté a la competición y apenas te conocía y en el viaje hasta compartí postre contigo (¡qué es mucho decir!) ahora ya tengo que partir el postre en dos antes de empezar porque sino te lo comes todo jajajaja. Gracias por todos los momentos, discusiones científicas, chistes malos, partidos de fútbol, volley, excursiones, cenas de gordos, fiestas... Al final hasta me encanta tu súper risa que todo el mundo conoce y con la que se te oye a kilómetros, y sabes que a mi tío (tu tocayo) también le encanta, porque es la risa

de felicidad, y es que sabes transmitir alegría y optimismo. Me encanta haber compartido todo este tiempo contigo y sé que aunque a veces nos tiremos de los pelos porque vamos muchas veces súper estresados, siempre vas a estar ahí para mí, y donde te vayas que sepas que te voy a ir a ver!!

Martita, me has enseñado tantas cosas. Siempre tan feliz, tan cariñosa, tan tú. Siempre me he llevado mejor con los chicos, porque soy un poco “rarilla” pero contigo he podido tener una amiga que me ha alegrado mi último año de tesis. Gracias por todo, por los cafés, los desayunos con churros, por ayudarme a hacer de mi pisito un hogar (cómo dice mi madre: “esto es para hacer hogar”), y sobre todo por aguantarme mis súper películas que me monto, que creo que soy peor que la vecina rubia, jajaja.

Kat, ya sabes que eres como la segunda hija de mi madre, lo que te hace prácticamente mi hermanita. Hemos compartido tanto momentos de escalada o de cervezas y cenas con gente del INA como en fiestas en Alcoy en los Reyes, Moros y Cristianos, ya eres como de la familia, dentro de nada hablas valenciano (alcoyano) perfectamente. Siempre vas a tener tu regalito de los Reyes Magos (y ya sabes que vienen de Alcoy eh, de ningún otro sitio). También te he confiado mil cosas, mil historias y agradezco tanto que sepas escuchar y que des consejos a esta cabecita loca, ya me decías: ¡la tesis, céntrate en la tesis! Eres una persona que es capaz de quitarle importancia a las cosas que de verdad no importan tanto y por las que yo a veces me preocupo demasiado, ¡gracias por dar ese enfoque a mi vida! Y muchas gracias a Tobi también! Ya sabéis que siempre tendréis casa en Alcoy. Danke!

Más gente del INA...y es que pasar tantos años aquí, que la tesis han sido 5...pero he estado 7 años en el INA, son tantos que prácticamente me sé de memoria el nombre y apellidos de todos...

A la gente del fútbol, Pablo, Omar, Fede, Deli, Roberto, Fabrizio, Hannah, Ernesto, Juan, el “nuevo bueno Pablo”, ¡espero no dejarme ningún nombre! Gracias chicos por hacerme pasar ratos tan divertidos y porque sé que soy mala en el fútbol, pero eso sí...se me da bien molestar y soy muy persistente y siempre me habéis animado a mejorar.

Seguro que me dejo a mucha gente del INA con la que he compartido muchas cosas, la gente con la que hice el máster o la gente con la que he compartido muchas “happy hour”. ¡Gracias chicos!

También tengo que agradecer a mucha gente que, aunque seguramente no entiendan ni de que va mi tesis, han estado ahí para que estos años sean más amenos para mí, la gente del roco, con la que he pasado días de entreno y también de escalada en la montaña, que tanto me gusta.

Sobre todo, quiero destacar a Vicente y a Jesús, ¡Quién diría que haríamos un grupete tan bueno! Me lo pasé tan bien en el viaje a Albarracín, ya no lo sólo por el hecho de ir a estar con la naturaleza, escalar un poquito, sino por el buen rollo que teníamos, los juegos, las cervezas al acabar, las siestas en los crashpads, las mil fotos que tenemos haciendo el tonto y durmiendo (cómo no). Y además de por el viaje, porque sé que puedo contar con vosotros para muchas otras cosas qué para escalar, como para irnos de cervezas, contarnos nuestras cosas, hasta pediros consejos amorosos (aquí siempre me la liáis por cierto, jajaja, nunca aprendo) y para comer chuches y dormirme en el cine (eh Jesús). ¡Gracias chicos!

Javi, te añado cuatro meses después de escribir la tesis. Gracias por formar parte de mi vida en esta última etapa de tesis, por darme fuerzas, por todo lo que hemos vivido tan intensamente en poco tiempo.

Saravanan, you have always been there for whatever I needed, I know we are quite far away from each other, but I also know than even if we cannot talk for weeks, I can talk to you whenever I need. You are also from the family, you know. I hope you can still come to a lot of more Christmas festivities in Alcoy and I also hope to do another trip to Chicago, it was wonderful! I will always remember when I met you in Lleida, I was doing practices in the lab and when we finished every day you always invited me to a Coca Cola and you told me: whenever you have your fellowship and earn money you will invite me! And now I have finished the thesis even... Thanks for all the moments, in Lleida (the mojito’s parties you loved) in Alcoy too, in Sevilla when I went there to see you and in Chicago of course. I know that wherever we are we will go to visit each other! And that is because you are a true friend for me, thank you!

Xavieret i Naxet! Los importantes, mis chicos. Sabéis que os quiero un montón y lo que os he echado de menos sobre todo los últimos momentos de escritura, me ha encantado que me animárais y que siempre habéis creído en mí. Siempre me habéis dicho que hasta ganaré un premio nobel, jajaja y es que sé que siempre me habéis tenido en alta estima y yo a vosotros, ¡muchísimo! Vaya trío hacemos, aunque no nos veamos muy de seguido, la quedada de Navidad de los importantes y la foto que lo demuestra nunca falla eh. Hasta el título de los importantes os quedaría corto chicos, y como bien has dicho, Xavi, tengo que acabar poniendo: a mis amores Javier Clement y el Dr. Ignacio Sanjuan :)

Mis otros amigos de Alcoy: Giovanna, Cris, Isaac, gracias chicos, este último tiempo he estado más distanciada, no he tenido tiempo de ir a Alcoy y es que la tesis me ha absorbido bastante, sé que no es del todo excusa, pero ahora espero poder veros ahora un poquito más. Aunque cada uno tenemos nuestras vidas, pero sé que puedo contar con vosotros cuando voy a Alcoy y sé que sacáis un hueco para verme, y eso que ya estáis todos con hijitos, jeje. Gracias por todo, chicos.

Por último, y los más importantes...mi familia. Sin ella esto no habría sido posible. Y es que aunque dicen que los amigos son la familia que se elige...para mí esta familia si la hubiera tenido que elegir...la elegiría sin duda alguna!

Mis padres, mis primos, tíos, mis abuelas. La iaia Carmen...siempre con sus mensajes motivadores, todo un ejemplo, cómo te quiero iaia, espero que estés en mi presentación de la tesis. Mi abuela Maruja, siempre preocupándose por todo y todos, ¡tan patidora com sempre! ¡Gracias a las dos! Mis tías, siempre ahí para apoyarme en todo, siempre tan positivas, porque somos los de Gracia y os merecéis una ola, otra ola ¡y un súper tsunami! Y mis tíos también, por supuesto tengo que nombrar a Juanma, que es el meu padrí! Gràcies!

Mi tía Maribel y mi tío Javier también, gracias por vuestra preocupación y por vuestro apoyo.

Mis primos, casi puedo decir primas porque somos casi todas chicas en esta familia, jejeje No hace falta que diga todos los nombres, porque sabéis que os quiero con locura y que habéis estado conmigo cuando lo he necesitado. Els “sempre xiquets” Lluís i Berta, sí que vos tenia que nomenar ja que heu sigut

com els meus germanets, totes les rises que hem tingut junt amb ma mare... es que estem un poquet loquets i qué divertit es estar amb vosaltres.

Javi y Hugo, primitos no me olvido de vosotros, estáis incluidos en los primos obviamente, aunque nos veamos mucho menos que con mis otros primos, sé que siempre os tengo porque sois mi familia, os quiero.

Els meus papis, us he deixat per al final perquè sou lo més important que tinc. Papa, sé que encara que no haja sigut el millor moment de la teua vida aquest últim any, has estat preocupant-se sempre ¿i com et va la tesis, tot bé? Gràcies pel teu suport i ja voràs com hi ha que ser optimista en aquest vida i tot passa. Et vull molt.

Mama, has sigut per mi no només ma mare, sino també la meua amiga, hem estat més unides que mai i sé que sempre m'has dit has de tirar endavant, tu pots amb tot, super! Sé que a vegades no sóc tan carinyosa o tan amorosa, però ho demostre a la meua manera i t'agraeixo tant el teu suport, que sé que encara que tu tingues els teus problemes, sempre el meu benestar ha estat per damunt de tot. També sempre he tingut els teus "tuppers" que tant m'han ajudat quan anava estressada (havia de dir-ho jajajaja). Sempre has vingut a vorem quan jo tenia temps de baixar a Alcoi i a més hem compartit viatges genials, i amb les teues amigues també, que són genials i se que et cuiden moltísim, gràcies a elles també que segurament voldran vindre a la meua tesis jeje, i a Andreu i Jaume, que son uns rebonicos!

A todos los que han pasado por mi vida en estos 5 años: GRACIAS, GRÀCIES, THANKS, DANKE!!

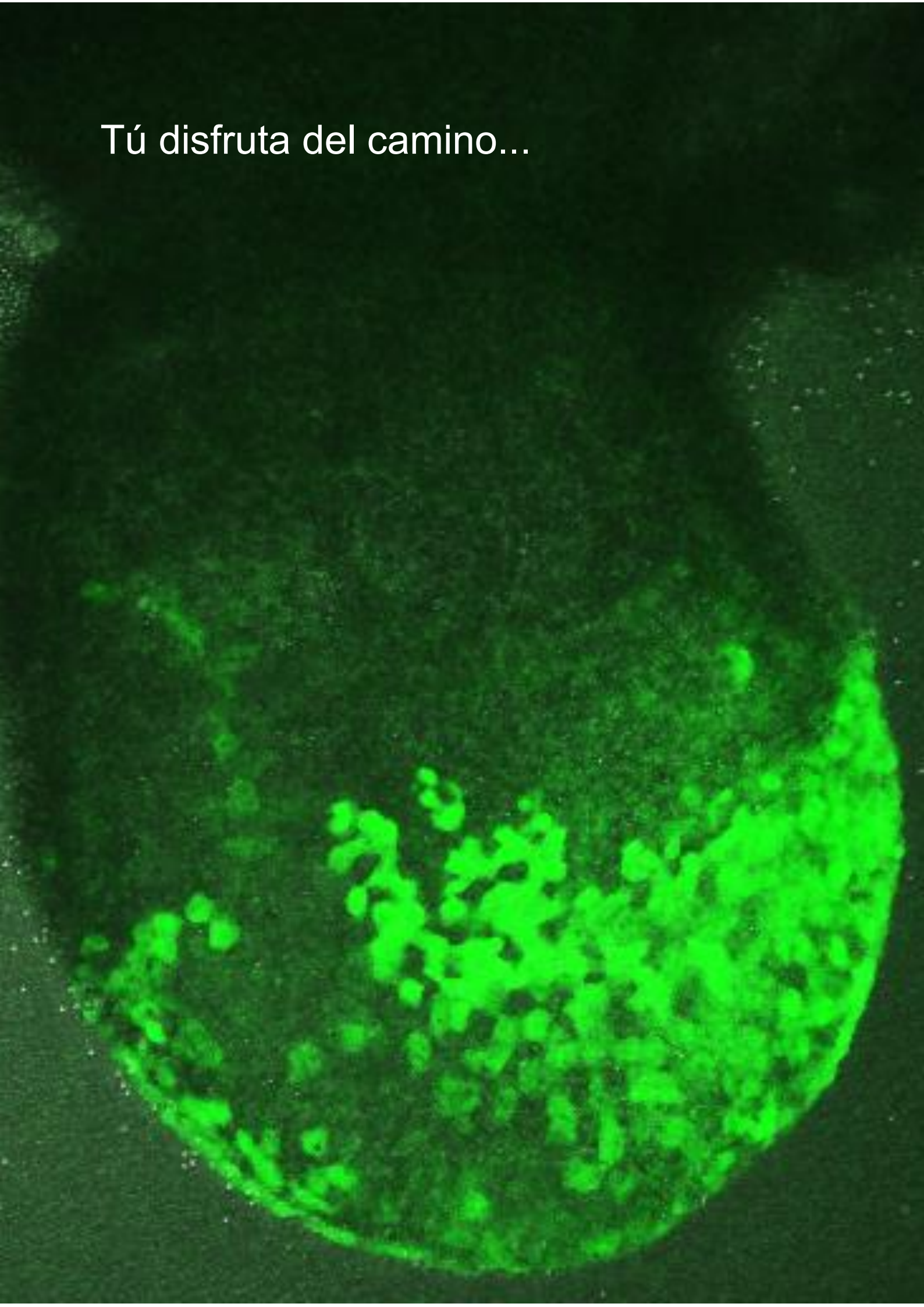
Tú disfruta del camino...

TABLE OF CONTENTS

ABBREVIATIONS

AP: Anterior–Posterior

AVE: Anterior Visceral Endoderm

BMP: Bone Morphogenic Protein

CNS: Central Nervous System

CoIP: Complex Immunoprecipitation

CRCs: Cajal Retzius Cells

Daam: Dishevelled Associated Activator of Morphogenesis

DRG: Dorsal Root Ganglia

DSH: Dishevelled

DVE: Distal Visceral Endoderm

EGF-CFC: Epidermal Growth Factor-Cripto-1/FRL-1/Cryptic

EMT: Epithelial-to-Mesenchymal Transition

Exe: EXtraembryonic Ectoderm

FGF: Fibroblast Growth Factor

Fmi: Flamingo

Fz: Frizzled

Gdf: Growth differentiation factor

GRN: Gene Regulatory Network

Gsc: Goosecoid

GSK3β: Glycogen Synthase Kinase 3β

Hhex: Hematopoietically Expressed Homeobox

HPE: Holoprosencephaly

ICM: Inner Cell Mass

LOF: Loss of Function

Lrp: LDL Receptor Related Protein

MITF: Microphtalmia Associated Transcription Factor/Microphtalmia Inducing Transcription Factor

NC: Neural Crest

Opa: Odd-paired

PCP: Planar Cell Polarity

Pk: Prickle

PS: Primitive Streak

PVE: Posterior Visceral Endoderm

RGC: Retinal Ganglion Cell

Ror: RAR Related Orphan Receptor

TF: Transcription Factor

TGF-β: Transforming Growth Factor-β

Vang: Van Gogh or Strabismus

VE: Visceral Endoderm

Zic: Zinc Finger Protein of the Cerebellum

ZOC: Zic-Opa Conserved

ZFD: Zinc Finger Domain

ZFNC: Zinc Finger N-terminal Conserved.

ABSTRACT

ZIC2 is a transcription factor that, when mutated in humans, causes holoprosencephaly type 5 (HPE5) and other neurodevelopmental disorders. However, the molecular mechanisms by which ZIC2 deficiency leads to this kind of pathologies remain unclear. Here we first demonstrate that Zic2 is expressed transiently in cells of the three germ layers of the epiblast, as well as in the premigratory neural crest cells (NCCs) in mice. Then, by analysing Zic2 occupancy profiles during gastrulation and neurulation stages and the transcriptome of Zic2 mutant embryos, we observe that this transcription factor majorly binds to sequences near or in the TSS in both epiblast and NCCs. These analyses also define the gene program directly regulated by Zic2 in NCCs, including a highly significant number of genes involved in the epithelial-to-mesenchymal transition (EMT) process that belong to the Wnt, cadherin or TGF-β pathways. By functional experiments *in vivo* we then demonstrate that Zic2 blocks the Wnt pathway in premigratory NCCs at the time that activates the TGF-β signalling pathway to facilitate their delamination. Altogether these results reveal the importance of EMT deregulation in the etiology of Zic2-associated pathologies and may help to improve the diagnosis and genetic counseling of these conditions.

RESUMEN

ZIC2 es un factor de transcripción que cuando está mutado causa holoprosencefalia tipo 5 (HPE5) y otros trastornos del desarrollo en humanos. Sin embargo, los mecanismos moleculares por los que la deficiencia de ZIC2 conduce a este tipo de patologías siguen sin estar claros. En este trabajo de tesis demostramos que Zic2 se expresa de forma transitoria en las células de las tres capas germinales del epiblasto de ratón, así como en las células premigratorias de la cresta neural. Analizando los perfiles de ocupación de Zic2 y comparando el transcriptoma de embriones de ratón durante gastrulación y neurulación, observamos que Zic2 se une principalmente a regiones cercanas al TSS e intragénicas tanto en las células del epiblasto como en la cresta neural. Nuestros análisis genómicos definen también el programa genético directamente regulado por Zic2 durante la gastrulación y neurulación, que incluye muchos genes relacionados con cascadas de señalización involucradas en el proceso de transición epitelio-mesenquima (EMT) tales como las vías Wnt, cadherina y TGF-β. Además, mediante experimentos funcionales in vivo, demostramos que Zic2 bloquea la ruta mediada por Wnt en las células premigratorias de la cresta neural a la vez que activa la ruta de señalización de TGF-β para facilitar su delaminación. Estos resultados revelan la importancia de la desregulación de EMT en la etiología de las patologías asociadas a Zic2 y pueden ayudar a mejorar el diagnóstico y el asesoramiento genético de estas afecciones.

INTRODUCTION

1. Embryogenesis in vertebrates

Embryonic development starts with the formation of the zygote after fertilization of the oocyte. The zygote acquires complexity when is transformed into a two layered embryo in the stage of blastocyst. These two layers, the inner cell mass (ICM) or primitive endoderm and the trophectoderm are defined as the two first tissue lineages (Wang and Chen, 2016). In mammals, the blastocyst then hatches from the zona pellucida (the outer part of the oocyte) and is ready for implantation in the uterus. In this step, the embryo suffers subsequent cell divisions and grows exponentially in cell number (Kojima et al., 2014). The polar trophectoderm and the ICM develop into an elongated structure that is made up of the ectoplacental cone (which connects the embryo to the uterus), the extraembryonic ectoderm (ExE), the epiblast and a layer of visceral endoderm (VE) (also known as primitive endoderm or hypoblast). The epiblast or primitive ectoderm cells, which are pluripotent, are the ones that have a higher ratio of proliferation when the embryo is implanted in the uterus and they will give rise to all the embryonic structures (Nagy et al., 2003).

The translocation of the distal visceral endoderm (DVE) to the anterior side transforms the proximal–distal polarity into the prospective anterior–posterior (AP) axis and then gastrulation, one of the most important steps in the mammalian embryogenesis, begins (Tam and Loebel, 2007; Tam, Loebel and Tanaka, 2006). As Lewis Wolpert, an expert in embryology, said: “It is not birth, marriage or death, but Gastrulation which is truly the most important time in your life”.

1.1 Gastrulation

Gastrulation involves the generation of a complex and organized embryo conformed by 3 primary germ layers from a group of unstructured cells (the inner mass) to later allow organogenesis.

Gastrulation starts at E6.5 with the formation of the primitive streak (PS) at the posterior part of the embryo. In this posterior region, epiblast cells start to ingress to form the mesoderm and the endoderm. Together with the ectoderm, these two layers form the three primary germ layers, which contain the progenitors for all the tissues (Tam and Loebel, 2007; Wang L and Chen, 2016).

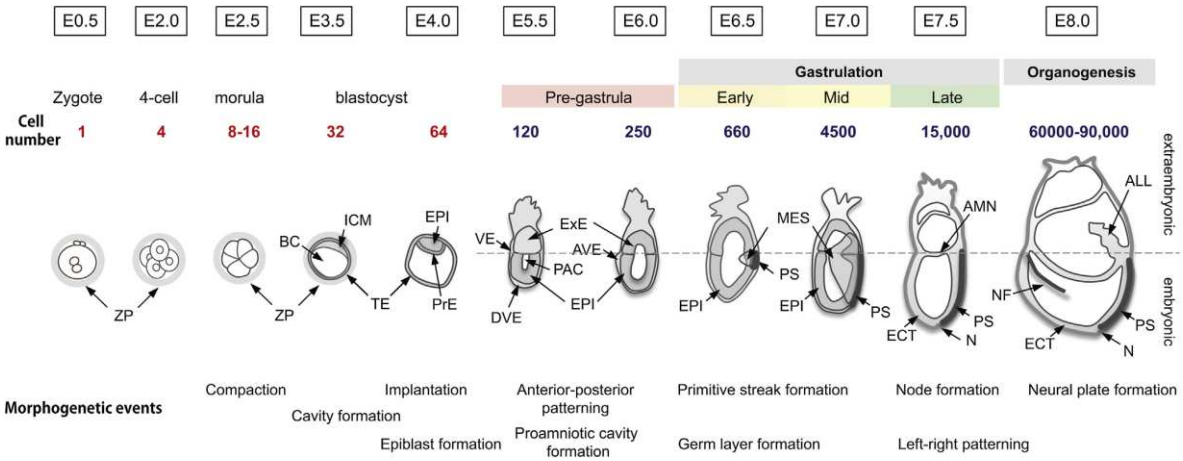

Figure 1. Timeline of preimplantation and early postimplantation development. Schematic drawings illustrate characteristic anatomical features of the mouse embryo at each embryonic age (E0.5–E8.5). The range or average cell numbers of the whole conceptus (E0.5–E4.5) (numbers in red) or the epiblast and the germ layers (E5.5–E8.0) (numbers in blue), and the key morphogenetic events/milestones at each chronological age are listed. Abbreviations: ALL: allantois, AMN: amnion, AVE: anteriorvisceral endoderm, BC: blastocyst cavity, DVE: distal visceral endoderm, ECT: ectoderm, EPI: epiblast, ExE: extraembryonic ectoderm, ICM: inner cell mass, MES: mesoderm, N: node, NF: neural fold, PAC: proamniotic cavity, PrE: primitive endoderm, PS: primitive streak, TE: trophectoderm, VE: visceral endoderm, ZP: zona pellucida. (Kojima et al., 2014).

1.1.1 Establishment of the anterior-posterior axis and formation of the primitive streak.

Although the PS becomes visible at E7.0, the establishment of the anterior-posterior (AP) axis has been proposed to occur earlier. At E5.5 the VE shows regionalized gene expression, which becomes crucial for the anterior-posterior patterning. Thus, at this stage, the secretable protein Wnt3 is detected in the prospective posterior visceral endoderm (PVE) while the anterior visceral endoderm (AVE) expresses the Nodal antagonists Lefty1 and Cer1 to antagonize posteriorizing signals coming from the Wnt and Nodal pathways (Tam and Loebe, 2007). Therefore, these two processes, establishment of the AP axis and the initiation of the primitive streak, are mainly controlled by the transforming growth factor superfamily (TGF-β) and the Wnt signalling, although FGF signalling might also be involved.

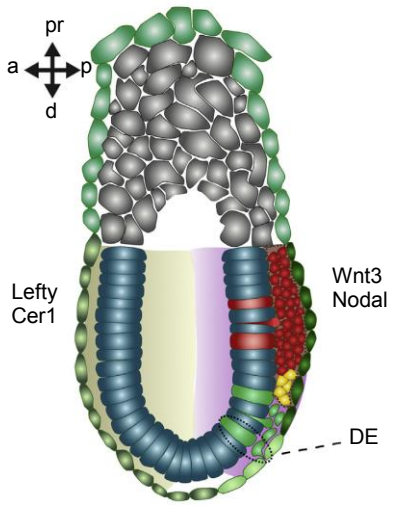

Figure 2. Schematic representation of major pathways involved in anteroposterior patterning. Wnt3 and Nodal signalling are present at the posterior side of the embryo. The Nodal antagonist Cer1 and Lefty are present at the anterior part. The definitive endoderm (DE) starts to arise at this stage. a: anterior, p: posterior, pr: proximal, d: distal. Modified from Scheibner et al., 2019.

Transforming growth factor-β (TGF-β) superfamily

The members Activin/Nodal and bone morphogenetic proteins (BMPs) are implicated in the establishment of the AP axis and/or the formation of the PS as well as in cell specification (Tam and Loebel, 2007; Lolas et al., 2014). BMPs are secreted proteins that bind to Type I and II BMP receptors. Upon BMP binding, these receptors promote phosphorylation and activation of Smads proteins (Smad1/5/8), which in turn, regulate gene transcription. For instance, *Bmp4*, expressed by extraembryonic tissues, is crucial for embryonic patterning as induces the expression of PS markers and also plays an important role in cell fate determination. Indeed, mutants for this gene show defects in gastrulation (Tam and Loebel, 2007).

Nodal signalling is mediated by EGF-CFC (epidermal growth factor-Cripto-1/FRL-1/Cryptic) co-receptors and type I and type II Activin receptors, which are serine/threonine kinases. It exerts a similar effect as BMP, as receptor activation triggers the phosphorylation of the receptor-associated SMADs Smad2 and Smad3. This phosphorylation makes possible the interaction with Smad4, which, in turn, goes to the nucleus to regulate gene transcription (Tuazon and Mullins, 2015; Houtmeyers et al., 2016). In zebrafish, Nodal signalling is involved in the AP axis establishment by inducing posterior identity (Tuazon and Mullins, 2015). In chick embryos, Nodal activity and its antagonists in the AVE appear to be also necessary for the formation of the PS (Chuai et al., 2012). In mice, Gdf3 (Growth differentiation factor 3) displays Nodal-like signalling activity and is involved in patterning the embryo by the blockage of BMP signalling (Tam, Loebel and Tanaka, 2006). Also in mouse, an even earlier role of this signalling pathway appears in the proximal–distal patterning of the visceral endoderm which is

necessary for the following AP patterning. In this step, Nodal helps differentiating the extraembryonic VE from the embryonic VE for this first axis, proximal-distal, to appear (Tam, Loebel and Tanaka, 2006). Indeed, miss-expression of BMP or Nodal proteins in the anterior part of the embryo ectopically induces tissues that are characteristic of posterior regions (Tam, Loebel and Tanaka, 2006).

Wingless/Int (Wnt)

Wnt proteins are a group of secreted glycoproteins that control a variety of cellular events such as cell proliferation, differentiation, migration and cell polarity, and they have critical roles in embryogenesis (Clevers and Nusse, 2012; Wang and Chen, 2016).

Wnt signalling is composed by a family of secreted ligands that bind to Frizzled and Lrp5/6 receptors (LDL Receptor Related Protein 5/6) in the cell membrane to induce an intracellular response. It can be subdivided in canonical and non-canonical pathways. In the absence of Wnts, β-catenin is sequestered by a destruction complex, formed by Adenomatous Polyposis Coli (APC), Axin and the glycogen synthase kinase 3β (GSK3β), phosphorylated and degraded. In the canonical pathway, when a Wnt ligand binds to Frizzled/LRP receptors, the protein Dishevelled (DSH) is activated to inhibit the formation of the destruction complex, thereby promoting the stabilization of β-catenin. β-catenin is then translocated to the nucleus to form a complex with TCF (T-cell specific transcription factor)/LEF (lymphoid enhancer-binding factor) proteins (Mayor and Theveneau, 2014; Prasad et al., 2019) and activate the transcription of Wnt target genes. The non-canonical pathways are independent of β-catenin-induced transcription. Instead, the non-canonical responses include induction of the

planar cell polarity pathway (PCP), calcium fluxes and Jnk and Src kinase activation (Arkell et al., 2013). The PCP non-canonical pathway involves small G-proteins such as Rho/Rac, which influence actin cytoskeleton remodelling, it often requires cell–cell contacts. Some of the molecules included in this pathway are Fmi (Flamingo), Vang (Van Gogh or Strabismus) and Pk (Prickle), Fz (Frizzled), Dsh, Ror (RAR Related Orphan Receptor) and Daam (Dishevelled Associated Activator of Morphogenesis) (Mayor and Theveneau, 2014).

Wnt3 participates in the formation of the primitive streak during gastrulation. Through β-catenin, LRP5 (low-density lipoprotein receptor- related protein 5) and LRP6, Wnt3 promotes the expression of genes important for the patterning of the posterior part of the epiblast (Wang and Chen, 2016; Tam, Loebel and Tanaka, 2006; Tuazon and Mullins, 2015). On the other hand, the antagonistic role of the secreted proteins Frizzled-related (sFRPs) and Dickkopf (Dkk) is necessary in the prospective anterior epiblast. sFRPs contain domains homologous to the Wnt binding site of Fz receptors and as a result, they block Fz activation. Dkk proteins are membrane-bound and bind LRP co-receptors to prevent the propagation of Wnt signalling (Tuazon and Mullins, 2015).

Fibroblast Growth Factor (FGF)

FGFs are secreted growth factors that bind and activate FGF receptors (FGFRs). FGF signalling presents a similar role to Wnt, as it functions emitting posteriorizing signals. However, the precise effect in AP axis establishment during gastrulation has not been addressed. These receptors belong to the tyrosine kinases type (RTKs) and upon FGF binding they become dimerized and

phosphorylated intracellularly. This, in turn recruits the effectors of this pathway, for instance GRB2 and Ras, which will activate MAPK (mitogen activate protein kinase). Activated MAPK then phosphorylates various transcription factors that will activate or repress gene expression. Other cascade of proteins that FGF signalling activates implies PKC, and PLCγ, which, in turn, promotes again the activation of the MAPK pathway (Turner and Grose, 2010). One of the FGFs ligands expressed during gastrulation is FGF8, which is present in the PS (Tam and Loebe, 2007).

1.1.2 Pluripotency regulation

After ingression and before the final lineage allocation, embryonic cells are pluripotent. This pluripotency is maintained thanks to the expression of several factors, such as OCT4, SOX2, Nanog and SALL4. These factors act in two transcription factor complexes, OCT4 and SOX2 on one hand and Nanog and SALL4 on the other. These two complexes activate gene transcription in a way that they promote expression of genes that encode their own and each other's constituent members (Tam and Loebel, 2007). Polycomb proteins help maintaining this pluripotency by suppressing the expression of genes that promote differentiation.

Although these are main factors required for pluripotency maintenance, it has been shown that Nodal is also involved, as mutant embryos for Nodal differentiate prematurely (Tam and Loebel, 2007). The role of Wnt signalling in pluripotency is still debated because inhibition of GSK3β which causes accumulation of β-catenin promotes the undifferentiated state; however, by

expressing a constitutively active form of β-catenin, cells differentiate precociously in mesoderm-like cells. Moreover, in the absence of Wnt3, the epiblast continues to express the pluripotency marker Pou5f1 (OCT4) (Tam and Loebel, 2007). During gastrulation the PS contains precursor cells of different mesodermal and endodermal tissues. Both Wnt and Nodal pathways activity in the PS are involved in the formation of different populations of mesoderm and endoderm cells. However, the precise moment of when these cells differentiate into morphological and molecular distinct cell populations is not clear (Burtscher and Lickert, 2009).

1.1.3 Epithelial-to-Mesenchymal Transition (EMT).

A key event in the initiation of gastrulation is the loss of cell-cell adhesion in the epiblast to undergo Epithelial-to-Mesenchymal Transition (EMT). EMT enables the ingression of the mesendoderm through the PS (Wang and Chen, 2016). The remaining cells that will form the ectoderm/epiblast, do not ingress in the PS and therefore they do not undergo an EMT process (Tam and Loebel, 2007). The process of EMT involves first a myosin mediated apical contraction and breaking cell-cell and cell-basement membrane connections to detach from the neuroepithelium and delaminate (Nieto et al., 2016). The cells, upon EMT, acquire the capacity of migratory cells and move through the extracellular matrix (ECM) (Acloqué et al., 2009). Thus, the ECM, which is a three-dimensional fibrillar network composed mainly of collagens and fibronectin plays an important role in delamination. Mice lacking fibronectin cannot complete gastrulation and have severe defects in mesoderm formation and migration. Typical epithelial markers are E-cadherin, occludins and cytokeratins whereas N-cadherin and

vimentin label mesenchymal cells, the expression of these different markers at the correct time is crucial for the EMT process.

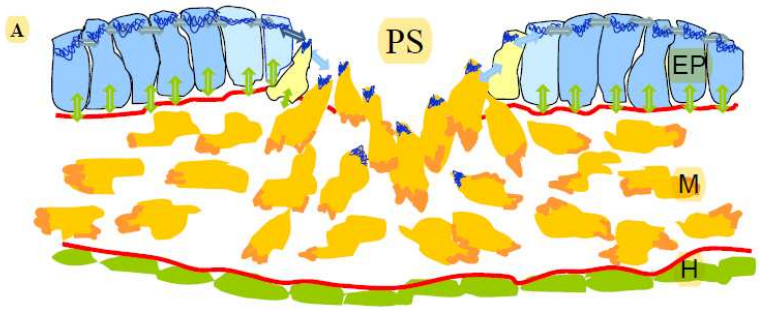

Figure 3. Cell ingression in the primitive streak. A: Diagram showing changes occurring during ingression in the streak. A signal secreted by the mesoderm cells (light-blue and yellow) results in apical contraction of these cells by myosin (apical blue line). Simultaneously the cells reduce the strength of E-Cadherin medicated interactions (blue double arrows between cells), break down the basal lamina (redline) and down regulate integrin mediated signalling to the matrix (green double arrows), polarise by synthesizing actin at their leading edges (orange) and migrate in the internal space of the embryo in response to repulsive ad attractive guidance factors (Chuai et al., 2012).

In mice, the FGF-Snail pathway is thought to control the switch from E- to N-Cadherin because Snail mediates transcriptional repression of E-cadherin (Chuai et al., 2012). In *Fgfr1*-mutant embryos, epiblast cells fail to undergo EMT, *Snai1* is not upregulated (Snail1) and *Cdh1* (E-cadherin) downregulated (Tam and Loebel, 2007). As a consequence, epiblast cells cannot ingress through the PS. In addition, post-transcriptional regulation of E-cadherin also takes place. This regulation exerts a more rapid effect in EMT. For example, an activator of p38 MAPK, the p38-interacting protein (p38IP), promotes the rapid degradation of E-cadherin (Zohn et al., 2006).

Snail is also known to negatively regulate Sox3 and in consequence, these transcription factors show complementary expression patterns. In fact, Snail1/2 (1 in mouse and 2 in chicken) positive cells ingress through the PS, while Sox3 positive cells give rise to ectodermal cells. Epiblast cells are able to respond to

extracellular signals that initiate EMT and their delamination is also influenced by the canonical Wnt signalling pathway, which is active in the posterior part of the embryo (Acloqué et al., 2009). Nodal signalling also constitutes an EMT inducer and low activity of this pathway is sufficient to induce delamination. Some studies have also described a role for mesoderm posterior (Mesp) transcription factors in stimulating EMT in a Wnt-independent manner (Tam and Loebel, 2007).

A crucial step during EMT is the loss of cell polarity, this is caused by the disassembly of tight junctions between the neighbour cells, that are normally maintained by the protein Par6, which is regulated by the membrane protein ephrinB1. For EMT to finish, cells must pass through the basal membrane. Several metalloproteases (MMP2/3/9) have been implied in the degradation of the basal membrane, and it is though that they are activated by *Snail* genes. Furthermore, RhoA, a small GTPase, which regulates microtubule dynamics, has been also related to the control of basal membrane integrity in the chick PS (Chuai et al., 2012).

1.1.4 Migration and ingression of PS cells.

Cells ingressing in the PS have been shown to migrate in a collective migration manner. The sequence of cell migration occurs in the way that cells move from posterior positions in the epiblast to anterior along the central midline and are replaced by cells moving in from more lateral positions. Endoderm and mesoderm cells begin to allocate in the correct place once the streak is extended halfway over the epiblast (Chuai et al., 2012).

Little is known about the molecules that guide epiblast cells migration, but there are some studies suggesting that chemotaxis drives mesendodermal ingression (Chuai et al., 2012). Mesoderm cells from the anterior part of the streak respond positively to FGF4 and this response is inhibited when these cells express a dominant negative FGFR1 receptor. However, they are repelled by FGF8, expressed in the PS. Thus, the migration of mesodermal cells is achieved by a balance between chemo-attraction and chemo-repulsion (Tam and Loebe, 2007). PDGF signalling has also been proposed to be an important mechanism controlling the migration of mesoderm cells to more anterior positions, while the cells that leave the most posterior positions of the streak would be attracted by factors such as VEGF (Chuai et al., 2012). The cytokine SDF1 through the receptors CXCR4 and CXCR7 are also important for mesendoderm cells to migrate towards the midline (Chuai et al., 2012).

Most *in vivo* studies on cell migration have been performed in chicken, *Xenopus* and zebrafish embryos. Studies in mouse gastrulation are scarce due to the difficulty of accessing to the embryo or culture them *in vitro*. However, it seems clear that in later stages of gastrulation, cell movements are more passive and are caused by the deformations of the extracellular matrix due to shape changes in the embryos in other places, movements that are the consequence of chemokinetic changes (which in contrast to chemotaxis do not imply active migration with directionality) (Chuai et al., 2012).

1.1.5 Germ layer differentiation

As gastrulation progresses, the streak elongates from its origins at the embryonic/extraembryonic junction toward the distal tip of the embryo. By mid-streak stages, cells on the anterior tip start to form the node, that is comprised by 20 cells in diameter and at late-streak stages becomes morphologically visible (Warr et al., 2008). The node is a bilaminar structure that patterns the midline axis of the embryo. The ventral cells of the node form the notochordal plate and, anterior to this, there is a population of cells that form the head process and underlie the future forebrain. The node also gives rise to most of the axial mesoderm and some definitive endoderm. When the process of regression starts, the node moves in a posterior direction and forms the notochord and the floor plate (Chuai et al., 2012). The notochord is laid down along the midline of the anteroposterior axis, underlying the neuroectoderm and the paraxial mesoderm on either side of the notochord is divided into pairs of somite blocks.

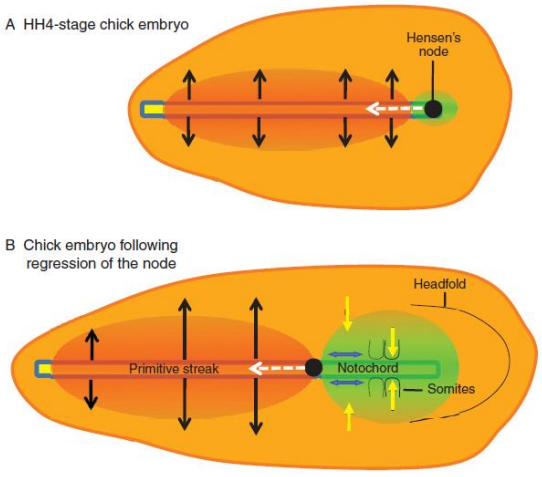

Figure 4. Collective cell migration of mesoderm cells during the early streak regression stages of chick gastrulation. Shown are two early chick embryos at successive stages of gastrulation. (A) Embryo at stage HH4, the fully extended streak stage. The tip of the primitive streak forms Hensen's node (black dot), which starts to regress in the posterior direction (dashed white arrow). Embryonic regions are shown by orange shading. Black arrows indicate the direction of cell movement. (B) Embryo after regression of the node. Here, the streak has started to regress; the first outline of the head becomes visible and the first somites are formed (Weijer, 2009).

Meanwhile, the dorsal ectoderm transforms into the neural plate (NP), which is an epithelial lamina formed through a process called neural induction or neurulation. When the ectoderm is still being patterned, between the NP and the nonneural ectoderm (NNE), two areas known as neural plate borders (NPB) emerge. The NPB domain will then contribute to the dorsal neural tube, the neural crest (NC), the NNE and, the placode progenitors in the anterior region (Rogers and Nie, 2018). The NP folds to form the neural tube between the border regions (neural folds) from opposite sides of the ectoderm and therefore, NC progenitors locate at the dorsal tip of the neural tube.

1.2 The Neural Crest

The neural crest (NC) is a transient embryonic structure that appeared in vertebrates during evolution (Chan and Tam, 1988; Le Douarin and Kalcheim, 1999). It was discovered in chick embryos by Wilhelm His in 1868 and, in 1878, Arthur Milnes Marshall called neural ridge to the cells that give rise to cranial and spinal ganglia (Hall, 2008). This term referred to the transient ridge that is formed on the dorsal surface of the neural tube of amphibians before migration and it appears before closure of the neural canal. But one year later, in 1879, Marshall realized that this name did not describe correctly this structure and replaced neural ridge for neural crest (Hall, 2008). The NC is composed by a multipotent and migratory cell population and it is originated at the border between the neural plate and the prospective epidermis (epidermal ectoderm or non-neural ectoderm) along the dorsal midline of the embryo, except in the most anterior part of the head (Duband et al., 1995; Kerosuo and Bronner-Fraser, 2012; Vega-Lopez et al., 2017). The formation of the NC extends rostrocaudally and it is

subdivided in different types depending on the site of origin. From anterior to posterior is called: cephalic, cardiac, enteric, trunk and sacral neural crest (Gouignard et al., 2018).

The NC has been proposed to constitute a fourth germ layer because, although NC cells derive from the ectoderm, they can give rise to derivatives not only coming from ectoderm but also from mesoderm layers, such as cartilage and bone (Hall, 2000, 2018). The molecular mechanism that could explain this dual potential has yet not been revealed, but there are studies in *Xenopus* suggesting that NC formation is underway during gastrulation and perhaps is initiated even during blastula stage (Basch et al., 2006; Patthey et al., 2008, 2009; Monsoro-Burq et al., 2005). This theory also postulates that the earliest anterior NC emerges independently from neural and nonneural ectoderm and mesoderm interactions, while later NC depends on the communication between these two tissues (Basch et al., 2006). Favouring this hypothesis, the expression of pluripotency inducing genes such as *Myc*, *Sox5* or *Id3*, is detected together with genes that specify the NC. However, these pluripotency genes are also expressed in the endoderm and mesoderm layers in a non-pluripotent state, suggesting that they might have another role in inducing lineage commitment (Sauka-Spengler and Bronner-Fraser, 2008; Buitrago-Delgado et al., 2015; Pshennikova et al., 2019).

The formation of the NC implies a sequence of phases that include induction and specification of the prospective NC territory-neural plate border, specification of *bona fide* neural crest progenitors, and differentiation into diverse derivatives. All these processes are controlled by regulatory circuits that can be assembled into a hierarchical network of regulatory genes (GRN) that has been

shown to be highly conserved across vertebrates (Taylor and LaBonne, 2007; Betancur et al., 2010).

1.2.1 Neural Crest Induction

Although the NC is induced in the ectoderm during gastrulation, NC cells do not become morphologically apparent until neurulation (Rogers et al., 2012; Pla and Monsoro-Burq, 2018). NC induction is thought to be the consequence of interactions between the epidermis (or nonneural ectoderm) and the neural plate when is elevated to form the neural folds (Betancur et al., 2010). So the NPB cells contain the NC precursors and they are located in-between the NP and the nonneural ectoderm, being the mesoderm also in contact with these cells, positioned underneath these two tissues. NPB cells are multipotent, so the neural plate expresses genes characteristic of these multipotent border cells, that are called neural plate border specifiers and are part of the GRN. These genes are crucial for NC induction and are expressed already in early neurulation. These GRN include the homeobox transcription factors Msx1/2, Dlx5, Pax3/7, and Gbx2, as well as zinc finger-containing Zic proteins (Nakata et al., 1997; Sauka-Spengler and Bronner-Fraser, 2008; Simoes-Costa & Bronner, 2015). In addition, NPB cells are influenced by morphogens such as FGFs, Wnt or BMPs.

In *Xenopus,* Msx1 is activated by the interaction of BMP, FGF, Wnt, and Notch signalling pathways (Monsoro-Burq et al., 2005, Tribulo et al., 2003) and Zic1 and Pax3 are also regulated by Wnt, BMP and FGF (Monsoro-Burq et al., 2005; Betancur et al., 2010). Pax7 is regulated by FGF, Wnt, and retinoids (Stuhlmiller and García-Castro, 2012; Prasad et al., 2019). Dlx5 is regulated by

low levels of BMP and GBX2 constitutes a direct target of Wnt signalling (Prasad et al., 2019). However, in mouse, Pax3 and Pax7 appear to have redundant roles and have even been proposed to be dispensable for NC formation (Zalc et al., 2015). The morphogens BMP, Wnt and FGF are secreted by the neural plate, the non-neural ectoderm and the paraxial mesoderm (Monsoro-Burq et al., 2003). Therefore, these tissues are essential to induce the NC. However, the contribution of the mesoderm has been a matter of controversy. Studies performed in zebrafish suggest that the mesoderm is not essential for NC induction because Nodal mutant embryos lacking mesoderm still express NC markers (Ragland and Raible, 2004). This is also supported by experiments in chicken, as chick nonneural ectoderm can respond to FGF signalling and activate NC markers expression in the absence of mesoderm induction (Yardley and García-Castro, 2012). Intriguingly, the requirement of the mesoderm in NC induction in mammals has not been fully confirmed *in vivo* because mesoderm removal does not seem to affect NC cells markers (Prasad et al., 2019).

Recently, it has been proposed by experiments in chicken and amphibian embryos that NC induction occurs in two-steps (Monsoro-Burq et al., 2003; Prasad, Charney and García-Castro, 2019). FGFs and Wnts act first and are essential for NPB formation (Monsoro-Burq et al., 2003), while BMP, Notch and again Wnt are needed a bit later in the maintenance of the induction and in NC specification (Monsoro-Burq et al., 2003; Tribulo et al., 2003). In addition to these signalling pathways, retinoic acid signalling would be important too.

BMP signalling

BMPs are present in the non-neural ectoderm and paraxial mesoderm. Initially, it was proposed from studies in *Xenopus,* that inhibition of BMP is required for neural induction, whereas high levels turn out to an epidermal fate (LaBonne and Bronner-Fraser, 1998). Later, it was proposed that intermediate levels of BMP are responsible for the induction of NC cells and can be obtained as a result of diffusion of secreted BMP molecules throughout the ectoderm (BMP gradient) (Knecht and Bronner-Fraser, 2002; Nguyen et al., 1998; Labonne and Bronner-Fraser, 1998) or by antagonistic interactions with Cerberus, noggin, chordin, and follistatins, ligands secreted by the forming neural plate (Sauka-Spengler and Bronner-Fraser, 2008; Tribulo et al., 2003; Wilson et al., 1997). Intermediate levels of BMP signalling would activate Zic3, Pax3, Msx1 and Hes4 in frog and zebrafish, which are the factors known as NPB specifiers. However, intermediate levels of BMP signalling alone cannot induce NC, suggesting that some other pathways, such as Wnt of FGF are needed in this process (Labonne and Bronner-Fraser, 1998; Garcia-Castro et al., 2002). In fact, in avian embryos it has been shown that BMP acts together with FGF to define the boundary of the ectodermal derivatives (Streit and Stern, 1999), and NC fate would be controlled by Wnt signalling (Wilson et al., 2001). A more recent model proposes an intermittent action of BMP signalling. In this model, BMP signalling attenuation together with the action of Wnt and FGF during gastrulation, promotes the formation of a “zone of competence” to promote NC induction. Later on, BMP is reactivated at the NPB to induce NPB and NC genes (Ragland and Raible, 2004; Steventon et al., 2009).

Several BMP signalling conditional KO mice, including those lacking BMP-receptor Alk2/3/5 or Tgfbr2 show severe craniofacial, pharyngeal and cardiac

defects. However, the expression of NC markers is not affected in these mutants until E9.5, suggesting that BMP likely plays a role in maintaining the induction phase (Prasad et al.,2019).

FGF signalling

At the time of NPB specification, several FGF ligands, including FGF3, FGF4, FGF8 are expressed in the dorsolateral marginal zone (DLMZ), i.e. the early precursor of paraxial and intermediate mesoderm. These ligands bind to FGF receptors and transduce an intracellular signalling via MAPK, PLCγ and PKC (Turner and Grose, 2010). In the prospective NC epiblast there is expression of FGFR1/4.

In *Xenopus*, FGF signalling has been involved in NC induction through the mesoderm tissue. FGF2 together with the attenuation of BMP induces the expression of Snail2 and overexpression of FGF8 transiently induces NC (Monsoro-Burq et al., 2003). In chick, inhibition of FGF signalling in the prospective NPB causes the loss of NC markers, but not its inhibition after gastrulation (Prasad et al., 2019). Although these experiments indicate that FGF signalling is necessary for the induction of most NPB specifiers *in vivo* in these two models, whether FGF plays a role in fish and mammals remains unclear because mice lacking FGF receptors or zebrafish without mesoderm have no phenotype related to NC formation (Jones and Trainor, 2005; Prasad et al., 2019). However, recent work suggests a mesoderm independent role of FGF signalling, being FGFR1/4 expressed in prospective NC epiblast during chicken gastrulation, but not in the mesoderm (Stuhlmiller and García-Castro, 2012).

Moreover, another study performed in rabbit using explants from gastrula shows a mesoderm-independent NC specification, dependent of FGF signalling (Betters et al., 2018). The fact that this mesoderm independent role has not been observed in mouse and zebrafish could be due to the redundancy of FGF factors in mouse; and to the differences in the stage where it has been analysed in the case of zebrafish. A better research on earlier stages should be performed to unveil solve this question (Prasad et al., 2019).

Wnt signalling

Several Wnt ligands including Wnt1, Wnt3a, Wnt6, Wnt7b and Wnt8a are expressed in the tissues involved in NC induction (Prasad et al., 2019). Actually, hence several Wnts are expressed in the developing neural tissue, Wnts appear to be the instructive signal to induce NC (Knecht and Bronner-Fraser, 2002). In the neural tube, Wnt signalling activates the expression of several NPB-TFs, such as *tfap2a*, *gbx2*, *pax3* and *msx1* as direct targets. As FGFs, Wnts have been shown to directly neuralize the NNE by inhibiting BMP4 expression in *Xenopus* caps assays.

The canonical Wnt/β-catenin signalling is necessary for NPB and NC induction in frog, fish and chick embryos *in vivo*. The ligands involved in this step are Wnt3a and Wnt8, which act in the neural tube and paraxial mesoderm, promoting posterior patterning and repressing anterior fates (Garriock et al., 2007). Conversely, Wnt6 has been proposed to act during late stages to extent the induction phase (Rogers et al., 2012). In mice, Wnts have been proposed to play a role in the migration and differentiation of NC derivatives (Prasad et al.

2019). β-catenin conditional knockout mice have been generated using a Wnt1-Cre driver, but because Wnt1 is not expressed during the induction phase, is still not clear whether the Wnt canonical pathway is involved in mammalian NC induction.

Although Wnt canonical signalling has been widely studied by LOF and GOF studies and by analysis on the expression of NPB specifiers, little is known about the molecular mechanisms triggering the phenotypes, i.e. it is unclear which are the gene targets for β-catenin-mediated transcription in this context. Axud1 has been reported to act downstream of Wnt signalling affecting FoxD3 expression and interacting with the NPB specifiers Msx1 and Pax7 (Simões-Costa et al., 2015). Also, Dkk2, acting through the LRP5/6 receptor, activates β-catenin and stimulate NC cell specification (Devotta and Saint-Jeannet, 2018). Other molecules have been also described to modulate Wnt signalling during NC induction. For example, the metalloprotease ADAM13 is involved in promoting Wnt signalling in *Xenopus* embryos (Prasad et al.,2019). It has been also shown that Ror2, a receptor tyrosine kinase known to be a major regulator of PCP signalling, upregulates the expression of the BMP ligand Gdf6 which in turn is essential for NPB/NC formation (Schille et al., 2016).

Notch/Delta signalling

Notch/Delta signalling is mediated by the activation of Notch membrane bound receptors upon Delta ligand binding that results in the cleavage of Notch intracellular domain (NICD). The NICD then translocates to the nucleus and

functions as a transcription factor in conjunction with a CSL protein (Rogers et al., 2012; Prasad et al., 2019).

This signalling is also present in NC induction; in chick, the Notch ligand Delta is expressed in the prospective epidermis whereas Notch is present in the neural folds and it has been reported that Notch-Delta signalling acts upstream of BMP4 (Endo et al., 2002). Intriguingly, defects in Notch signalling both by overexpression or by downregulation reduce BMP4 expression in the epidermis, indicating that intermediate levels of Notch signalling might be needed to induce NC indirectly by regulating BMP4 (Endo et al., 2002). In zebrafish, Notch is important to restrict neural fate, it appears to affect trunk but not cranial NC formation (Prasad et al., 2019). Delta1 null mutant mice have no apparent early NC defects even though cranial NC cells express several Notch genes, although they show later defects in migration and differentiation (De Bellard et al., 2002; Williams et al., 1995). All these findings do not demonstrate a role of Notch signalling in NC induction, and point to a more specific function in maintaining the inducing signals by regulation of BMP4 and the later specification of the NC (Knecht and Bronner-Fraser, 2002).

Signalling crosstalk

As explained above, there is signalling crosstalk between the different key pathways. Wnt can activate BMP, i.e. Wnt3a induces BMP in gastrula stage neural explants and inhibition of Wnt in NC explants downregulates BMP signalling (Patthey et al., 2009). FGF can also modulate BMP in *Xenopus*, it regulates positively BMP inhibitors, while induces Wnt expression. Thus, FGF

and Wnt work together to induce the NC gene regulatory network (GRN) at NPB and then modulate BMP, which is required for the induction maintenance and for the activation of the battery of genes needed for the NC specification. For example, *tfap2a* and *msx1* are both activated by FGF signalling and are direct targets of the Wnt/β-catenin pathway (Pla and Monsoro-Burq, 2018; Prasad et al., 2019). The combination of all these signals (BMP, Wnt and FGF) with the NP border specifiers activates another battery of TF (NC specifiers) which regulates downstream effectors to produce *bona fide* NC cells.

The NP border specifiers also interact with each other in a way that depletion of any of them alters the expression of all other NB specifiers, resulting in deficient NC induction (Prasad et al., 2019).

Table 1 | **Steps in neural-crest induction**

Stage	Process	Genes/proteins
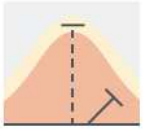	Induction of neural plate and neural-plate border (Solid line indicates the strong inhibition of BMPs by their antagonists, which come from the organizer region and which induce the neural plate. Dotted line represents a weaker antagonism that induces the neural plate border.)	BMPs and BMP antagonists
	Induction of neural crest potential as assayed by *Slug* expression	Wnts, FGFs and retinoic acid from epidermis or lateral mesoderm
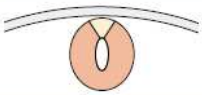	Maintenance, proliferation and non-differentiation of neural crest precursors	BMPs, *Wnt1*, *Wnt3a* and *Pax3* in the dorsal neural tube
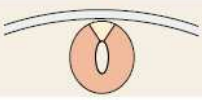	Subdivision of neural crest/neural tube lineage	Notch/Delta, *Foxd3*
	Emigration of neural crest	BMPs, *Slug*

The proposed stage at which each process functions is indicated by the diagram in the left column, whereas genes/proteins that are implicated in each process are listed in the right column. Although processes are separated for clarity, they might actually occur simultaneously in the embryo. BMP, bone morphogenetic protein; FGF, fibroblast growth factor.

Table 1: explanation of the steps in neural crest induction and the pathways involved taking the chick embryo as a model (Knecht and Bronner-Fraser, 2002).

1.2.2 NC Specification (NC specifiers)

The NC specifiers initiate their expression in premigratory and early migrating NC progenitors. Transcription factors present in this group are the family of *SoxE/D*, *Snail1/2*, *AP2*, *Twist*, *cMyc*, *FoxD3*, *Ets1* and *Id* genes among others (Prasad et al., 2019). While some persist in migrating and differentiating NCCs (such as Sox10), others such as Snail2 are present only at the onset of the specification process and the EMT prior to their emigration. A third way of expression occurs for example with Sox9, that is expressed in NC progenitors, switches off and appears again later in differentiating derivatives (Betancur et al., 2010).

The NC specifiers are subdivided in early or late depending on the time of NC specification they affect. The “early ones” function to maintain pluripotency and the “later” are required to initiate the EMT program and initiate migration (Rogers et al., 2012). Some exceptions to this mode of expression are *AP2α*, *Snail1/2*, *Id*, *c-Myc* and *Twist*, which are expressed even before NC appearance (Sauka-Spengler et al., 2007), although this varies between species. This manner of expression brings up the possibility that these genes act as a link between the establishment of competence of NC progenitors at the neural plate and the specification of the NPB cells to NC cells (Betancur et al., 2010).

SoxE (*Sox8*, *Sox9* and *Sox10*) and *D* (*Sox5*) families play a crucial role both in NC formation and migration. *Sox* genes expression varies between species. In chick, the expression of *Sox5*, *Sox9* and *Sox10* goes before *Sox8*, while in *Xenopus SoxE* family are all coexpressed and *Sox5* is expressed even earlier, at blastula stages. In rabbit embryos, *Sox9* marks premigratory and migratory NC cells while *Sox10* appears later, only in migratory cells (Taylor and LaBonne, 2007; Prasad et al., 2019).

The role of *Sox* genes differs minimally between species; Sox9, in chick, has been involved in the maintenance of an undifferentiated state of NC and Sox5 acts as a modulator of Sox10 and affects NC cells EMT through regulation of *RhoB* expression. In *Xenopus*, Sox5 modulates BMP signalling to regulate neural plate border and NC specifiers (Buitrago-Delgado et al., 2015; Prasad et al., 2019). In general, SoxE transcription factors inhibit differentiation and consequently maintain multipotency in NC cells. Later on, Sox10 is essential for terminal differentiation of melanocytes and glia and Sox9 induces ecto-mesenchymal differentiation (Taylor and LaBonne, 2007). *Sox9* expression depends on AP2α and it can be also induced by Zic1 and Gbx2 (Betancur et al., 2010; Prasad et al., 2019). *Sox10* is regulated by Ets1, cMyb, and Sox9. Also in this model organism, both *Sox9* and *Sox10* can be repressed by Id factors (Light et al., 2005; Prasad et al., 2019).

Ets1 is specifically expressed in the cranial NC (Sauka-Spengler and Bronner-Fraser, 2008; Betancur et al., 2010) and might be the factor that explains the differences of cell cycle regulation and migration between the cranial and the trunk NC cells. cMyc and Id (Inhibitor of differentiation) factors function by connecting the NPB specifiers with the NC specifiers (Prasad et al., 2019). *Id* and *cMyc* genes are involved in the regulation of the cell cycle and help in the maintenance of the NC in a multipotent state (Light et al., 2005). Id proteins act as transcriptional repressors when they bind to genes of the *bHLH* family of transcriptional activators, as they impede the activation of their targets.

In *Xenopus* embryos, *Id* expression is regulated by cMyc (Light et al., 2005). However, in other organisms such as Lamprey, it has been found that *cMyc* expression starts before *Id3* is detected. This indicates that *Id3* expression

must be induced by other factors such as AP-2a or Zic1, and maintained by cMyc (Betancur et al., 2010). Finally, *Id* genes are also downstream targets of the BMP signalling pathway (Light et al., 2015; Prasad et al., 2019).

FoxD3 exerts a similar role to Id3, as it also maintains the multipotent state and prevents early differentiation (Lister et al., 2006). Notch signalling would be responsible of the regulation of this transcription factor, although Zic1 and Pax3/7 together with Wnt input appear to also promote FoxD3 expression (Betancur et al., 2010; Simões-Costa et al., 2012). In addition to this, Msx1 can also modulate this TF expression, as shown by LOF and GOF experiments in *Xenopus* (Tribulo et al., 2003). It has been found that in chick embryos, there are two separate enhancers controlling its expression in cranial or trunk NC (Simões-Costa et al., 2012).

cMyb, in turn, was added to the GRN because its downregulation affects *Slug* expression in trunk NC cells and it seems to regulate *Sox10* expression in cranial NC. In chick embryos, its expression is seen even before, at gastrulation stages (Betancur et al., 2010).

The *Snail* family is composed by *Snai1* and *Snai2*. This paralogous emerged in vertebrates from gene duplication from a single *Snail* gene in protochordates (Barrallo-Gimeno and Nieto, 2005; Taylor and LaBonne, 2007; Prasad et al., 2019). Their expression changes between species; *Snai1* is expressed in premigratory NC cells in mouse and zebrafish, while *Snai2* is present in these cells in chick and lizard (Locascio et al., 2002). *Snai1* is expressed already in blastula stage of *Xenopus* embryos (Buitrago-Delgado et al., 2015), suggesting a role of this transcription factor in mesendoderm

formation, conversely *Snai2* has not been detected in any species until NPB stage (Prasad et al., 2019). This lasts evidences, suggest a segregated role of these genes during NC development. *Snai2*, thus, is involved in specification and migration of NC cells, and both genes have been described to be important for EMT, but being Snail2 acting in chick and Snail1 in other vertebrate embryos (LaBonne and Bronner-Fraser, 1998). However, when Snail2 GOF is performed in chick embryos, it can induce cranial NC but not the trunk cells (del Barrio and Nieto, 2002). In mouse, both TF seem to be dispensable for NC formation, as a double knockout study in mouse epiblast does not show any NC defect at the cranial regions, at least until E9.5 (Murray and Gridley, 2006). In this animal, Twist and Sip are good candidates to mediate this function, as they are crucial for processes of EMT in tumour progression (Taylor and LaBonne, 2007).

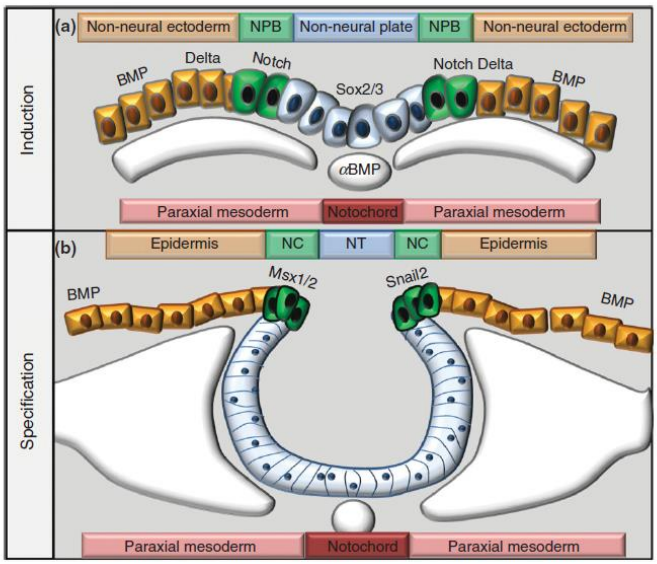

Figure 5. Neurulation and neural crest induction. (a) Secreted factors from the surrounding tissues [bone morphogenetic protein (BMP), fibroblast growth factor (FGF), Wnt] pattern the presumptive neural crest region or NPB. (b) As the neural tube closes, neural crest specification is complete and they begin to express neural crest specifier genes such as Foxd3, Slug, and Sox10 (Rogers, Jayasena, Nie and Bronner, 2012).

Snai2 (Slug) regulation has been extensively studied. In avian embryos, BMP4 can induce *Slug* expression and, in turn, Notch signalling pathway in chick and *Xenopus* helps maintaining *Bmp4* expression, required for NC specification,

and inhibits *Slug* (Endo et al., 2002, Glavic et al., 2004). *Slug* is also directly regulated by intermediate levels of BMP, which, in turn, are controlled by Wnt pathway. This TF contains binding motifs for *Smad1* and *Tcf/Lef1*, the mediator the β-catenin-dependent Wnt signal (Betancur et al., 2010; Prasad et al., 2019).

Moreover, the NPB specifiers Msx1, Pax3 and Zic1 are sufficient to induce *Slug* expression (Tribulo et al., 2003) and, at the same time, they interact with the Wnt signalling in *Xenopus* to help to this positive regulation of *Slug* (Betancur et al., 2010).

Epigenetic influence in NC formation

Regulation of the GRN is also influenced by epigenetic mechanisms involving chromatin remodelling. Post-translational modifications in the chromatin include methylation, acetylation, phosphorylation, ubiquitination, sumoylation, ADP ribosylation, etc (Prasad et al., 2019). These modifications exert positive or negative regulation of the genome. For example, trimethylation of the Histone 3 in the Lysine 4 (H3K4me3) and acetylation of the same histone in the Lysine 27 (H3K27ac) are marks for activation, while H3K9me3 and H3K27me3 are repressive marks (Rogers et al., 2012). Changes associated with H3K27me3 in enhancers influence them resulting in a poised enhancer state, and these are known to be important in steps such as gastrulation, neurulation and mesoderm formation (Rada-Iglesias et al., 2011; Rogers et al., 2012; Prasad et al., 2019).

Concerning the histone modifiers that could play a role in NC formation, JmjD2A, that is part of the Jumonji family of histone demethylases, is expressed in the NPB and removes H3K9me3 mark to activate the expression of NC

specifiers *Sox9*, *Sox10*, *FoxD3* and *Snai2* in chick (Strobl-Mazzulla et al., 2010). In addition to this, another histone modifier, CHD7, activates the expression of SOX9, TWIST1 and SNAI2 in human embryonic stem cell-derived NC cells (Bajpai et al., 2010). Finally, HDACs have been also investigated in this context, and it is known that *Hdac8* mutants show craniofacial defects and that high levels of Hdac1 are needed for NC specification (Bajpai et al., 2010).

1.2.3 NC Delamination and Migration

After specification of the NC, during or after neural tube closure (depending on the species), NC cells undergo an EMT to delaminate and migrate long distances. The beginning of this migration is related to the onset of somitogenesis (Kalcheim et al., 2016). The GRN also plays a role during this step, as they must not only maintain the precursors in a multipotent and proliferating state, but also activate or repress effector genes involved in the EMT process. Thus, *Sox9*, *Foxd3*, and *Snail* genes act together to activate genes involved in NC EMT (Betancur et al., 2010). One of the key features that takes place to ensure EMT is the change from type I Cadherins to type II Cadherins. For instance, in chicken, N-cadherin (type I Cadherin) is downregulated and Cadherin7 (type II Cadherin) is upregulated and this is thought to occur through FoxD3 and Sox10 actions. Another important Cadherin in avian embryos is Cad6B, in fact, LOF experiments for this protein show premature EMT (Kalcheim, 2016). In addition, changes in Cadherins at the protein level also occur, as N-cadherin is processed by an enzyme to obtain a soluble fragment that can enter the nuclei and regulate gene transcription. Changes in other types of cell adhesion molecules are also required, such as in

the expression of occludins, claudins, connexins and integrins (Vega-Lopez et al., 2017).

Similar to the EMT in gastrulation, in NC delamination, Snail1 is responsible for the downregulation of one of the type I Cadherins, E-cadherin and other factors, so together with the Zeb family of TF, have an inhibitory function onto E-cadherin.

FoxD3, which is expressed in premigratory and migratory NC cells, in addition to regulate Cadh7, induces the expression of human natural killer antigen-1 (*HNK1*), a marker for migratory NC cells. However, FoxD3 alone is not sufficient to induce EMT (Acloqué et al., 2009). In contrast, Snail2 is necessary and sufficient to induce NC cell delamination in chicken although only in the trunk region. At the same time, *Sox* genes are able to induce EMT and expression of HNK1, but they are sufficient only when several *Sox* family genes are introduced in combination, which could be explained by a compensation mechanism among these genes (Cheung et al., 2005).

Other molecules, such as the GTPase Rho, through the Rho-associated kinase (Rock), are involved in triggering EMT. Rho inhibits the process of G1/S transition, which is crucial to allow delamination, and they act downstream of BMP signalling. Rho impedes the processing of N-cadherin and negatively modulates EMT. Therefore, Rho is downregulated to allow EMT. As a consequence, Rac1, another Rho GTPase, is activated. Rac1 is highly concentrated in the leading edge of migrating NC cells to control actin polymerization enabling cell motility. Rho is again activated in migrating cells in an inverse distribution of that of Rac1 (Kalcheim, 2016). Also similar to EMT during gastrulation, metalloproteases such as MMP2 are important for the degradation of extracellular matrix proteins,

including several types of collagen, laminin, aggrecan, etc (Kuriyama and Mayor, 2008).

BMPs, Wnt, Notch and FGF signalling pathways are also involved in NC EMT. BMP signalling activity enables EMT. A gradient of Noggin is present across the AP axis that generates a gradient of BMP allowing the NC specification. When this gradient disappears by downregulation of Noggin, the inhibition of BMP is progressively released, allowing NC EMT (Kalcheim, 2016). Particularly, Bmp4 is expressed in the neural folds and triggers cMyb that evokes the activation of Snail2 and Msx1 to allow EMT. The downregulation of *Noggin* in the NT appears to be mediated by somitic factors, as the expression of this molecule is temporally correlated with somite development (Morales et al., 2005; Kalcheim, 2016). Thus, FGF and retinoic acid, which have opposing gradients in the paraxial mesoderm, might control the timing of NC EMT (Martínez-Morales et al., 2011). Actually, a decrease in FGF signalling in the somites is required for Noggin downregulation and for the expression of Wnt1. On the other hand, retinoic acid triggers *Wnt1* transcription at axial levels containing already specified NC progenitors, although it is not able to influence on Noggin expression (Martínez-Morales et al., 2011). So opposite gradients of FGF and retinoic acid are needed to control BMP and WNT signalling activities to regulate the onset of EMT (Martínez-Morales et al., 2011).

BMP4 induces ADAM10, which produces proteolysis of N-Cadherin which gives rise to a soluble fragment called CTF1, then is further processed by γ-secretase to be converted into CTF2 (Burstyn-Cohen et al. 2004; Gouignard et al., 2018). This fragment goes to the nucleus and stimulates transcription of *CyclinD1*. CyclinD1, in turn, promotes cells cycle progression and induces the S

phase synchronous entrance of NC cells, that were previously arrested in G1, to promote separation from the neuroepithelium and therefore, the delamination (Kalcheim, 2016). However, the caudal most NC cells, do not seem to delaminate thanks to the BMP4/WNT1 signalling, instead, they rely on WNT3A and they do not downregulate Noggin as a consequence of the somitogenesis step (Gouignard et al., 2018). There is also extensive crosstalk between different signalling pathways during this step. BMP signalling increases Wnt1 expression, whereas inhibition of Wnt1 downregulates BMP targets (Acloqué et al., 2009). Wnt1 protein is also responsible for the cell cycle transition from G1 to S (Burstyn-Cohen, 2011).

Intriguingly, although WNT canonical signalling is crucial for EMT, a transient inhibition must be achieved to allow delamination, and this is favoured by the proteins DACT1/2 (Dishevelled antagonist of β-catenin 1 and 2) (Rabadán et al., 2016). After completing EMT, cells start to migrate to arrive to their final destination and differentiate into one of the NC cell derivatives (Kerosuo and Bronner-Fraser, 2012).

There exist two different migratory pathways in trunk NC cells: a dorsolateral pathway between the ectoderm and the somites and a ventro-medial pathway between the neural tube (NT) and the posterior sclerotome (Erickson et al., 1992; Krull et al., 2001; Gammill and Roffers-Agarwal, 2010). The ventromedial route starts first. NC cells migrating through this path differentiate into sensory and sympathetic ganglia. The dorsolateral pathway, that initiates later, will give rise to melanocytes (Gammill and Roffers-Agarwal, 2010, Krispin et al., 2010, Richardson et al., 2016). In addition to these differences in the cell fates of NC cells migrating on these two pathways, the organization of their

migration is also distinct. NC cells that migrate ventromedially travel in a segmental manner through the somitic mesoderm, entering the rostral half of the somitic sclerotome while avoiding the caudal half-sclerotome. In contrast, dorsolaterally-migrating NC cells travel in a uniform, unsegmented fashion (Keynes et al., 1990).

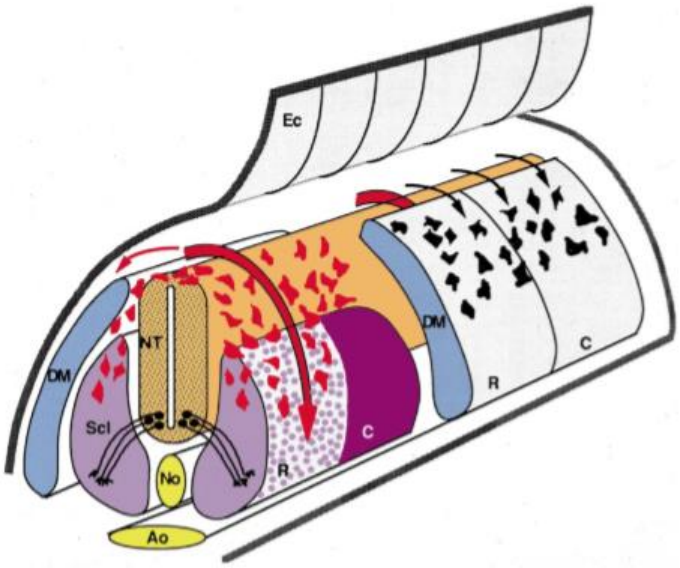

Figure 6. Avian trunk neural crest cells travel on two distinct pathways after emigration from the neural tube. Schematic diagram of a longitudinal view of the trunk region of an avian embryo. Some trunk neural crest cells (red) travel ventromedially, through the rostral, but not caudal, somitic sclerotome. Other neural crest cells (black) migrate dorsolaterally in a uniform manner between the somites and overlying ectoderm. DM, dermomyotome; Scl, sclerotome; No, notochord; Ao, aorta; Ec, ectoderm; NT, neural tube; R, rostral; C, caudal. (Krull et al., 2001).

NC cells are in a constant interaction with each other in a mode of migration called collective cell migration, moving in streams (Mayor and Theveneau, 2014). This way of movement is controlled by a process called contact inhibition of locomotion, that triggers a polarization on the cells to allow directional migration (Mayor and Theveneau, 2014).

During migration, NC cells express different molecules (normally signalling receptors) that respond to guidance cues expressed in the somites and mesoderm that will guide them by the different pathways (Sauka-Spengler and

Bronner-Fraser, 2008; Betancur et al., 2010). Eph-ephrin signalling is one of the pathways that NC cells use to migrate. In avian embryos, Ephb3 is expressed in the rostral half of the sclerotome and in the NC while its ligand, ephrinB1, is present in the caudal half-sclerotome. The complementary expression of the receptor and the ligand mediates repulsion and cells avoid the posterior part of the somite (Sauka-Spengler and Bronner-Fraser, 2008; Schwarz et al., 2009; Vega-Lopez et al., 2017). In addition to this, Ephs are implicated in the control of dorsolateral vs ventromedial migration. Melanoblasts express several Ephb receptors that help in their migration. If Eph signalling is downregulated, melanoblasts do not migrate dorsolaterally (Vega-Lopez et al., 2017). Thus, this pathway exerts two functions: first, it controls the segmentation of ventromedially migrating cells, and second, allows melanoblasts to migrate through the dorsolateral pathway (Vega-Lopez et al., 2017).

Another crucial guidance signal implicated in NC migration is the one involving Semaphorins and its receptors. Trunk NC cells express the receptor Neuropilin2 (Npn2/Nrp2) while Sema3F is restricted to the posterior half-somite (Schwarz et al., 2009). Both mutant mice show NC cells segmental migration defects, proposing that they are needed for signalizing the migration of NC cells through the anterior half of the somite (Schwarz et al., 2009).

Finally, the guidance molecules Slits, and their receptors the Robos, are also important for NC cells migration. While Slits are expressed in the dermomyotome, early migrating crest cells expressed Robo1 and 2. This evokes a repulsion to repress the entry of the NC into the dorsal pathway (Jia et al., 2005; Kuriyama and Mayor, 2008; Vega-Lopez et al., 2017).

Intriguingly, all these signalling pathways are involved in restricting NC cells path through a specific place, but not much is known about positive guidance cues that direct NC cells migration. Some molecules with a permissive effect on NC migration have been described; ECM proteins are permissive substrates to migration (Kerosuo and Bronner-Fraser, 2012; Gammill and Roffers-Agarwal, 2010), some examples are Collagen, Laminin and Fibronectin. Possible attractant cues for NC cells are: The glial cell lines derived neurotrophic factor (GDNF) and the netrin/deleted colon cancer protein (DCC), as loss of function studies for these proteins show failures in NC migration (Gammill and Roffers-Agarwal, 2010) and also members of the VEGF (vascular endothelial growth factor), PDGF (platelet-derived growth factor) and FGF families (Mayor and Theveneau, 2014).

Despite knowing that these proteins may exert attraction and contribute to the migration of NC cells, it is still not proven that NC cells migration is mediated by chemotaxis. Some results obtained from LOF studies propose the possibility that NCCs migrate by chemokinesis, which is the migration of cells stimulated by a factor and with no directionality. Evidence for chemotaxis are however strong as NC cells show typical mesenchymal morphology and are highly polarized in the direction of migration. One of the signalling pathways that control this polarity is the PCP (planar cell polarity) non-canonical Wnt signalling pathway (Mayor and Theveneau, 2014). As the canonical pathway, PCP may be activated by Frizzled receptors. But instead of activating β-catenin induced-transcription, the binding of Wnt to the receptors induce dishevelled (Dsh) proteins intracellularly and this regulates cellular polarity by rearrangement of the cytoskeleton. Downregulation of several PCP factors such as Wnt11, Fzd7 and Dsh leads to NC inhibition. In

fact, Wnt11 and Wnt11R are expressed adjacent to premigratory NC before the onset of NC delamination. Studies *in vitro* show that PCP is needed to stabilize cell protrusions that the cells need to direct the migration and important factors taking part on these processes are the small GTPases Rho and Rac (Kuriyama and Mayor, 2008). These cell protrusions form when the NC cells collide between each other, and upon this cell-cell contact, Rac is inhibited in the place of collision and Rho is activated (Theveneau et al., 2010).

1.2.4 NC cells derivatives

Before expressing typical markers for the new cell fate that NC acquire when becoming one of the derivatives, they must downregulate the expression of Snail1/Snail2, FoxD3, Id, and AP-2 (known as NC specifiers) (Betancur et al., 2010). However, some of these genes, such as FoxD3, persist in the population of cells that will give rise to sensory neurons, and it prevents the expression Microphtalmia-associated transcription factor (MITF), characteristic of melanocytes. Sox10 in turn, is retained in melanoblasts and in cells of the peripheral nervous system (Betancur et al., 2010).

Then, NC cells can give rise to a broad variety of neural and mesodermal derivatives (Le Douarin, 1982; Le Douarin, 1993; Stemple and Anderson, 1993), including neurons, glia, Schwann cells, cartilages, bones, smooth muscles, pigment cells, and cells of the adipose tissue, endocrine system and dental tissue (Pshennikovaa and Voronina, 2019). The first cells to migrate go towards the dorsal aorta and become sympathetic ganglia, followed by Schwann cells precursors, dorsal root ganglia (DRG) sensory neurons and finally melanocytes

of the skin. After that, the dorsal neural tube becomes the roof plate (RP) and will generate the dorsal neurons in the spinal cord (Kalcheim, 2016).

Regarding fate-restriction, it has been shown that melanoblasts are specified before they enter the dorsolateral route (Krispin et al., 2010). Conversely, ventral migrating NC cells are more plastic and can change their fate depending on the environment. This was shown in transplantation studies were NC cells derived structures were transplanted to an “early environment” of NC cells (Raible and Eisen, 1994, 1996). It has been hypothesized that multipotent progenitors exist ventrally, and they displace the dorsal pool of more committed cells on their arrival (Krispin et al., 2010). Taking this into account, the dorsal neural tube (NT) will be, therefore, a dynamic area during NC ontogeny in which progressive NC replacement takes place until formation of the definitive RP and separation of CNS from PNS migration (Krispin et al., 2010). However, a study in zebrafish postulates that NC cells are already fate-restricted when they start EMT (Raible and Eisen, 1994, Henion et al., 1997). This could be due to differences between species or different techniques used.

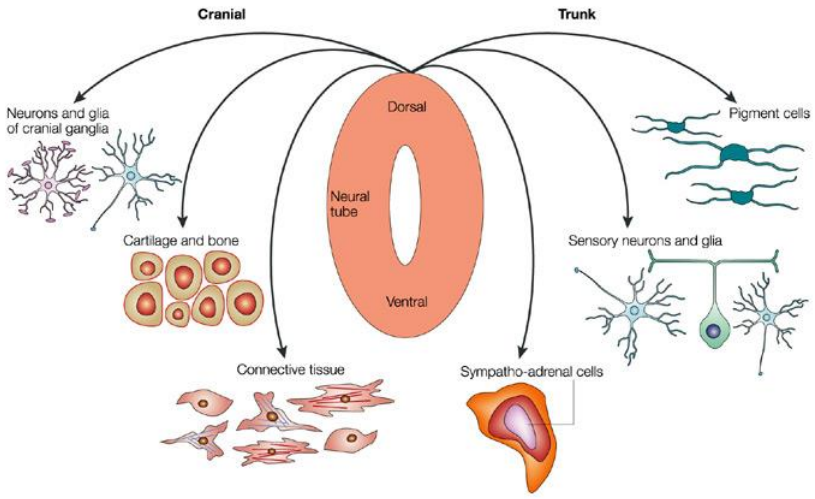

Figure 7. Neural crest cells migrate throughout the body and differentiate into many different cell types. Although neural crest cells are pluripotent, differences exist between cells that are generated from different anteroposterior levels: neural crest cells in the trunk form melanocytes and several neuron and glia cell types, whereas neural crest cells in the cranial (the embryonic head region) also have the potential to form mesenchymal derivatives, such as cartilage, bone and connective tissue (Knecht and Bronner-Fraser, 2002).

1.2.5 Differences between cranial and trunk NC cells

The two major populations of NC cells are cranial and trunk cells. They differ in several aspects regarding delamination, way of migration and the derivatives they give rise to. Only cranial NC cells contribute to craniofacial cartilage, while sympathetic neurons and glia are trunk-specific NC derivatives. Cranial NC also gives rise to connective tissue and smooth muscle while both give rise to pigment cells (Rogers et al., 2012; Prasad et al., 2019).

There are differences also in gene expression regarding the AP position: some examples are *bmp2* being expressed in trunk neural crests while *bmp4* in head, an existing AP gradient of *noggin* only in the trunk (not in the head) and the cranial unique expression of *ets1* (Rogers et al., 2012). Moreover, some genes have different enhancers depending if they are expressed in cranial or trunk NC

cells, for example in the gene *foxd3* or *sox10* (Simoes-Costa et al., 2012; Betancur et al., 2010; Prasad et al. 2019).

In addition, there exist differences in delamination, in mouse and chicken cranial NC cells, Sip1 (a.k.a Zeb2) is essential for delamination (Rogers et al.,2013) while δEF1 is also for trunk NC cells (Yasumi et al., 2016). Another difference is that, while trunk cells synchronously enter the S phase upon delamination, cranial NC cells do not (Betancur et al., 2010).

Regarding the way of migration, cranial NC cells are a homogeneous population relying on cell-cell interactions or directional migration, while trunk NC cells are a heterogeneous population with leader cells instructing directionality (Richardson et al., 2016). While trunk NC cells use two pathways to migrate, cranial NC cells migrate into three streams: adjacent to the neural tube from the diencephalon to rhombomere 2 (r2), adjacent to r4, and adjacent to the postotic region from r6 to r8. NC cells from r3 and r5 migrate rostrally and caudally to join adjacent streams (Kulesa *et al.*, 2010, Kuriyama and Mayor, 2008, Lumsden and Guthrie, 1991).

1.2.6 Differences between species

In amphibians the NC populations form a transient ridge on the dorsal surface of the neural tube before migration. These cells do not form such a ridge in birds and mammals and therefore, they cannot be distinguished from the rest of the neural tube prior to migration. In birds, NC cells undergo separation from the neural epithelium at the levels of the forebrain, midbrain and rostral hindbrain at the time that NC folds are fusing and before separation of the epidermal ectoderm

from the rest of the neural tube (Gouignard et al., 2018). In mammals, dispersion of the NC cells at the forebrain, midbrain and rostral hindbrain begins before the closure of the neural folds. In caudal hindbrain and trunk, neural fold fusion and separation of the overlying ectoderm from the neural tube occur well before NC cell emigration commences, both in mammals and in birds (Tosney, 1978; Erickson and Weston, 1983; Rogers and Nie, 2018). In these species, neural fold fusion does not occur exactly parallel to the wave of segmentation of the axial mesoderm into somites but it in the line with the EMT of the somite to form the sclerotome (Newgreen and Erickson,1986).

In mouse, NC cells in the two paths (ventromedial and dorsolateral) travel with much overlapping, while in chicken, these routes separate in time (Krispin et al., 2010). In zebrafish there are two ways of migration: medial and dorsolateral, and in contrast to other species, melanocytes come from both (Krispin et al., 2010). In *Xenopus* the preferred route is the ventromedial, as very few cells migrate in a lateral way, and another difference is that they migrate through the caudal somite (Gouignard et al., 2018).

The GRN genes show a high interdependence in lower organisms such as frog, while in mouse and zebrafish have more redundant functions during specification and a more restricted function in differentiation processes, as mutants in these genes show later phenotypes in the kind of derivatives NC cells give rise to. This could be due to the duplication of some genes during evolution or because of the techniques used in mammals are not appropriate (Barriga, Trainor, Bronner and Mayor, 2015).

2. The Zic family of transcription factors

The Zic (zinc finger protein of the Cerebellum) family of transcription factors (Zic1-5) play critical roles in vertebrate development including gastrulation and neurulation. In particular, Zic2 is highly associated to defects in gastrulation and neural tube closure (Warr et al., 2008; Nagai et al., 2000). The murine and human *Zic2* genes are highly conserved and mutations in these genes produce holoprosencephaly (HPE; MIM 236100), which is a group of developmental disorders that feature a failure of forebrain midline development that are typified by the presence of fused cerebral hemispheres and incomplete separation of the eyes.

Zic genes are the vertebrate homologues of the *Drosophila* gene odd-paired (opa) (Aruga et al., 1994). They encode multifunctional transcription regulators that contain five C2H2-type zinc fingers (Cys2, His2) (Inoue et al., 2007), which enable several functions: DNA binding, protein binding, transcriptional activation, and nuclear localization. They have been shown to act as classical transcription factors and as co-factors to regulate gene expression (Ali, Bellchambers and Arkell, 2012). Other known domains are the ZOC domain at the amino-terminal end that is conserved between Zic and fly Odd-paired domains (Zic-Opa conserved domain-ZOC) and the ZFNC (ZF-N-terminal conserved) domain that is immediately amino-terminal to the Zinc Finger Domain (ZFD). The ZOC domain only known function is the interaction with the proteins Pax3 and I-mfa, while the ZFNC domain that still has not an assigned function (Houtmeyers et al., 2013).

Zic genes are distributed in all metazoans except Porifera (sponges) and Ctenophora (comb jellies) and in vertebrates there are 5 to 7 *Zic* paralogs

(zebrafish has 7, vertebrates 5) (Houtmeyers et al., 2013). Zic and the family of transcription factors Gli are proposed to come from a common ancestor gene (Hatayama and Aruga, 2010).

Zic genes are clustered on the same chromosomes in a head to head orientation in mouse, humans and *Xenopus*. *Zic1* is in the same chromosome of *Zic4*, *Zic2* with *Zic5* and *Zic3* is located in a different chromosome (Houtmeyers et al., 2013).

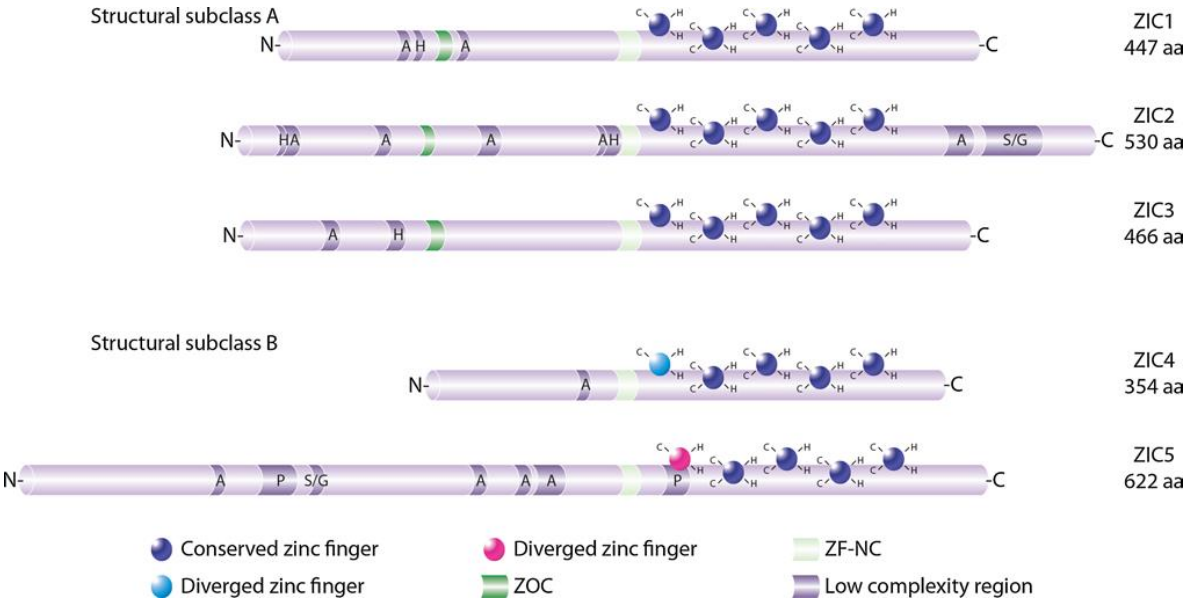

Figure 8. Structural features of the Zic proteins. Each of the five human Zic proteins is depicted. All contain a zinc finger domain that consists of five tandem C2H2-type zinc fingers. This domain is highly conserved with only the first zinc fingers of ZIC4 and ZIC5 showing some divergence. All five proteins also contain a short (14–21 amino acid) highly conserved domain immediately upstream of the zinc fingers, called the ZF-NC domain. Three of the proteins (ZIC1, ZIC2, and ZIC3) share another small domain (9–10 amino acid) of homology towards the N terminal of the protein called the ZOC motif. All proteins also contain low complexity regions with the major amino acid found at each low complexity region shown by the associated letter (A alanine, H histidine, P proline, S/G serine/glycine). Expansion of the alanine repeat region located C-terminal of the ZIC2 zinc finger domain or at the N-terminus of the ZIC3 protein is associated with human pathology. On the basis of the presence or absence of the ZOC motif and the degree of conservation within the first zinc finger domain the Zic proteins can be divided into two distinct structural subclasses (Houtmeyers et al., 2013).

Some of these roles are conserved in different species, mainly regarding the nervous system (Aruga, 2004). For example, several *Zic* genes have been involved in neural induction, more specifically in neuroectodermal differentiation in amphibian embryos (Nakata et al., 1998). Similarly, the process of lineage commitment from a non-neural cell to a neural cell has been tested in cultured mammalian cells. However, some studies in nematodes do not validate this, because loss of function of some *Zic* genes shows no phenotype (Bertrand and Hobert, 2009). These genes have been also proposed to participate in neurogenesis. For example, Zic1 enhances the expansion of neuronal precursors by inhibiting neuronal differentiation in the chick spinal cord (Aruga et al., 2002b). Moreover, *Zic* genes have been involved in the generation of NC cells (Elms et al., 2003; Nakata et al.,1997; Nakata et al.,1998). Additional functions postulated for *Zic* genes are the generation of mesoderm, as they are expressed in this and its derivatives notochord and paraxial mesoderm and mutants show skeletal defects (Aruga et al.,1999; Nagai et al., 2000). Although the functions are conserved, the mechanisms and the particular Zic protein involved in each process appear to be different between species.

2.1 Murine Zic2

Zic2 mRNA has been shown to be expressed at E5.5 in the epiblast (Elms et al., 2004) and even at 3.5 in the ICM of blastocyst (Brown and Brown, 2009).

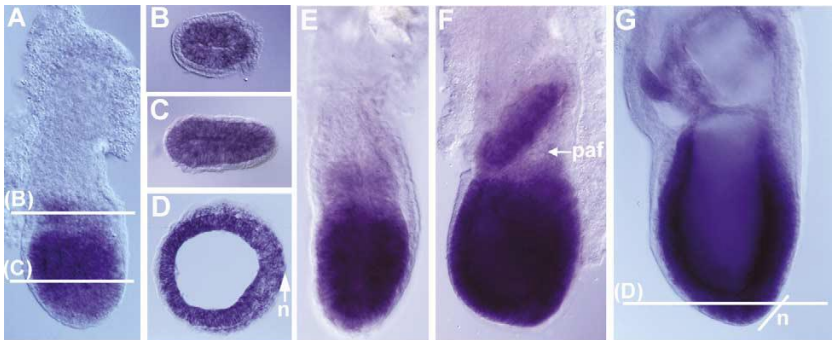

Figure 9. Zic2 expression during mouse gastrulation. In all pictures of embryos at stages where the anterior can be distinguished (after 6.0 dpc) the anterior is to the left and all intact embryos are shown in lateral view. (A) A 5.5 dpc, pre-streak stage embryo. (B) A transverse section through the extra embryonic region of a pre-streak stage embryo at the level shown in (A). (C) A transverse section through the embryonic region of a pre-streak stage embryo at the level shown in A. (D) A transverse section through the embryonic region of a 7.0 dpc, late-streak stage embryo at the level shown in G. The primitive streak and node are to the right. (E) A 6.5 dpc, early-streak stage embryo at the onset of gastrulation. (F) A 6.75 dpc mid-streak stage embryo with mesoderm moving into the posterior amniotic fold. (G) A 7.0 dpc late-streak stage embryo. The node is now visible and Zic2 transcripts are seen in the node. n: node, paf: posterior amniotic fold. Scale bar, 50 mm (A–D), 100 mm (E–G), 200 mm (Elms et al., 2004).

Later on, when development proceeds, *Zic2 mRNA* is also expressed in the anterior ectoderm and mesoderm of the headfold and even later in dorsal neural folds, somites and the segmenting trunk (Inoue et al., 2007). Zic2 has been also detected in differentiated neurons during late brain development, including Cajal Retzius cells (Murillo et al., 2015), granule cells in the cerebellum (Aruga et al., 2002a), ipsilateral interneurons in the dorsal the spinal cord (Escalante et al., 2013) and ipsilateral retinal ganglion cells in the retina (Herrera et al., 2003).

2.1.1 Zic2 in early embryonic development

Zic2-associated holoprosencephaly shows high penetrance (93%) (Solomon et al., 2010a). Mutations in Zic2 accounts for the majority of severely affected HPE cases (Solomon et al. 2010b) and is one of the four genes that are routinely analysed on a clinical basis in human patients with this disorder (Raam et al., 2011). Zic2 is the only member of Zic family that has been linked to HPE

(Houtmeyers et al., 2013) and pathogenic variants of ZIC2 are associated with both classic and middle interhemispheric variant (MIHV) HPE. Moreover, Zic2 associated HPE has been correlated with other phenotypes such as neural tube defects, hydrocephalus, skeletal anomalies, cardiac anomalies and renal anomalies (Solomon et al., 2010a).

There are three Zic2 mutant mouse lines. A null mouse line that carries a spontaneous missense mutation in the 4th zinc finger domain originated spontaneously (Kumba mutants (Zic2^{ku}), that impedes DNA binding and thus activation of transcription by Zic2 (Elms et al., 2003) , a hypomorphic Zic2 line (Zic2^{kd}) that resulted from wrong homologous recombination while genetic manipulation and a mutant found in a recessive ENU mouse mutagenesis screen searching for novel mutants for cardiovascular anomalies called Zic2^{iso} which contains a disruption of the fifth zinc finger domain of the protein.

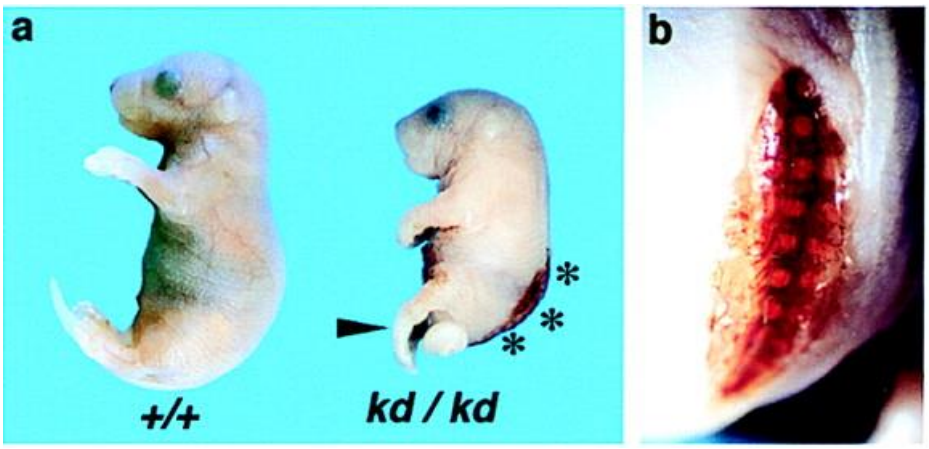

Figure 10. Neural tube defects found in *Zic2$^{kd/kd}$* mice. (a) Lateral views of P0 Zic2$^{+/+}$ (Left) and *Zic2$^{kd/kd}$* (Right) newborns. Heads of *Zic2$^{kd/kd}$* animals were significantly smaller (microcephaly). Arrowhead, pes equinus; *, spina bifida. (b) Dorsal close-up view of the P0 *Zic2$^{kd/kd}$* embryo. Spina bifida was always observed. (c) Lateral close-up view. Tails were irregularly curled (Adapted from Nagai et al., 2000).

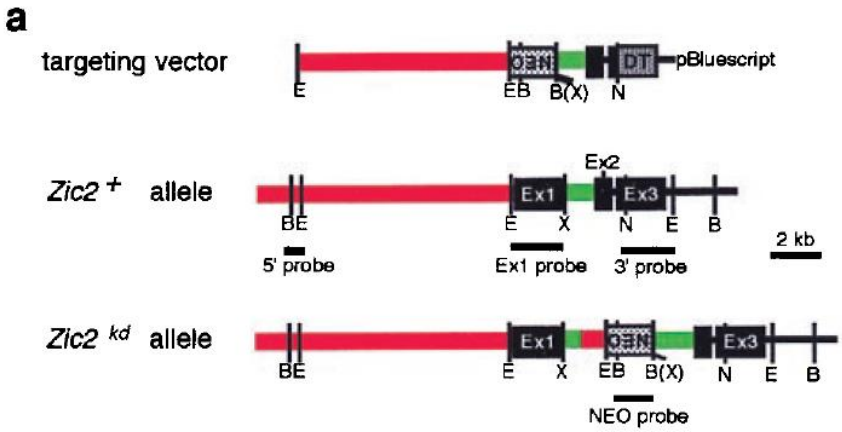

Figure 11. The Zic2 knockdown mutation. (a) Mouse Zic2 gene, targeting construct, and mutated Zic2 gene (Zic2^{kd}). The targeting vector (Top) contains an 8.0-kb and a 2.3-kb region homologous to the Zic2 gene and a neomycin resistance gene, respectively, driven by the phosphoglycerate kinase gene (PGK) promoter (NEO). The diphtheria toxin A fragment gene driven by the MC1 promoter (DT) was inserted in the 39 end of the Zic2 gene. In the Zic2^{kd} allele, a homologous recombination occurred in the 39 end, whereas a large portion of the 59 homologous region (red) was deleted and the remaining part was connected to the first intron (green) illegitimately. The connecting point contains the three bases of the overlapping sequence between the 59 and intron sequence as determined by nucleotide sequencing (data not shown). As a result, PGKneo and 622 bp of the 59 homologous regions were inserted into the first intron (Nagai et al., 2000).

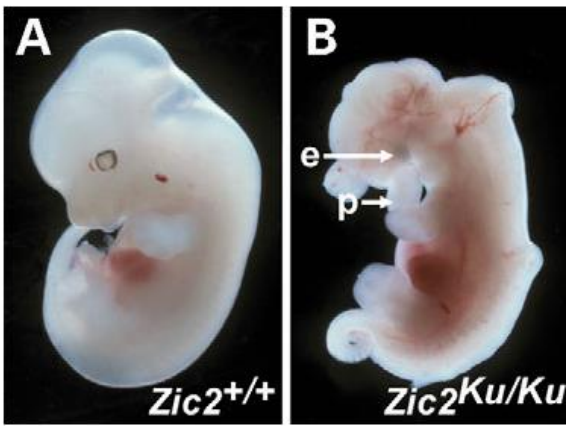

Figure 12. Zic2 mutation causes cyclopia with proboscis. Lateral view of intact embryos or transverse sections through the head of 12.5 dpc embryos. (A) A wild-type embryo. (B) A *Zic2$^{Ku/Ku}$* embryo with exencephaly, spina bifida, a looped tail, an internally located eye and a proboscis. e, eye; p, proboscis. (Adapted from Warr et al., 2008).

Kumba mutants have defects in neural tube closure, abnormal forebrain, eyes dysmorphologies and a reduction in the number of NC cells (Elms et al., 2003; Warr et al., 2008). In addition to these phenotypes, it has been also reported an earlier defect in the node or gastrula organizer of these mutants. Some node markers as Hhex, Foxa2 and Gsc are depleted or absent. This causes a decreased number of differentiated cells that come from the node,

implying a failure of anterior notochord specification and a loss in the maintenance of cell identity in the prechordal plate (Warr et al., 2008). This defect in the specification of the prechordal plate has been proposed to be caused by a defective Nodal signalling (Houtmeyers et al., 2016). Classic HPE implies a defective ventral forebrain patterning so it was logical to think that a failure in the prechordal plate signalling was the main cause of this disease. The prechordal plate is generated during mid-gastrulation, from cells coming from the node, that are the cells arising from the anterior PS. Warr and colleagues revealed that *Zic2* is the only member of *Zic* family expressed at the node and they claim that *Zic2* mutants fail to specify the anterior notochord and the prechordal plate, as they do not generate sufficient precursors at the node that give rise to these structures (Warr et al., 2008). Supporting this idea, they showed aberrant expression of some node markers, such as Hhex, Gsc and FoxA2. In a more recent article, these authors propose that HPE5 must be caused by a defective Nodal signalling, by physical interaction of Zic2 with the signalling transductors of the TGF-β cascade Smad2 and Smad3 to activate FoxA2, which is important for the formation of the anterior notochord (Houtmeyers et al., 2016).

In the *Zic2*^{kd} mutants, the phenotypes varied from HPE and microcephaly to exencephaly and anencephaly. In addition to this, mouse mutant for Zic2 have some skeletal abnormalities. Already at E9.5 these mutants show higher number of mitotic cells in the dorsal telencephalon and a failure in apoptosis that is known to occur at E10.5 in the roof plate and as a consequence, the dorsal forebrain is not properly developed in *Zic2*$^{kd/kd}$ (Nagai et al., 2000). Moreover, several markers were examined to go deeper in the forebrain defects. Pax6 (ventral NT) and Shh (notochord and floor plate) were expressed as in wildtype, whereas

Wnt3a was significantly reduced both in the brain and the spinal cord. These indicates that although dorsoventral patterning is correct, roof plate is defective in these mutants (Nagai et al., 2000). Together with Zic3, Zic2 has been shown to control the segmentation of paraxial mesoderm and the combined mutants have skeletal abnormalities as a consequence. *Zic2*$^{kd/kd}$ mutants also showed somite compartment defects, seen by the expression of Uncx4.1 and deficiencies in the formation of ganglia and spinal nerve axons (Inoue et al., 2007).

Recently, the examination of an additional *Zic2* mutant line (*Zic2*^{iso}) has also revealed that Zic2 is required for left-sided identity in the lateral plate mesoderm (Dykes et al., 2018).

Gain of function studies of Zic2 in *Xenopus* have suggested a role for this protein in neural induction, because according to the authors it promotes an expansion of the neuroectoderm (Nakata et al., 1998). Also in *Xenopus*, it was pointed a role for Zic2 in NC development, as overexpression of this gene causes an increase in the number of NC cells in the dorsal mesenchyme. *Zic2*$^{kd/kd}$ embryos also have more NCAM expression, which lead to the idea that Zic2 may induce neural fate (Nakata et al., 1998).

2.1.2 Zic2 in neural circuits development

At late developmental stages Zic2 is also expressed in different populations of migrating neurons. For instance, it is present in Cajal Retzius cells, where is crucial for their motility during the migration. Zic2 mutants exhibit an uneven distribution of the CRCs across the telencephalic surface (Murillo et al., 2015) and defects in cortical lamination (Inoue et al., 2008, Murillo et al., 2015). These

mice also show defects in other populations of migrating neural progenitors expressing *Zic2* which are the LOT cells (cells that integrate in the nucleus of the lateral olfactory tract), neuroepithelial cells in the caudal tier of the dorsal pallium moving to the amygdala via the caudal amygdaloid stream (CAS), as well as prethalamic subventricular neuroepithelial cells traveling to the ventral LGN (vLGN) (Murillo et al., 2015). *Zic2* is also expressed in the precursor granule neurons in the cerebellar nuclei. Compounds *Zic1/2* mutants show marked cerebellar folial abnormality, the cerebellum is missing a lobule in the anterior vermis and has a truncation of the most posterior lobule (Aruga et al., 2002a).

Zic2 is also involved in axon pathfinding and was reported as the first transcription factor controlling the laterality of optic axons in binocular species. Moreover, this TF controls axon midline avoidance in two other tracts of the CNS: the thalamocortical axons and the spinofugal projections (Escalante et al., 2013). Finally, Zic2 has been also involved in stablishing the topography of ipsilateral retinal ganglion cell axons in the superior colliculus (García-Frigola et al., 2010).

2.1.3. Transcriptional regulation by Zic2

Using classical candidate approaches, several studies revealed some of the Zic2 target genes, such as EphB1 and SERT in retinal ganglion cells, and EphA4 in dorsal spinal cord neurons and Tgif1 in a mouse cerebellar granule cell line (García-Frigola et al, 2008; Escalante et al, 2013; García-Frigola et al., 2010; Ishiguro et al., 2018). More recently, unbiased approaches (ChIP-seq and RNA-seq) have been used to identify other possible Zic2 targets.

One of these studies uses ChIP-seq analysis and Zic2 *shRNAs* functional studies in a mouse embryonic stem cell (mESC) line. In this article, Luo et al propose that Zic2 binds to enhancers of genes implied in pluripotency maintenance acting mainly as a repressor. They find that 80% of Zic2-bound sites are far from the transcription start site (TSS) and have chromatin modification signatures that are known to be in enhancers. They also show that Zic2 interacts with Mbd3, a protein that is part of the NuRD chromatin remodelling complex.

This function was corroborated using *Zic2 shRNA* in this cell line to downregulate Zic2 and measuring crucial pluripotency gene expression (Luo et al., 2015). Based on these experiments, they proposed that Zic2 regulates the chromatin state in ESCs, a step crucial for stem cell specification.

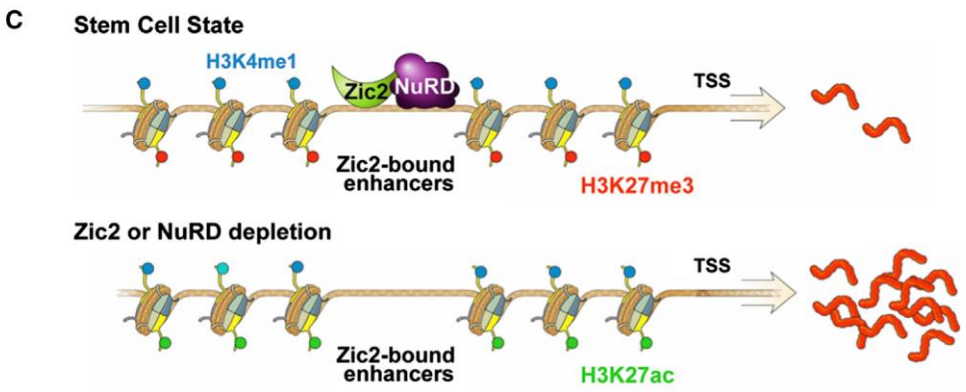

Figure 13. Zic2 and ESC Pluripotency. (C) Model: In the stem cell state (top panel), the zinc finger-containing protein Zic2 functions together with the NuRD repressor complex, setting a poised, yet to be activated state of developmental genes. Knockdown of Zic2 (bottom panel) and/or NuRD subunits leads to de-repression of the same group of developmental genes. Adapted from Luo et al., 2015).

Another Zic2 ChIP-seq analysis was done in mEpiSCs. This cell line is obtained from epiblasts of egg-cylinder stage mouse embryos and is maintained in feeder-free culture conditions supplemented with activin and bFGF (FGF2) (Matsuda et al., 2017). Using this cell line and transfecting it with biotinylated Zic2, they see Zic2 peaks within the 50kb of a transcription start site (TSS),

overlapping extensively with the ones observed for the TF Otx2 and that these overlapping peaks are associated with chromatin modifications present in active or poised enhancers (Matsuda et al., 2017). This study compared also the peaks found in ESCs (Luo et al., 2015) with the ones they obtained in mEpiSCs (Matsuda et al., 2017) and there were less peaks described in ESCs than in EpiSCs, but 80% of the peaks were in common. In this study, they suggest that early binding of Zic2 to the same or nearby enhancer regions in both types of stem cells is needed in ESCs for enhancer priming and later on in EpiSCs for regulating gene transcription.

Another study using CoIP (Complex Immunoprecipitation), found that Zic2 physically interacts with the proteins SMAD2 and SMAD3 in HEK293T cells and that the region responsible for this binding was the N-terminal domain, where the ZOC box is present. By this union, Zic2 represses SMAD-dependent transactivation. These authors also suggest that Zic2 binds to the *foxa2* promoter in the presence of SMAD3 (Houtmeyers et al., 2016).

Zic2 has been proposed to interact with the Wnt signalling pathway. It has been shown that REF-2, the paralog of Zic2 in *C.elegans*, is involved in an atypical regulation of TCF and βcatenin, which repress gene transcription when are complexed together and these genes are activated only when TCF is present but not β-catenin (Murgan et al., 2015). In vertebrates, Zic2 has been proposed to bind to TCF4 to block the transcriptional activation exerted by TCF/βcatenin complexes (Pourebrahim et al., 2011). Furthermore, we have recently found that Zic2, in differentiated neurons, controls an alternative non-canonical Wnt signalling in which cytoplasmic accumulation of β-catenin plays a role in the

repolarization of the growth during axonal navigation (Morenilla-Palao et al., BioRxiv).

Despite all this information, the gene program triggered by Zic2 to control early and late stages of embryonic development causing the HPE phenotype when is absent, is still unclear.

OBJECTIVES

This work aimed to uncover the function of Zic2 in early embryogenesis and define the relevance of this transcription factor and the gene program that regulates in the etiology of HPE5. For this purpose, we defined the following objectives:

1. To characterize the spatiotemporal expression pattern of Zic2 during gastrulation and neurulation stages.
2. To perform functional studies in mouse and chick to precisely define the role of Zic2 during early stages of development.
3. To unveil the molecular program induced by Zic2 in early stages of development.

MATERIALS AND METHODS

Mouse lines

BDF1 mice were obtained by crossing DBA2 and C57/B6 mice.

The Tg(Zic2^{EGFP}) HT146Gsat/Mmcd line (identification number RP23-158G6) was generated by GENSAT (Gong et al., 2003) and obtained from the Mutant Mouse Regional Resource Center (http:// www.mmrrc.org/strains/17260/017260.html). The hypomorphic *Zic2$^{kd/kd}$* mouse line (*Zic2^{tm1Jaru}*) was obtained from the RIKEN repository. Transgenic mice Tg(Zic2EGFP) were crossed with the heterozygous mice for Zic2 (Zic2$^{kd/+}$) and the resulting F1 progeny was crossed [(Zic2$^{+/kd}$; Tg(Zic2 EGFP) X (Zic2$^{+/kd}$; Tg(Zic2EGFP)] to generate [Zic2$^{+/+}$; Tg(Zic2EGFP)] and [Zic2 $^{kd/kd}$; Tg(Zic2 EGFP)] embryos into the same litter. These mouse lines allowed us to visualize, by EGFP fluorescence, both Zic2 cells in the control embryos and cells with no (or very low) levels of Zic2 in the Zic2 mutant embryos. The day of vaginal plug was considered as embryonic day (E). All mouse lines were congenic on a C57BL/6J background and were kept in a timed pregnancy-breeding colony at the Instituto de Neurociencias. The animal protocols were approved by the Institutional Animal Care and Use Committee and met European and Spanish regulations.

Constructs

For gain of function (GOF) experiments of Zic2, pCAG-Zic2 was used at 1µg/µl together with CAG-EGFP at 0’5µg/µl as a reporter to visualize the electroporated cells or CAG-EGFP (0’5µg/µl) with and pCAGGS/ES (1µg/µl) as a control.

Loss of function (LOF) experiments in chicken were performed using an RNA interference pRFPRNAiC cZic2RNAi6 at 3'5µg/µL using the following target sequence AGATCCACAAACGGACGCAC as described in Escalante et al., 2013 or the corresponding control pRFPRNAiC-cRNAi-scramble at the same concentration using the sequence ACGAATGACGCAACCACACG.

Regarding the experiments of Wnt reporter activity in the LOF, the plasmids used for the RNA interference experiments were electroporated together with TopFlash TK d26F (named also as TOPd2GFP) at 0'75µg/µL.

Related to the GOF with the Wnt reporter activity the plasmid pCAG-Zic2 (1 µg/µL), Δ90-CAT-GFP (1 µg/µL) and TopRFP (0'75µg/µL) or the control substituting pCAG-Zic2 by pCAGGS/ES.

In ovo electroporation

Fertilized White Leghorn chicken eggs were incubated at 38ºC until desired developmental stage according to Hamburger and Hamilton (Hamburger and Hamilton, 1951).

Plasmidic DNA solution was injected in the lumen of the neural tube. Platinum electrodes were used with 5 x 10ms pulses at 25V generated with a TSS20 Ovodyne electroporator. Embryos were then incubated for 1-3 days before analysis.

Immunohistochemistry and in situ hybridization

For immunohistochemistry, chicken embryos were fixed overnight at 4ºC and mouse embryos for 2-3 hours (E6.5-E7.5) or 4-5 hours from E8.5 with Paraformaldehyde (PFA) 4% /Phosphate Buffer Saline (PBS) and were washed

twice with PBS. Chicken embryos were sectioned at the vibratome (70μm sections) (VT1000S, Leica) or at the cryostat (40μm sections) (Mnt, Slee). Mouse embryos were sectioned at the cryostat (26μm sections) or were used in whole mount immunohistochemistry. Sections or whole embryo were blocked with Bovine Serum Albumina (BSA) 5%/ PBS-Triton (PBST) (0'5% Triton X-100) for 2 hours at room temperature, then incubated with the correct primary antibody in BSA 3%/PBST (0'3% Triton X-100) overnight at 4ºC. Afterwards, sections/embryos were washed with PBS and incubated with the correct secondary antibody: for 2 hours at room temperature, washed again with PBS and stained with DAPI.

The primary and secondary antibodies used are described in the following tables:

Primary Antibody	Host	Dilution	Reference
Zic2	Rabbit	1/1000	Homemade, described in Brown et al., 2003
GFP	Chicken	1/2000	Aves Labs
RFP/DsRed	Rabbit	1/1000	Clontech,632496
Sox2	Goat	1/500	R&D Systems, AF2018
Sox10	Goat	1/500	Santa Cruz Biotechnology, sc-17342
FoxD3	Goat	1/500	R&D Systems, AF5090
Otx2	Rabbit	1/500	Millipore, AB9566
FoxA2	Mouse	1/500	Abcam, ab60721
T/Brachyury	Goat	1/500	Santa Cruz Biotechnology, sc-17743

Mitf	Mouse	1/200	Abcam, ab12039

Table 2: Primary antibodies used for immunohistochemistry.

Secondary Antibody	Host	Dilution	Reference
Alexa 546 anti-mouse	Donkey	1:1000	Invitrogen, A10036
Alexa 647 anti-mouse	Donkey	1:1000	Invitrogen, A31571
Alexa 546 anti-goat	Donkey	1:1000	Invitrogen, A11056
Alexa 488 anti-rabbit	Donkey	1:1000	Invitrogen, A21206
Alexa 647 anti-rabbit	Donkey	1:1000	Invitrogen, A31573
Alexa 488 anti-chicken	Donkey	1:1000	Jackson Immunoresearch, 703-545-155

Table 3: Secondary antibodies used for immunohistochemistry.

For *In situ hybridization*, RNA probes were synthetized and labeled with digoxigenin (DIG; Roche Diagnostics) in cryostat sections, both mouse and chicken embryos were fixed overnight at 4ºC with PFA 4%/PBS. Chicken embryos were sectioned at 40µm and mouse embryos were sectioned at 26µm and kept at -20ºC until used. Microscope slides with mounted sections were left drying for 4 hours at room temperature, then were washed in PBS, postfixed with PFA4%/PBS and washed again with PBS. Then, sections were incubated with hybridization buffer (50% deionized formamide (Ambion), Salt solution containing 0'2M NaCl, 0'88M Tris-HCl, 0'11M Tris Base, 5mM Na $H_2PO_4x2H_20$, 5mM Na_2HPO_4 at pH7.5, 10% Dextran sulfate (Sigma), 5X SSC pH 4'5, 0'2% t-

RNA(Invitrogen) , 1x Denhardt solution (from 50x stock, Sigma)) for 1 hour and incubated again with the hybridization buffer containing the correct antisense digoxigenin labelled riboprobe (previously denaturalized at 85ºC for 5 min) at 58ºC-64ºC (depending on the temperature of hybridization of the riboprobe) overnight. Afterwards, sections were washed with a solution containing 50% formamide, 2x SSC and 0'5%Tween20 three times at the same temperature of hybridization, washed at room temperature with MABT solution (containing maleic acid, NaOH, NaCl and 0'1% tween20) twice and blocked with 10% sheep serum and 10% blocking reagent in MABT solution for 3 hours. Then, it was incubated with anti-digoxigenin antibody 1/3500 (Invitrogen) overnight at 4ºC in blocking solution again. The day after, sections were washed with MABT (8-10 washes every 30 minutes), washed three times with NTMT (NaCl 100mM, MgCl2 50mM, Tris-HCl pH9.5 100mM, 1% Tween20) and developed with 3'4µg/ml nitroblue etrazolium (NBT) and 3'5µg/ml 5-bromo-4-chloro-3-indolyl phosphate (BCIP) in NTMT. When the signal was the desired, the developing was stopped with PBS (2 washes) and mounted with Mowiol or further processed for immunohistochemistry.

The antisense riboprobes used for this study were: mouse Draxin, chicken Draxin (both probes were provided from Hideaki Tanaka, reported in Zhang et al., 2017).

iDISCO

Whole embryos were fixed overnight at 4ºC with 4%PFA/PBS. Immunolabeling was performed before the clarification, all the steps of immunolabeling were performed at 37ºC. First, embryos were incubated in permeabilization solution

(20%DMSO, Glycine 23g/L in 0'2%Triton X-100/PBS) for half day, then blocked in blocking solution (10% DMSO, 6% donkey serum in 0'2%Triton X-100/PBS) for one day. Then, the embryos were incubated with the primary antibody in PTwH (0'2%Tween20, 0'01%Heparin) /5%DMSO/3% Donkey Serum for one day and washed in PTwH for 4-5 times until the next day. Afterwards they were incubated with secondary antibody in PTwH/3% Donkey Serum for one day and washed in PTwH for 4-5 times until the next day.

For the clarification, embryos were dehydrated in a series of methanol/H_2O: 20%, 40%, 60%, 80%, 100%, 100%; 1hr each at room temperature. Then, incubated 3 hours with shaking in 66% DiChloroMethane (DCM, Sigma 270997-12X100ML) / 33% Methanol, washed in 100% DCM 15 minutes twice (with shaking) to remove the MeOH. Finally, the embryos were incubated in DiBenzyl Ether (DBE, Sigma 108014-1KG) and the tubes were inverted a couple of times to finish mixing the solution. The primary antibodies used here were anti-Zic2 and anti-GFP (described in the table). The secondary antibodies were Alexa 546 donkey anti-rabbit (Invitrogen, A10040) and Alexa 647 goat anti-chicken (Invitrogen, A21449)

Image acquisition

Immunohistochemistry Images were captured with an Olympus FV1000 confocal IX81 microscope/FV10-ASW Software.

In situ hybridization images were taken with a Leica DM 2500 microscope and a DFC7000T Leica camera and the LAS AF software Leica.

Images of iDISCO clarified embryos were taken with the Ultramicroscope II (LaVisionBiotec).

Image analysis

For quantification of Sox10 or FoxD3 cells in [*Zic2*$^{+/+}$,Tg(Zic2EGFP)] and [*Zic2*$^{kd/kd}$,Tg(Zic2EGFP)] embryos, four/five sections were analyzed per embryo and 4/5 embryos were used per genotype. Number of Sox10 and FoxD3cells were quantified per slice, normalizing by the length of the neural tube and the ratio of FoxD3 cells inside the neural tube compared to the total number of cells was obtained. The quantification of GFP were done delineating a ROI outside the neural tube (in the migration zone) and measuring the fluorescence (IntDen Parameter in Fiji) and normalizing by the total fluorescence of the image using a ROI equal in all images.

For the quantification of GFP fluorescence in electroporated chicken embryos two complementary squared areas were delineated along the migratory stream in each section. FI was measured in the area proximal to the dorsal tube (ventromedial pathway) and distal to the neural tube (dorsolateral area). Corrected total area fluorescence was calculated from ImageJ measurements according to the following formula: integrated density (selected area _ mean of background fluorescence).

For the quantification of TOPRFP or TOPd2GFP fluorescence in electroporated chicken embryos a ROI was used delineating the dorsal part of the neural tube, this fluorescence was normalized by the fluorescence of the electroporation with GFP or DsRed and the background fluorescence was subtracted for each channel. 3/5 embryos per condition were used for statistical analysis.

Images of iDISCO clarified embryos were projected in 3D in IMARIS software.

ChIP-seq

BDF1 mice were used for this experiment. E6.5 embryos were dissected from the decidua in cold sterile PBS, generally, 4 litters were dissected the same day, each one containing 8-10 embryos. Embryos were then fixed with fresh 1'1% PFA/PBS for 20 minutes to covalently crosslink proteins to DNA, incubated with glycine 0'14M to quench the unreacted paraformaldehyde for 10minutes and washed with fresh PBS three times every 5 minutes. After that, embryos were lysated with ChroIP lysis buffer (50mM HEPES-KOH pH8'1, 1mM EDTA, 0'5mM EGTA, 140mM NaCl, 10% Glycerol, 0'5% NP40, 0'25% Triton X-100) with proteinase inhibitor cocktail (Roche) and homogenized with a homogeniser of 0'1mL (GPE limited, 20404), leaving them with the lysis solution for 10 minutes shaking on ice. Then, the cell suspension was centrifuged at 600g for 5 min at 4ºC to pellet the nuclei. Nuclei were washed with Chro-IP wash buffer (10mM Tris-HCl pH 8.0, 1mM EDTA, 0'5mM EGTA, 200mM NaCl) 10 minutes shaking on ice and then nuclei were pelleted using the same procedure as before. The pellet was resuspended with SDS lysis buffer (1% SDS, 10mM EDTA, 50mM Tris pH 8.0) and sonicated in a bioruptor 5 cycles (30''on/30''off). Finally, the samples were centrifuged 6 minutes at 13000rpm at room temperature and the supernatant was kept at -80ºC.

For immunoprecipitation, beads were previously blocked with BSA 5% 2 hours at 4ºC with shaking, then were centrifuged 5 minutes at 3000G, washed with Tris-EDTA (TE) and diluted in the same volume of TE, having a mixture 1:1. Then, for each N, 18 pools of embryos were used and they were put together in an Lobind Eppendorf ® (to avoid sample loss) and diluted in 10 times dilution buffer (0'01% SDS, 1'1% Triton X-100, 1'2mM EDTA, 16'7mM Tris-HCl pH8.1, 167mM NaCl),

having 9 tubes per N (Total N=2 per condition). We performed a preclearing step of the samples with the mixture of beads/TE (40µl) for 1 hour at 4ºC with shaking, centrifuging then at 3000g for 1 minute to take the supernatant to a new tube. From each tube (we had 18 tubes) 80µl of sample were taken for the input samples and these were frozen at -80ºC until next step. 3'5ul of Zic2 antibody (Millipore, AB15392) per tube were used to immunoprecipitate at 4ºC overnight. The next day we added 65µl of beads for each immunoprecipitation and we incubated for 1'5 hours at 4ºC shaking, we centrifuged again and kept the pellet that will be the complex of antibody and beads, next we performed a series of washes, each one of 5 minutes, with the following buffers:

-one wash with low salt wash buffer (0'1% SDS, 1% Triton X-100, 2mM EDTA, 20mM Tris HCl ph8'1, 150mM NaCl)

-one wash with high salt wash buffer (0'1%SDS, 1% Triton X-100, 2mM EDTA, 20mM Tris-HCl pH 8'1, 500mM NaCl)

-one wash with LiCl wash buffer (0'25M, 1% IGEPAL-CA630, 1% deoxycholic acid (sodium salt), 1mM EDTA, 10mM Tris pH 8'1)

-two washes TE buffer (10mM Tris-HCl, 1mM EDTA, pH8'0)

Each wash followed by a 1minute centrifugation of 3000g. Then, the samples were kept at 4ºC until the next day. The input samples that were kept at -80ºC the first day, were precipitated with NaCl 1/10, glycogen (100ng/µl) and 2 volumes of Ethanol 100% overnight at -20ºC.

The third day, the inputs were centrifuged 30 minutes, washed once with ethanol 70%, centrifuged 5 minutes and let dry. Meanwhile, the samples were eluted: for that we centrifuge, remove the TE and add 100µl of the elution buffer (1% SDS, 0'1M $NaHCO_3$) and kept it for 15 minutes shaking at 25ºC, then we performed a

centrifugation at 3000rpm and recover the supernatant in a new tube, we repeat again the procedure with the other 100µl of elution buffer and put together the two elutions. We added to the inputs 200µl of elution buffer and to all the samples we added 0'2M NaCl and incubate at 65ºC for 5 hours to reverse the DNA-Protein crosslinks, treated with RNAse A for 30 minutes and with proteinase K for 1'5 hours at 45ºC. Finally, we used the Microchip Diapure columns (Diagenode, C03040001) kit to purify the DNA with spin columns and get the final samples, which we kept at -80ºC until we sent them for sequencing.

ChIP-seq bioinformatic analysis

ChIP-seq was performed in a HiSeq 2000 machine using Flow Cell v3 in single-end configuration (50bp). Quality control of the raw data was performed with FastQC. Additional quality control analyses were performed using the R package Repitools (Statham et al., 2010). (http://www.bioinformatics.babraham.ac.uk/projects/fastqc/). Libraries were trimmed from adapters and low-quality bases using Trimmomatic v0.36 (Bolger et al., 2014) and were aligned to the mouse genome (Mus_musculus.GRCm.38.83) using bowtie2 (v2.2.9) (Langmead and Salzberg, 2012) and further processed using Samtools (v1.3.1) (Li et al., 2009b) and bedtools (v2.25.0) (Quinlan and Hall, 2010) Peak calling for Zic2-ChIP-seq was performed using MACS2 (v2.1) (Zhang et al., 2008) with the following parameters: -q 0.01 --nomodel --extsize 131, and -p 1.00e-05 –bw 300 -m 10,30. Read counts on aligned bam files were obtained using featureCounts (Rsubread v1.22.3) (Liao et al., 2014). Differential binding analysis of ChIP-Seq peak data was calculated by DiffBind (Stark R, Brown G, 2011) and csaw (Lun ATL, Smyth

GK, 2016). Further data processing was performed with custom scripts in the R programming language (https://cran.r-project.org/)(v3.6.0“Planting of a Tree”). De novo DNA motif discovery at Zic2-bound regions was performed using MEME suiteand MEME suite (Bailey et al., 2009) in an area of 151 bp (average genomic fragment length) around each peak summit. GO enrichment analyses were performed using the platform Panther (Mi et al., 2019a), with Fisher´s exact test and with and with the Benjamini-Hochberg False Discovery Rate for multiple test correction for the nominal p values. GO terms were obtained using the following filters: P adj < 0.1, ratio enrichment > 2, number of genes enriched term > 3, number of GO family group genes between 3 and 2000. Heatmaps of ChIP-seq read density and aggregate density plots were performed using SeqMiner (v1.3.4) (Ye et al., 2011) and R custom scripts. ChIP-seq peaks were annotated using ChIPpeakAnno (Zhu et al., 2010). ChIP-seq tracks were visualized using IGV (v2.3.72) (Robinson et al., 2011).

Sample Library type Nº of reads Type pf sequencing Read length

Input_E6_A ChIP DNA 65266394 Single end 50

Input_E6_B ChIP DNA 77255825 Single end 50

Zic2_E6_A ChIP DNA 66594058 Single end 50

Zic2_E6_B ChIP DNA 81770692 Single end 50

Input_E8_A ChIP DNA 85329966 Single end 50

Input_E8_B ChIP DNA 88252911 Single end 50

Zic2_E8_A ChIP DNA 82017718 Single end 50

Zic2_E8_B ChIP DNA 86772494 Single end 50

RNA-seq

Mouse embryos *Zic2*$^{kd/kd}$ and its control littermates *Zic*$^{+/+}$ were used at E6.5 for RNA extraction. Embryos were dissected from the decidua in cold sterile PBS and were immediately frozen in dry ice and kept at -80ºC until a sufficient pool of embryos was obtained. The ectoplacental cone was dissected apart for genotyping. A pool of 4 embryos for each N and a total of 3N per genotype were used. For RNA extraction, ARN ARCTURUS® PicoPure® (KIT0204) kit was used, RNA was kept at -80ºC until sent for sequencing

***RNA*-seq bioinformatic analysis**

ChIP-seq was performed in a HiSeq 2000 machine using Flow Cell v3 in single-end configuration (50bp). Quality control of the raw data was performed with FastQC. Additional quality control analyses were performed using the R package Repitools (Statham et al., 2010). (http://www.bioinformatics.babraham.ac.uk/projects/fastqc/). Libraries were trimmed from adapters and low-quality bases using Trimmomatic v0.36 (Bolger et al., 2014) and were aligned to the mouse genome (Mus_musculus.GRCm.38.83) using bowtie2 (v2.2.9) (Langmead and Salzberg, 2012) and further processed using Samtools (v1.3.1) (Li et al., 2009b) and bedtools (v2.25.0) (Quinlan and Hall, 2010) Peak calling for Zic2-ChIP-seq was performed using MACS2 (v2.1) (Zhang et al., 2008) with the following parameters: -q 0.01 --nomodel --extsize 131, and -p 1.00e-05 –bw 300 -m 10,30. Read counts on aligned bam files were obtained using featureCounts (Rsubread v1.22.3) (Liao et al., 2014). Differential binding analysis of ChIP-Seq peak data was calculated by DiffBind (Stark R, Brown G, 2011) and csaw (Lun ATL, Smyth

GK, 2016). Further data processing was performed with custom scripts in the R programming language (https://cran.r-project.org/) (v3.6.0“Planting of a Tree”). De novo DNA motif discovery at Zic2-bound regions was performed using MEME suiteand MEME suite (Bailey et al., 2009) in an area of 151 bp (average genomic fragment length) around each peak summit. GO enrichment analyses were performed using the platform Panther (Mi et al., 2019a), with Fisher´s exact test and with and with the Benjamini-Hochberg False Discovery Rate for multiple test correction for the nominal p values. GO terms were obtained using the following filters: P adj < 0.1, ratio enrichment > 2, number of genes enriched term > 3, number of GO family group genes between 3 and 2000. Heatmaps of ChIP-seq read density and aggregate density plots were performed using SeqMiner (v1.3.4) (Ye et al., 2011) and R custom scripts. ChIP-seq peaks were annotated using ChIPpeakAnno (Zhu et al., 2010). ChIP-seq tracks were visualized using IGV (v2.3.72) (Robinson et al., 2011).

Sample Library type Nº of reads Type pf sequencing Read length

Input_E6_A ChIP DNA 65266394 Single end 50

Input_E6_B ChIP DNA 77255825 Single end 50

Zic2_E6_A ChIP DNA 66594058 Single end 50

Zic2_E6_B ChIP DNA 81770692 Single end 50

Input_E8_A ChIP DNA 85329966 Single end 50

Input_E8_B ChIP DNA 88252911 Single end 50

Zic2_E8_A ChIP DNA 82017718 Single end 50

Zic2_E8_B ChIP DNA 86772494 Single end 50

Both RNA-seq and ChIP-seq bioinformatic analysis were performed by Mª Teresa López Cascales.

Quantitative and statistical analysis

All quantifications were presented as the mean_SEM. Minimal statistical significance was fixed at p_0.05 for the results of the Student's t test and are represented in the figures as follows: *p _ 0.05; **p _ 0.01; ***p _ 0.001.

RESULTS

1. Zic2 is expressed in the mouse epiblast during gastrulation.

Zic2 protein was reported to be expressed as soon as E3.5 in the ICM of blastocysts although this staining is faint and not nuclear (Brown and Brown, 2009). Later, although the expression of *Zic2 mRNA* has been detected in pregastrula stages (E5.5) in mouse embryos (Elms et al., 2004), Zic2 protein expression has not been characterized.

To precisely define the spatiotemporal expression pattern of Zic2 during gastrulation, we performed immunohistochemistry with an antibody specific to Zic2 in E6.0-E7.5 embryos. At E6.0, we found very few nuclei stained for Zic2 **(Figure 14A)**. In E6.5 embryos, a higher number of Zic2 positive cells were detected **(Figure 14B)**, which partially colocalized with the epiblast marker Sox2 **(Figure 14C)**. Interestingly, those cells positive for Zic2 but negative for Sox2 had higher sizes and bigger nuclei **(arrow in Figure 14C)**. At E7.0 we distinguished two type of Zic2 expressing cells, a population with high levels of Zic2 and another with low levels **(Figure 14D)**. A distinctive feature of cells undergoing EMT is the downregulation of E-cadherin. Intriguingly, when we performed triple immunostaining for Zic2, Sox2 and E-cadherin, we observed that cells expressing high levels of Zic2 that were negative for Sox2, expressed very faint levels of E-cadherin, suggesting that these cells are undergoing EMT **(Figure 14F, G)**.

To track Zic2 cells during early developmental stages we used a previously reported mouse line [Tg($Zic2^{EGFP}$)] that allows fate-mapping of Zic2 cells (Escalante et al., 2013, Murillo et al., 2015; Marcucci and Murcia-Belmonte, 2016). In E6.5 Tg($Zic2^{EGFP}$) embryos, we observed low EGFP staining (data not shown). At E7.0, although more GFP protein than Zic2 positive cells were

observed reflecting that EGFP is more stable than Zic2, the two stainings mostly colocalized **(Figure 14E, I)**. Typical markers of the three germ layers (FoxA2 for endoderm, Brachyury/T for mesoderm and Otx2 for ectoderm) may be normally detected at E7.5. Co-immunostaining of these markers with Zic2 and/or EGFP in Tg(Zic2^{EGFP}) embryos revealed colocalization of Zic2 positive cells with both Brachyury and FoxA2 cells **(Figure 14J-L)**, although there were some Zic2 positive cells negative for FoxA2 and Brachyury as well as FoxA2 or Brachyury cells that were negative for Zic2. Although cells with the highest levels of EGFP did not express Otx2, few cells co-expressed Otx2 and EGFP suggesting that they also expressed Zic2 at some point **(Figure 14M, N)**. Together with the observation that the majority of the epiblast cells express EGFP at different levels, these results indicate that most, if not all, the cells in the epiblast expressed Zic2 at some point. By the time that cells are allocated in their respective layers Zic2 is downregulated.

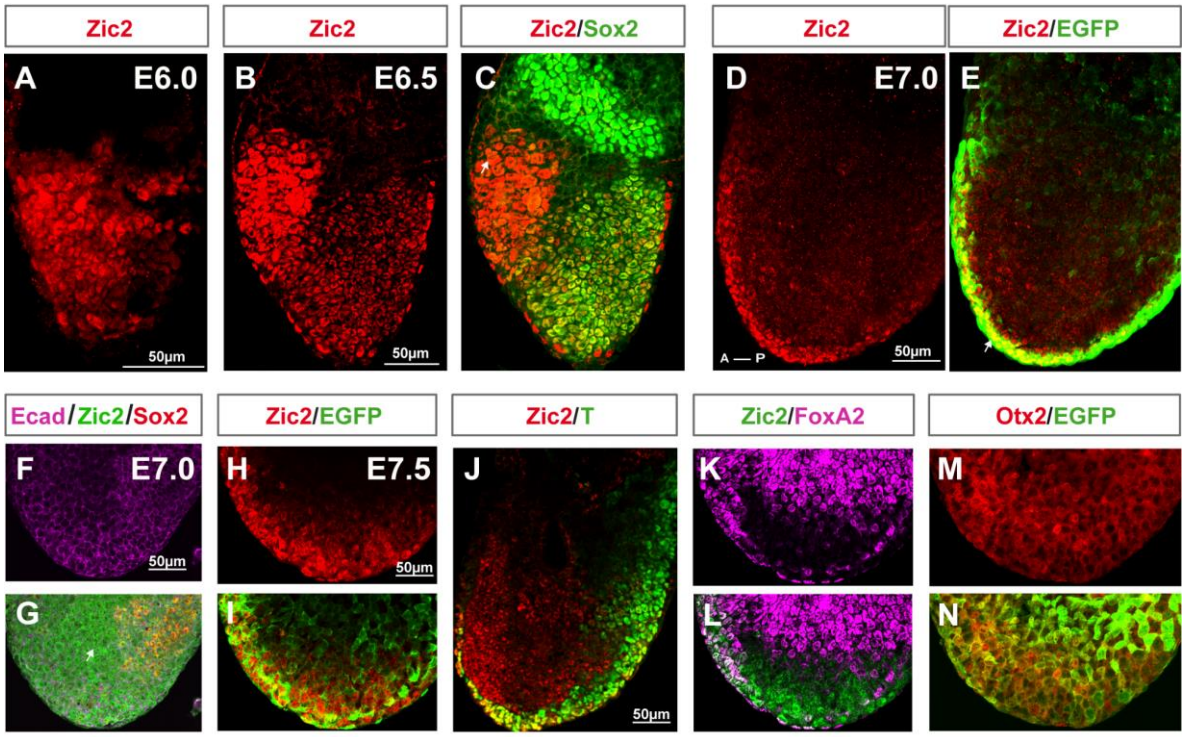

Figure 14. Zic2 expression in the mouse epiblast during gastrulation. (A,B,D,H) Immunohistochemistry for Zic2 at different stages from E6.0 to E7.5. (C) Double immunohistochemistry for Zic2/Sox2 at E6.5 (E,I) Double immunohistochemistry for Zic2/EGFP at E7.0 (E) and at E7.5 (I). (F,G) Triple immunohistochemistry for E-cadherin, Zic2 and Sox2. Note that $Zic2^{+}/Sox2^{-}$ big cells are negative for E-cadherin (arrows in G).(J-L) Double immunohistochemistry for Zic2 and markers for mesoderm (T also called Brachyury) (J) and endoderm (FoxA2) (K,L) at E7.5. (M,N) Double immunohistochemistry for EGFP and the marker for neuroectoderm Otx2 at E7.5.

2. *Zic2*$^{kd/kd}$ mutant embryos show defects in the formation of the notochord

To determine whether downregulation of Zic2 affects the differentiation of the cells to the germ layers we analysed the expression of the different markers in *Zic2*$^{kd/kd}$ embryos and found that in these mutants, epiblast cells appear to express correctly endoderm and mesoderm markers **(Figure 15A-D)**.

In the kumba mutants (*Zic2*$^{ku/ku}$) failures in the specification of the node leading to defects in the formation of the anterior notochord have been reported (Warr et al., 2008). By performing immunohistochemistry for Brachyury (T) to label the notochord in whole mount E8.5 embryos we confirmed that this phenotype is also exhibited by the *Zic2*$^{kd/kd}$ mutants **(Figure 15E, F)**.

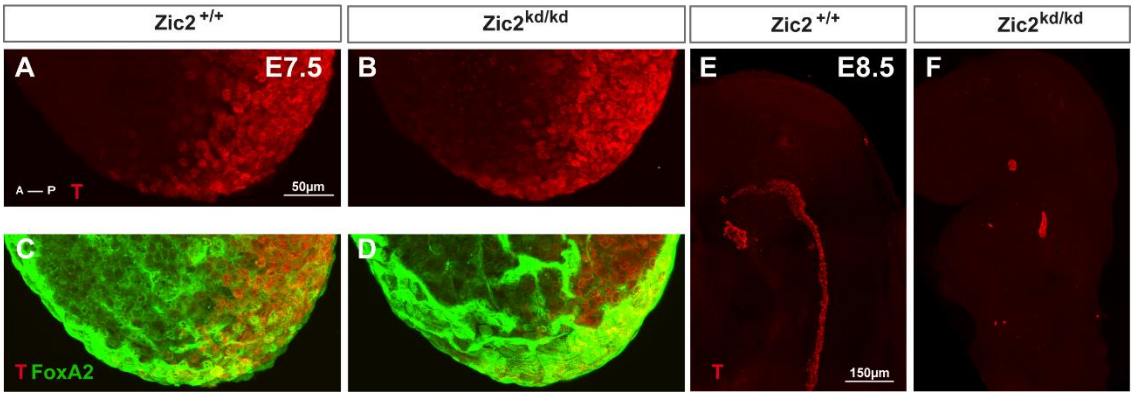

Figure 15. Epiblast cells from *Zic2*$^{kd/kd}$ differentiate correctly to the germ layers but present defects in the notochord formation. (A-D). Double whole mount immunohistochemistry of FoxA2 (endoderm) and T (mesoderm) in E7.5 of *Zic2*$^{kd/kd}$ and control littermates. (E, F) Whole mount immunohistochemistry in E8.5 of *Zic2*$^{kd/kd}$ and control littermates.

3. Zic2 is expressed in premigratory neural crest cells.

The first phenotype we detected in *Zic2*$^{kd/kd}$ was during the formation of the notochord. However, Zic2 is not expressed in the notochord and in the kumba mutants this phenotype was attributed to defects in the specification of the node (Warr et al., 2008). Our detailed characterization of Zic2 positive cells during gastrulation suggested that rather than provoking defects in the specification of any particular germ layer or notochord cells **(Figure 16A-D)**, Zic2 is involved in the EMT that epiblast cells undergo during the differentiation process. Unfortunately, mouse gastrula embryos are not easy to manipulate and therefore, we decided to analyse Zic2 expression in more tractable cells undergoing EMT, such as NCCs when they delaminate from the dorsal neural tube.

The expression of *Zic2 mRNA* in NCCs has been described in several organisms, including mouse and zebrafish (Teslaa et al., 2013; Elms et al., 2003), but Zic2 protein expression remained unknown. Thus, we performed immunostainings with a specific antibody for Zic2 at two crucial points of NC

formation, E8.0 when cells are starting to delaminate and E9.5, when most of the cells are already migrating.

In Tg(Zic2^{EGFP}) E8.0 embryos, we found Zic2 positive cells in the dorsal neural tube and in the somites **(Figure 16A)** and EGFP colocalized with Zic2. However, Zic2 cells located outside the neural tube, previously described as sclerotome cells (Gaston-Massuet et al., 2005), were not positive for EGFP **(Figure 16D, I)** likely indicating that this transgenic line does not fully recapitulate the expression of Zic2.

To further characterize Zic2 expression in dorsal neural tube cells, we used markers for premigratory NCCs (FoxD3) and migratory NCCs (Sox10). At E8.0, immunostaining for FoxD3 in Tg(Zic2^{EGFP}) embryos demonstrated that Zic2 is expressed in premigratory NCCs **(Figure 16C, E)**. At E9.5, Zic2 expression at the dorsal neural tube declined although, it could be still detected in the sclerotome **(Figure 16F)**. Many EGFP cells located outside the tube were positive for the migratory NCCs marker Sox10 **(Figure 16G, H, J)**, but they were negative for Zic2 **(Figure 16F, I)**. EGFP cells travelled through both the dorsolateral (DL) and the ventromedial (VM) pathways **(Figure 16J)**. These results demonstrated that Sox10 positive cells migrating through the DL and the VM tracts derive from premigratory Zic2 NCCs and that Zic2 expression is downregulated as soon as they leave the tube. Therefore, Zic2 is transiently expressed in premigratory NCCs and it is turned off as they exit the tube to initiate their migration.

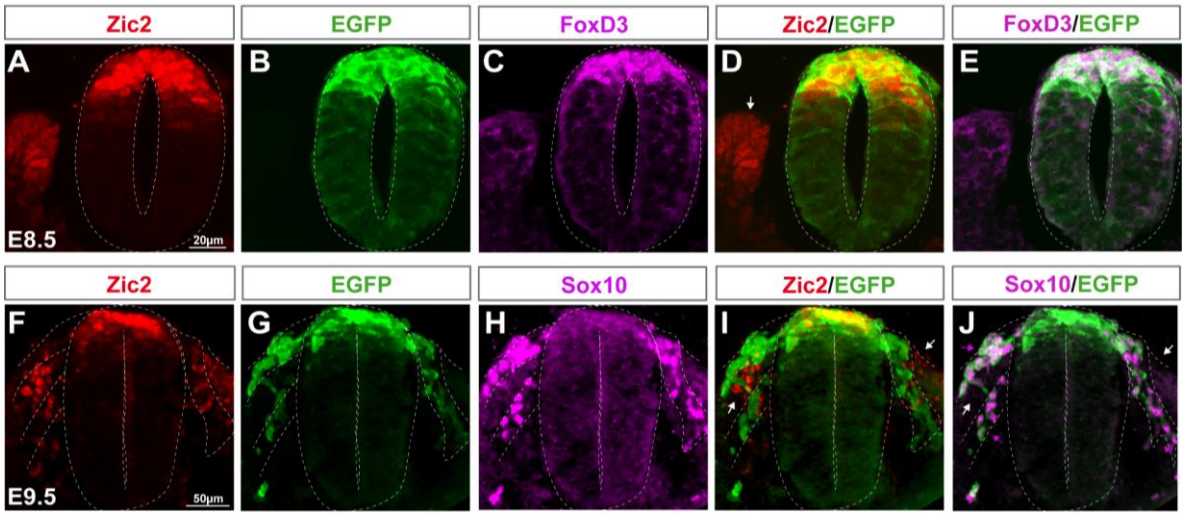

Figure 16. Zic2 is expressed in premigratory NC cells. Triple immunohistochemistry for Zic2, GFP and markers for premigratory neural crest cells (FoxD3) at E8.5 (A-E) or migratory neural crest cells (Sox10) at E9.5 (F-J) in transverse sections from the neural tube of Zic2 reporter mice [Tg(Zic2^{EGFP})]. Note that cells positive for Zic2 outside the neural tube are not EGFP positive (arrow in D). In contrast, inside the tube Zic2 cells are EGFP and also positive for FoxD3. Note that cells positive for Zic2 outside the neural tube are not EGFP positive (white arrows in I) or Sox10 positive (white arrows in J). In contrast, EGFP cells outside the neural tube are positive for Sox10 (pink arrows in J).

4. Zic2 binds to many genomic regions near or in the TSSs

To define the Zic2 bound-genomic regions in pluripotent cells *in vivo*, we investigated the binding profile of Zic2 in gastrula and neural crest cells. For that, we collected E6 and E8 mouse embryos and performed ChIP-seq assays using Zic2 specific antibodies. We found a much larger number of Zic2-peaks at E6 (7192) than at E8 (4736) (**Figure 17A**). Most peaks were located into the TSS or in intragenic regions (67,5% in E6 and 77,5% in E8) (**Figure 17B**), contrasting with the previously reported scenario in an embryonic stem cell (ESC) line in which only 21% of the Zic2-peaks were found in TSS or intragenic regions and more than 50% were in intergenic regions (Luo et al., 2015). In addition, peaks located in intergenic regions were mostly found into the 50kb upstream the TSS

(**Figure 17B**), coinciding previous results performed in Epi-like cells (Epi-SCs) differentiated *in vitro* (Matsuda et al., 2017).

From the Zic2-peaks that can be associated to genes (according to UCSC genome TxDb.Mmusculus.UCSC.mm10.knownGene), 4057 were common in E6 and E8, while 2680 were exclusively found in E6 embryos (**Figure 17C**) indicating that a large fraction of Zic2 peaks in E8 were already present in E6. A small subset of peaks (453) were exclusively found in E8 but not earlier. Panther pathways analysis of the genes associated to the Zic2 peaks revealed that an elevated number of them were related to the Wnt, PDGF, CCKR and EGF/TGF-β signaling pathways or with angiogenesis **(Figure 17D, E)**, suggesting that Zic2 has the potential to regulate all these pathways. Interestingly, while a large number of peaks were located in intergenic regions among those exclusively found at E6 **(Figure 17D)**, the distribution of common peaks was clearly biased to the TSSs **(Figure 17E)**. However, Panther pathway analysis focused on peaks distribution, revealed that peaks associated to a particular pathway do not concentrate at specific locations but are distributed all across the genome at both stages.

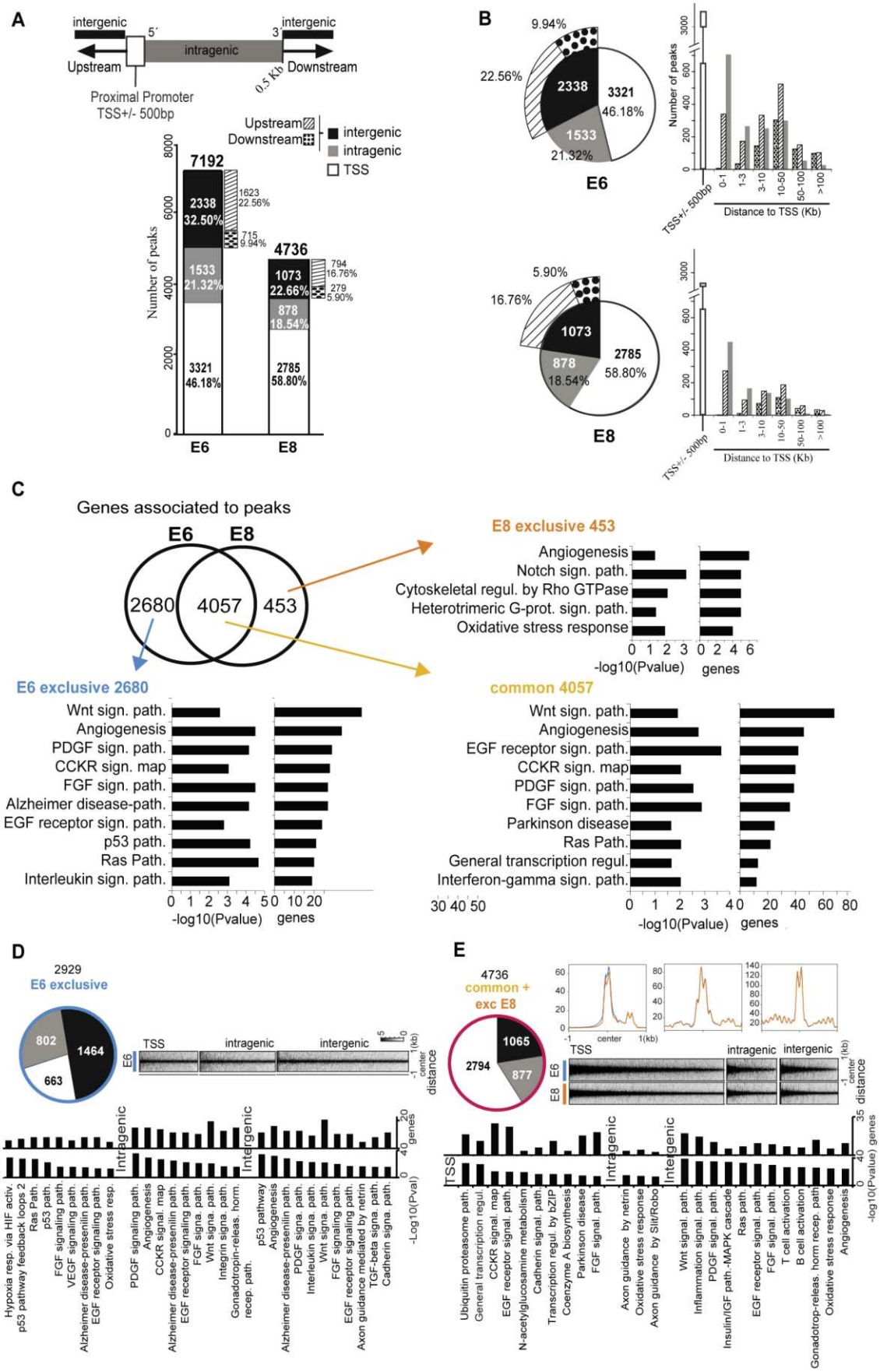
A
intergenic
5´
3
intergenic
intragenic
Upstream
0.5 Kb
Downstream
Proximal Promoter
TSS+/- 500bp
Upstream
Downstream
intergenic
intragenic
TSS
Number of peaks
7192
2338
32.50%
1623
22.56%
715
9.94%
1533
21.32%
3321
46.18%
4736
1073
22.66%
794
16.76%
279
5.90%
878
18.54%
2785
58.80%
E6
E8
B
9.94%
22.56%
2338
3321
46.18%
1533
21.32%
E6
Number of peaks
0-1
1-3
3-10
10-50
50-100
>100
TSS+/- 500bp
Distance to TSS (Kb)
5.90%
16.76%
1073
2785
58.80%
878
18.54%
E8
C
Genes associated to peaks
E6
E8
2680
4057
453
E8 exclusive 453
Angiogenesis
Notch sign. path.
Cytoskeletal regul. by Rho GTPase
Heterotrimeric G-prot. sign. path.
Oxidative stress response
-log10(Pvalue)
genes
E6 exclusive 2680
Wnt sign. path.
Angiogenesis
PDGF sign. path.
CCKR sign. map
FGF sign. path.
Alzheimer disease-path.
EGF receptor sign. path.
p53 path.
Ras Path.
Interleukin sign. path.
-log10(Pvalue)
genes
common 4057
Wnt sign. path.
Angiogenesis
EGF receptor sign. path.
CCKR sign. map
PDGF sign. path.
FGF sign. path.
Parkinson disease
Ras Path.
General transcription regul.
Interferon-gamma sign. path.
-log10(Pvalue)
genes
D
2929
E6 exclusive
802
1464
663
TSS
intragenic
intergenic
E6
distance
Intragenic
Intergenic
genes
-Log10(Pval)
Hypoxia resp. via HIF activ.
p53 pathway feedback loops 2
Ras Path.
p53 path.
FGF signaling path.
VEGF signaling path.
Alzheimer disease-presenilin path.
EGF receptor signaling path.
Oxidative stress resp.
PDGF signaling path.
Angiogenesis
CCKR signal. map
Alzheimer disease-presenilin path.
EGF receptor signaling path.
FGF signa. path.
Wnt signa. path.
Integrin signa. path.
Gonadotropin-releas. horm. recep. path.
p53 pathway
Angiogenesis
Alzheimer disease-presenilin path.
PDGF signa. path.
Interleukin signa. path.
Wnt signa. path.
FGF signaling path.
EGF receptor signaling path.
Axon guidance mediated by netrin
TGF-beta signa. path.
Cadherin signa. path.
E
4736
common +
exc E8
1065
2794
877
TSS
intragenic
intergenic
E6
E8
distance
Intragenic
Intergenic
genes
-log10(Pvalue)
Ubiquitin proteasome path.
General transcription regul.
CCKR signal. map
EGF receptor signal. path.
N-acetylglucosamine metabolism
Cadherin signal. path.
Transcription regul. by bZIP
Coenzyme A biosynthesis
Parkinson disease
FGF signal. path.
Axon guidance by netrin
Oxidative stress response
Axon guidance by Slit/Robo
Wnt signal. path.
Inflammation signal. path.
PDGF signal. path.
Insulin/IGF path.-MAPK cascade
Ras path.
EGF receptor signal. path.
FGF signal. path.
T cell activation
B cell activation
Gonadotrop-releas. horm recep. path
Oxidative stress response
Angiogenesis

Figure 17. Zic2 regulates different pathways. (A) Bar chart of the genomic location distribution of ChIP-seq peaks in E6 and E8 embryos. (B) Pie charts of the genomic location distribution of ChIP-seq peaks at both stages. Graph represent peaks distance to the TSS. (C) ChIPpeakAnno annotate peaks to genes and can be visualized with a venn diagram that determines the overlapping peaks from different ChIP-seq experiments. Panther pathways analysis for each specific group is shown. (D) Pie chart of the genomic location distribution of ChIP-seq E6 specific peaks (2929). Row-linked heatmaps show RPKM normalized number of reads across a 1kb genomic interval in to the midpoint of enriched regions at E6 specific peaks. Heatmaps were generated from merged biological replicate pairs for each sample, and divided by K-means clustering representation (k-means=3; TSS, intragenic, intergenic). Regions are sorted in descending order based on average row tag density for Zic2 ChIP-seq. Each row represents a gene. Black and white reflect high and low read densities (gray scale), respectively. (E) Pie chart of the genomic location distribution of ChIP-seq common (4263) + E8 specific peaks (473). Row-linked heatmaps show RPKM normalized number of reads across a 1kb genomic interval in to the midpoint of enriched regions at common peaks (E6 + E8). Composite plots on top of each cluster heatmap quantify the normalized tag density generated. Composite plots and Enrichment analysis were generated with equal methodology than in D. Enrichment analysis with Panther pathways database for peaks is shown for each cluster.

5. Zic2 is required to allow NCCs delamination

Then, to define the regulatory networks controlled by Zic2 during gastrulation and neurulation, we compared the transcriptomes of E6 and E8 $Zic2^{kd/kd}$ mutant embryos with their control counterparts. We found that the Zic2 locus remains active and is normally transcribed in E6 embryos. However, the produced transcripts are, as expected, aberrant and include extra sequences that interfere with their translation. As a result, we detected a very robust downregulation at the protein level and almost no cells in $Zic2^{kd/kd}$ E6 embryos were identified as Zic2-positive by immunohistochemistry (**Figure 18A, B**). Despite the severe loss of Zic2 proteins, we did not retrieve significant differences in the transcriptome of E6 mutant embryos when compared to their controls (**Figure 18C, D**), suggesting that Zic2 does not play a prominent role regulating transcription at this early stage or, alternatively, the number of cells expressing Zic2 at this stage is too low to observe a significant impact in the gastrula total RNA after removing Zic2 and consequently the changes would be diluted because control samples contain few Zic2 cells. This situation radically changes at E8. At this stage, we detected 1097

differentially expressed genes (DEG) including 272 upregulations and 825 downregulations and principal component analyses (PCA) revealed a good separation between mutant and control samples (**Figure 18C-E**). As expected, *Zic2* was the most downregulated gene in Zic2 E8 mutant embryos.

Combination of the ChIP-seq and RNA-seq analysis revealed that Zic2 directly binds to the regulatory sequences of a high percentage (42%) of the DEG genes, and showed significant overlap between the studies (*p*-value = 2.23^{e-143}) (**Figure 18F**). In most of the DEG, Zic2 peaks were found in or near the TSS (**Figure 18G**).

Associated to these differences in gene expression detected at neurulation stages, we also observed a strong phenotype in E8 $Zic2^{kd/kd}$::Tg(*Zic2*^{EGFP}) embryos derived from $Zic2^{+/kd}$ mice crossed with the Tg(*Zic2*^{EGFP}) reporter line. EGFP cells migrate in an stereotyped manner through the mesenchymal surface in wholemount preparations of control $Zic2^{+/+}$::Tg(*Zic2*^{EGFP}) embryos (**Figure 18H, J**), contrasting with Zic2 mutants where very few EGFP cells were detected in the dorsal surface (**Figure 18I, K**). In transverse sections we observed an accumulation of EGFP cells in the dorsal neural tube in the mutants compared to the controls (**Figure 18L, M, P**). As previously reported for the kumba mutants, we observed an overall reduction in the expression of FoxD3 in the $Zic2^{kd/kd}$ mutants, but in addition, we noticed that the ratio of FoxD3 cells inside versus outside the tube was higher in the mutants compared to the controls (**Figure 18N, O, Q**). This result indicated again an aberrant accumulation of NCCs into the tube. In agreement with these observations, we found a reduced number of migratory Sox10/EGFP cells in the mesenchyme of Zic2 mutants both in wholemount embryos and in sections (**Figure 18R-V**). These results suggested that a large

majority of NCCs do not delaminate and remain inside the tube in the Zic2$^{kd/kd}$ mutants.

Consistent with this result, previous experiments also performed in our laboratory (by Gerald Muça) showed that temporal downregulation of Zic2 by in ovo electroporation of Zic2 shRNAs in chick embryos at the moment that NCCs are leaving the tube (HH10/12), lead to a significant decrease in the number of NCCs at the dorsal mesenchyme compared to the controls. As in mice, both the DL and the VM pathways were dramatically affected at E3 and one day later the number of EGFP in the dorsal root ganglia (DRG) was also significantly reduced.

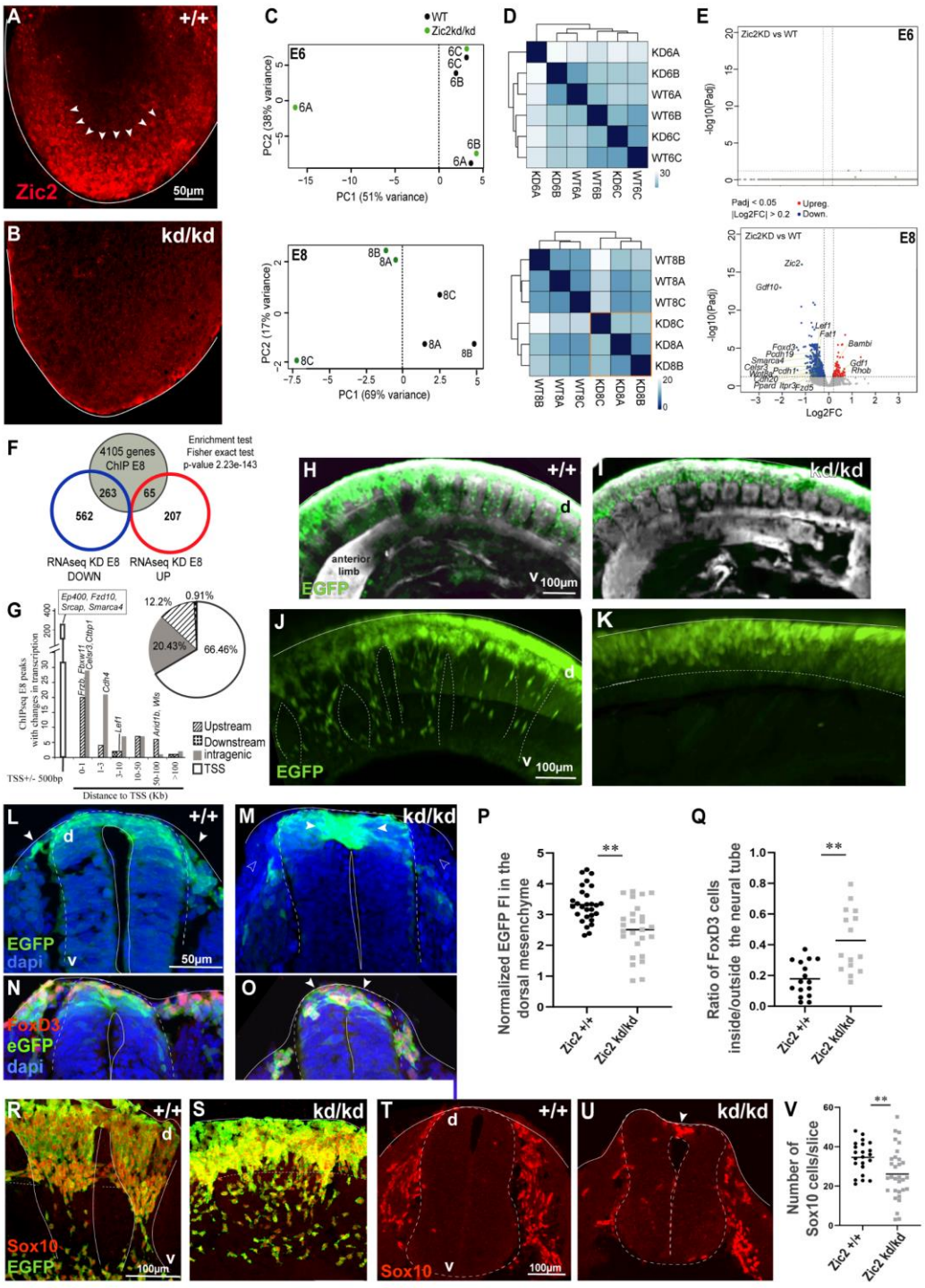

Figure 18. Zic2 is essential for neural crest cells exit. (A, B) Zic2 immunostaining in E7.0 Zic2$^{kd/kd}$ and littermate control (Zic2$^{+/+}$) embryos. (C) Principal component analysis (PCA) of pools of E6 and E8 embryos revealed differential gene expression in Zic2 mutants at the late but not the early stage compared to the controls. (D) Heatmap of distance matrix provides an overview of similarities and dissimilarities between samples according to hierarchical clustering. (E) Volcano plots show the significance value of differential expression genes after DESeq2 analysis in the transcriptome of E6.0 and E8.0 samples. (F) Overlap between Zic2-genes (4736 peaks, 4433 genes) and transcripts found in E8 embryos that are either downregulated (825 transcripts) or upregulated (272 transcripts). Fisher exact test p-value 2.23e-143 indicates significant overlap.

(G) The pie chart despite the distribution of Zic2 peaks associated to DEG genes in E8 Zic2 mutant embryos. Note that in almost 66.5% of the DEG Zic2 peaks locate in the TSS. Bar graph shows that the rest Zic2 peaks associated to DEG mostly locate into the 50kb from the TSS. (H-K) Representative images of wholemount immunohistochemistry in E9.5 Tg($Zic2^{EGFP}$)::$Zic2^{kd/kd}$ embryos and control littermates reveal no EGFP cells migrating in the mutants contrasting to the controls in which EGFP cells were visualized migrating in a segmented manner. (L, M) Representative images of transverse sections from E8.5 $Zic2^{kd/kd}$::Tg($Zic2^{EGFP}$) embryos and control littermates. (N, O) FoxD3 immunostaining in transverse sections from E8.5 $Zic2^{kd/kd}$::Tg($Zic2^{EGFP}$) embryos and control littermates. (P) Quantification of GFP fluorescence intensity in the dorsal mesenchyme of $Zic2^{kd/kd}$::Tg($Zic2^{EGFP}$) embryos and control $Zic2^{+/+}$ ::Tg($Zic2^{EGFP}$) littermates (N=4 embryos/genotype and a minimum of 5 slices/embryo). (Q) Quantification of FoxD3 cells inside the neural tube compared to the total number of Fox3 cells in Zic2 mutants and controls (N=5 embryos/genotype and a minimum of 5 slices/embryo). (R, S) Representative images showing double immunohistochemistry for Zic2 and Sox10 in longitudinal sections from E11.5 $Zic2^{kd/kd}$::Tg($Zic2^{EGFP}$) embryos and control littermates. (T,U) Sox10 immunostaining in transverse sections from E10.5 $Zic2^{kd/kd}$::Tg($Zic2^{EGFP}$) embryos and control littermates. Some cells accumulate in the dorsal part in the Zic2kd/kd::Tg(Zic2EGFP) embryos (white arrowshead) (V) Quantification of the number of Sox10 cells in the $Zic2^{kd/kd}$ compared to $Zic2^{+/+}$ embryos (N=5 embryos/genotype and a minimum of 5 slices/embryo).

6. Zic2 blocks the canonical Wnt signalling pathway in NCCs

To precisely define the gene programs regulated by Zic2 in NCCs, we carried out Panther Pathway enrichment analysis from the RNA-seq dataset from E8 embryos and observed again that a significant number of DEG genes belong to the Wnt signaling pathway (**Figure 19A**). When combined with ChIP-seq data set from E8 embryos the Wnt pathway was highly enriched (**Figure 19A**), indicating that Zic2 has a direct effect on the regulation of this pathway.

The analysis of the Wnt pathway at Reactome using Gene Set Enrichment Analysis (GSEA) revealed both the downregulation and upregulation of many genes in this pathway (**Figure 19B**). Most of the DEG found in this pathway had a Zic2-peak into or near the TSS although not Zic2 peaks associated were found in some cases (**Figure 19C**), implying that Zic2 does not regulate it directly or controls its regulation through enhancer sequences that cannot be associated to that particular gene because are located too far away. To determine whether Zic2 regulation of genes related to Wnt signaling leads to a net activation or repression

of the pathway in NCCs, we performed loss-of-function by *in ovo* electroporation experiments in chicken because it allows the targeting of NCCs.

Plasmids bearing Zic2 or scramble *shRNAs* were electroporated together with a plasmid that encodes for a Wnt-responsive reporter that drives the expression of a non-stable form of GFP (Top-d2GFP). Upon activation of the canonical Wnt signaling, β-catenin translocates to the nucleus and forms a complex with the transcription factor TCF that recognizes the TCF motif present in the plasmid and activates d2GFP transcription (Rabadán et al., 2016). d2GFP is a non-stable form of GFP and as a consequence, only those cells with the Wnt pathway activated in that particular moment are visualized. Embryos electroporated with Zic2 *shRNAs* showed an increase in the number of cells with the Wnt canonical pathway activated (**Figure 19D-F**), indicating that Zic2 is actually required to repress the activation of the canonical Wnt pathway in NCCs.

We then performed the converse Zic2 gain-of-function experiment. Because electroporation of Topd2GFP plasmids in control embryos revealed that only few NCCs into the tube have the Wnt pathway activated at the same time at this stage (**Figure 19D-F**), we thought that a repressive effect of Zic2 on the Wnt pathway would be difficult to detect using this reporter. Therefore, to better visualize the repression of the Wnt pathway after Zic2 induction, we utilized a plasmid encoding a more stable reporter form (Top-RFP). At the same time, we artificially activated the Wnt pathway through the ectopic expression of a non-degradable form of βcatenin (Δ90βcat). In these conditions, red fluorescence levels were significantly reduced in the dorsal tube of embryos expressing Zic2 compared to the controls (**Figure 19G-I**), demonstrating that Zic2 is able to inactivate the canonical Wnt signaling in NCCs before they leave the neural tube.

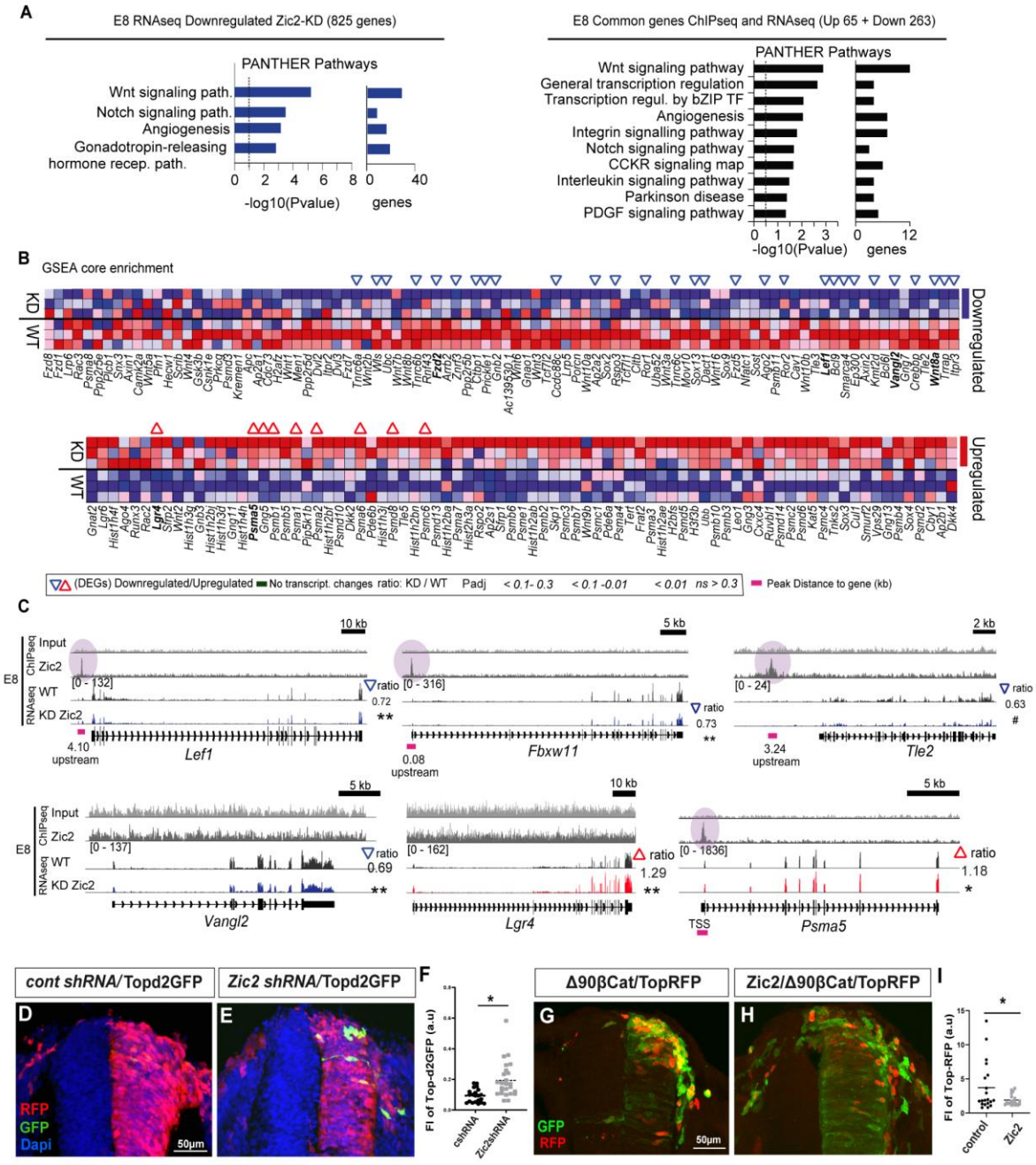

Figure 19. Zic2 regulates many genes from the Wnt signaling pathway. (A) Enrichment analysis with Panther Pathways database in the RNA-seq downregulated genes obtained by differentially expressed analysis data set from E8 embryos. (B) Enrichment analysis with Panther Pathways database on the combined datasets from ChIPseq and RNAseq experiments. (C) Heatmap of gene set Wnt signaling pathway with the genes that contribute most to the Enrichment Score, i.e., genes that appear in the ranked list before or at the peak point of ES, are defined as core enrichment genes. Genes are represented as colors according to their expression values. The range of colors: red, pink, light blue and dark blue indicates expression values high, moderate, low, and lowest, respectively. Triangle arrows indicate the DEGs (Differentially Expressed Genes) obtained with DEseq2 (blue downregulated and red upregulated). (D) Gene profiles of some of the genes belonging to the Wnt pathway directly regulated by Zic2. (E, F) Representative images of neural tube transverse sections from HH16-18 chicken embryos labeled with antibodies for RFP and GFP after electroporation of control shRNA or Zic2 shRNA

together with Topd2GFP at HH12 (n= 4 embryos per condition and a minimum of 4 slices per embryo) (G) Quantification of GFP fluorescence intensity normalized by RFP fluorescence in transverse sections from HH16-18 chicken embryos electroporated as in E and F (n=6 embryos per condition and a minimum of 3 slices per embryo). (H, I) Representative images of neural tube transverse embryos stained with RFP and GFP antibodies in HH16-18 chicken embryos electroporated at HH12 with Δ90βCat/TOPRFP plus Zic2/EGFP or EGFP control plasmids. (J) Quantification of RFP fluorescence intensity normalized by GFP fluorescence inside the neural tube in transverse sections from HH16-18 chicken embryos electroporated as in H, I.

7. Zic2 is sufficient to induce the expression of Draxin, an inhibitor of the canonical Wnt signaling pathway

It has been recently shown that Draxin/Neucrin, a secretable molecule known to be an antagonist of the Wnt canonical signalling pathway (Miyake et al., 2012) is crucial for cranial NCCs delamination (Hutchins et al., 2018, 2019). Moreover, in a microarray performed in the lab, we identified Draxin/Neucrin as highly upregulated in chicken embryos electroporated with Zic2 compared to control embryos **(Figure 20A)**. This result was also confirmed by injecting Zic2 encoding plasmids in chick embryos **(Figure 20D)**. This gain-of-function experiment demonstrated that Zic2 is able to regulate Draxin/Neucrin expression in the neural tube. However, we also noticed that although Zic2 upregulates Draxin/Neucrin inside the tube, Zic2-expressing cells outside the tube did not ectopically express Draxin/Neucrin **(Figure 20D)**. Interestingly, *in situ* hybridization for Draxin/Neucrin compared with Zic2 immunostaining showed that although they are both expressed in the dorsal neural tube of E8.0-8.5 embryos, Draxin/Neucrin is not expressed in the most dorsal cells **(Figure 20B)**. To evaluate whether Zic2 is not only sufficient but also necessary to regulate Draxin/Neucrin, we analyzed *Draxin mRNA* levels in Zic2 mutant embryos and found a diminished expression compared to $Zic2^{+/+}$ controls **(Figure 20C)** demonstrating that Draxin/Neucrin expression inside the tube is regulated by Zic2**.**

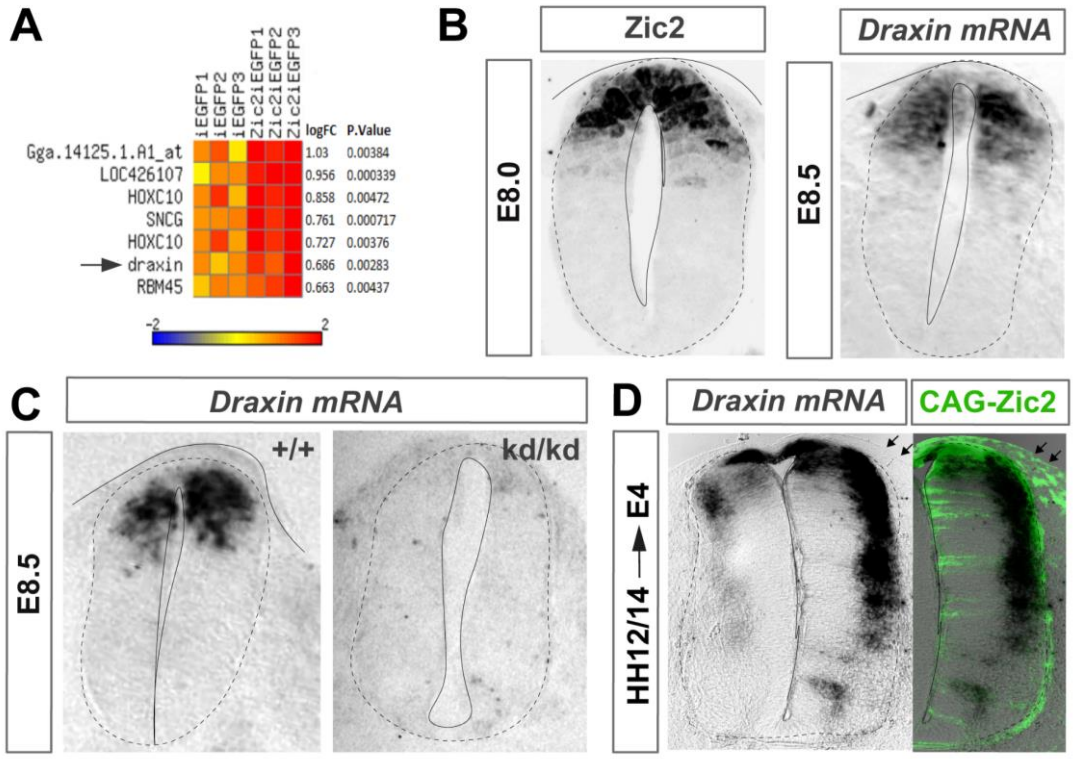

Figure 20. Draxin is expressed in the dorsal neural tube and Zic2 is sufficient to induce Draxin expression in chicken embryos. (A) Hit map generated from the DNA microarray data from embryos electroporated with Zic2/GFP encoding plasmids or GFP alone, *performed by Augusto Escalante*. Seven probe-sets/transcripts were significantly upregulated on samples overexpressing Zic2 with a fold-change larger than 0.5 ($p<0.05$). The probe-set ID, gene symbol, fold change and P values for each transcript are indicated. The color scale bar indicates up-regulation in red. (B) *Draxin/Neucrin mRNA* detected by in situ hybridization in sections from E8.5 mouse embryos (right) shows a similar pattern to Zic2 expression at E8.0 (left). (C) In situ hybridization for *Draxin mRNA* in sections of $Zic2^{+/+}$ and $Zic2^{kd/kd}$ mouse embryos show a strong downregulation in $Zic2^{kd/kd}$ mutants. (D) In situ hybridization in sections from E4 chick embryos electroporated with Zic2/GFP plasmids shows a strong upregulation of *Draxin mRNA* levels in the electroporated side. Note that Zic2 ectopically expressing cells outside the dorsal tube don't upregulate Draxin (black arrows).

8. Zic2 induces TGF-β signaling and promotes NC cells delamination

Our *in vivo* gain-of-function experiments demonstrated that Zic2 blocks the canonical Wnt signaling before NCCs delamination. However, while carrying out these experiments we also noticed that embryos electroporated with plasmids encoding Zic2/EGFP showed a remarkable accumulation of EGFP-cells at the dorsal mesenchyme outside the neural tube concomitant with a reduction of EGFP-cells in the dorsal root ganglia compared to the controls (**Figure 21A-C**).

This accumulation of NCCs in the dorsal mesenchyme after Zic2 gain-of-function was similar to previous observations in *Xenopus* embryos (Brewster and Lee, 1998; Nakata et al., 1998). Based on the fact that melanocytes migrate dorsally through the mesenchyme, the authors suggested a role for Zic2 as a determinant of the melanocytic fate. However, our RNA-seq screen in E8 mutant mice did not reveal DEGs related to any specific neural crest fate. In addition, transverse sections from electroporated chick embryos did not show an increase in the expression of melanocytic markers such as Mitf in cells ectopically expressing Zic2/EGFP **(Figure 21D, E)**. These results suggested that the accumulation of NCCs at the dorsal mesenchyme after ectopic expression of Zic2, is due to an increased NCCs delamination rather than a change in cell fate.

According to this idea, the transcriptome analysis of E8 Zic2 mutants retrieved *Gdf10* as the most downregulated gene after Zic2 itself (**Figure 21C**). *Gdf10* encodes for the growth differentiation factor 10 which is a secreted ligand of the TGF-β receptors which are involved in the recruitment and activation of the SMAD family of proteins (Upadhyay et al., 2011). The activation of the TGF-β pathway has been widely reported as required in the epithelial-to-mesenchymal transition (EMT) process, which in turn is essential for NCCs delamination (Acloque et al., 2009). Zic2 also regulates many genes of this pathway according to the differential expression screen conducted in Zic2-deficient E8 embryos (**Figure 21G**). For instance, activators of the pathway such as Sall4, *Foxh1* and Ski (Aragón et al., 2019; Sun et al., 1999; Zhang et al., 2018) were significantly downregulated in the Zic2 mutants while *Bambi*, that encodes a protein that when eliminated allows TGF-β signaling, was strongly upregulated (**Figure 21H**).

Together, these results suggest that Zic2 activates the TGF-β pathway in

NCCs likely to induce delamination. To test whether Zic2 induces delamination by regulating the aforementioned targets in the TGF-β pathway, we electroporated *shRNAs* against Bambi to mimic one of the molecular effects of this transcription factor. As expected, downregulation of Bambi increased the number of cells exiting the neural tube compared to the controls (**Figure 21I-K**) although contrary to the phenotype observed after Zic2 gain of function the cells with reduced levels of Bambi were able to migrate. Together, these results demonstrate that (i) Zic2 can induce NCC delamination by regulating Bambi and possible other genes associated to the TGF-β pathway, and (ii) Zic2 has to be downregulated a soon as the NCCs exit the tube to allow their correct migration.

These experiments demonstrate that Zic2 orchestrate the inhibition of the canonical Wnt signaling and concomitant induction of the TGF-β pathway to promote EMT in NCCs and support the idea that a temporally restricted expression of Zic2 in premigratory NCCs promotes their delamination. These results concur with previous data showing that activation of the TGF-β pathway and inhibition of the Wnt canonical signaling are both required for NCCs delamination (Kahata, 2018; Rabadán et al., 2016)

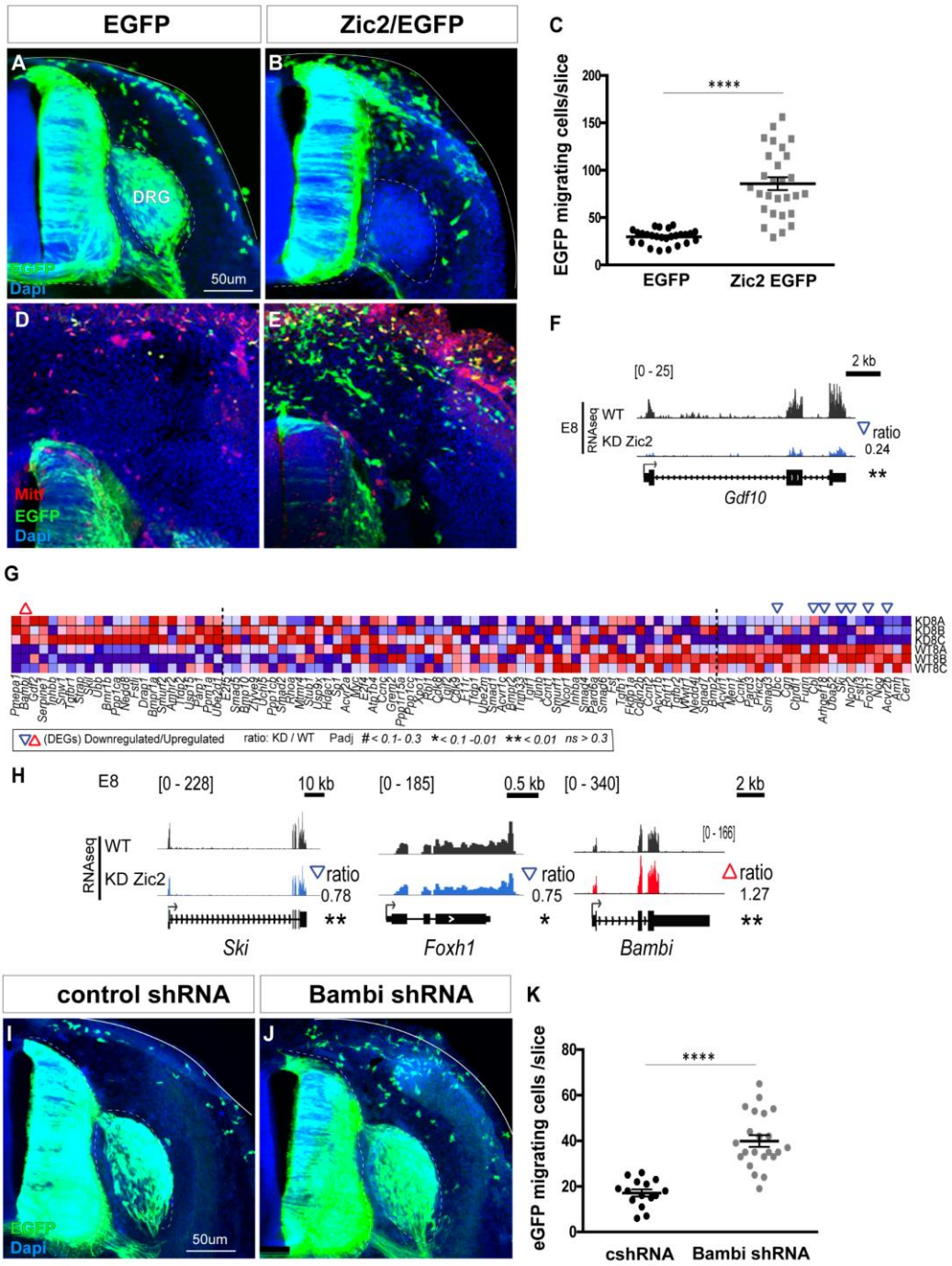

Figure 21. Zic2 induces neural crest cells delamination. (A, B) Transverse sections from E4 chick embryos electroporated at HH12/14 with plasmids encoding Zic2/EGFP or EGFP plasmid alone. (C) Graph represents the number of EGFP cells migrating in transverse sections of E4 chick embryos electroporated at HH12/14 with plasmids encoding Zic2/EGFP or EGFP plasmids alone. N=3 embryos per condition, 5-6 slices per embryo (D, E) Representative transverse sections from E5 chick embryos electroporated at HH12/14 with plasmids encoding Zic2/EGFP or EGFP plasmid alone and stained for the melanocytes marker MITF. (F) Gene profile of Gdf10 expression in E8 $Zic2^{kd/kd}$ (blue) vs $Zic2^{+/+}$ (gray) embryos. (G) Heatmap of the Reactome database focused on the TGF-β pathway. Genes are represented as colors according to their

expression values. The range of colors red, pink, light blue and dark blue indicates expression values high, moderate, low, and lowest, respectively. Triangle arrows indicate the DEGs (Differentially Expressed Genes) obtained with DEseq2 (blue downregulated and red upregulated) (H) Gene profiles of relevant genes related to the TGF-beta pathway are shown. (I-J) Transverse sections of E4 chick embryos electroporated at HH12/14 with plasmids encoding control shRNA or Bambi shRNA plus EGFP plasmids. (K) Graph represents the number of migrating EGFP cells in the mesenchyme of embryos electroporated with Bambi shRNA and control shRNA plasmids. N=3 embryos per condition, 5-6 slices per embryo. *This experiment was performed by Cruz Morenilla.*

DISCUSSION

Zic2 expression is detected already at E6 just before gastrulation commences, but transcriptional profiles of *Zic2*$^{kd/kd}$ embryos do not show differential gene expression compared to the wild type littermates. However, at this stage Zic2 is already bound to many places in the genome, as seen by ChIP-seq analysis, where we find more than 7000 peaks belonging to Zic2 binding. A significant number of these peaks are also found at E8. We observe changes on the binding profile of this TF over time likely reflecting its accessibility to open chromatin through development.

At E8 we demonstrate that Zic2 is able to inhibit the Wnt canonical signalling pathway in NCCs to enable EMT and that activates other signalling pathways implied in this process, such as TGF-β pathway. These results shed light on the function of Zic2 during early embryogenesis. These results might also serve to study and understand the functions of Zic2 in other developmental contexts such as the rhombic lip, the hem, the caudal amygdaloid stream, which are also tightly influenced by the Wnt signalling pathway. All these findings might have clinical relevance in pathological conditions such as HPE5 as may help to improve the diagnosis and genetic counselling of this pathology.

Zic2 in mouse gastrulation

Gastrulation is the process by which a two-layer embryo is transformed into a complex three-layer embryo by ingression of the epiblast cells through the primitive streak. Cells in this stage suffer a process called EMT, which consists of cytoskeleton rearrangements and detachment from an epithelial sheet. In this

process, several crucial signalling pathways interact. TGF-β (Nodal and BMP) and Wnt signalling act as posteriorizing signals whereas at the anterior epiblast expression of antagonists of Nodal signalling maintain an anterior fate. At mid gastrulation, while the three germ layers are being allocated and the primitive streak extends until the most anterior part of the epiblast, the node, also called the gastrula organizer becomes evident. This structure will give rise to the anterior mesendoderm and will also contribute to the notochord and prechordal plate. The spatiotemporal expression pattern of Zic2 through gastrulation is consistent with the idea that it is transient and dynamically expressed in cells from the three germinal layers when they undergo EMT.

Analysis of E7.5 *Zic2*$^{kd/kd}$ embryos showed expression of different markers of the three germ layers, suggesting that Zic2 does not control the differentiation of epiblast cells in any specific layer. The first phenotype we detected was at E7.75-E8.0, in the anterior notochord. This defect was previously described by Warr et al., 2008 in the kumba mutant mice. In this work, the authors showed that Zic2 is the only Zic member of the family expressed in the forming node, and that the lack of Zic2 causes defects in the formation of the precursors of the anterior cells of the notochord and the prechordal plate (Warr et al., 2008). Warr and colleagues also showed aberrant expression of some node markers, such as Hhex, Gsc and FoxA2. In a more recent article, these authors propose that HPE5 must be caused by a defective Nodal signalling. They suggest a physical interaction of Zic2 with Smad2/3 proteins to repress Smad-dependent transactivation during these stages by direct binding to Smad binding elements (SBE) upstream of FoxA2 (Houtmeyers et al., 2016). Our ChIP-seq assays do not show direct binding of Zic2 to any of the SBE domains close to the FoxA2

locus and RNA-seq does not reveal differential regulation of FoxA2 in the Zic2$^{kd/kd}$ mice. Instead, we find a very strong downregulation of Gdf10 in Zic2 deficient mice, which is known to activate Smad3 phosphorylation (Upadhyay et al., 2011). Although we cannot definitively rule out the possibility that Zic2 regulates the Nodal pathway at gastrula stages, our data suggest that Smad3-dependent transcriptional activation is controlled via Gdf10-dependent phosphorylation rather than for physical interaction between Zic2 and Smad3.

Remarkably, we found many Wnt-related genes (such as Apc2) that show Zic2-peaks close or in the TSS, implying that Zic2 regulates the Wnt pathway during gastrulation. Previous data from our laboratory have shown that Zic2 negatively regulates Apc2, which in turn induces an accumulation of βcatenin. However, we also observed that Zic2 blocks the canonical Wnt pathway. Although an increase in the levels of βcatenin and concomitant blockage of the canonical Wnt pathway appeared contradictory at the first glance, we have recently demonstrated that in differentiated neurons, Zic2 activity increases the levels of βcatenin and mediates a Wnt dependent response but do not activate the canonical pathway (Morenilla-Palao et al., BioRxv). This novel Zic2-Wnt pathway may be essential in early stages of development as well.

Our transcriptomic profiling at E6 in Zic2 hypomorphic mice compared to the wild type littermates aiming to find an earlier phenotype, did not detect genetic changes at early stages. It is quite possible that *Zic2 mRNA* in the wildtype is too low to detect differences with the *Zic2$^{kd/kd}$* mutants and it might be too early to detect further changes in the transcriptome.

Zic2 in NCCs delamination

Neural crest cells are induced during late gastrulation in the neural plate border, however, they do not become morphologically apparent until neurulation. Then, NCCs are specified and start a process of EMT to detach from the neuroepithelium and be able to migrate long distances to populate several organs in the body. Zic2 is expressed at this stage in the neural folds in the premigratory NCCs (FoxD3^{+}) and its expression is downregulated when these cells exit the neural tube. To unveil the gene program directly regulated by Zic2, we performed a ChIP-seq analysis at E8 which threw an enrichment of the Wnt signalling pathway. At this stage we observed that 77,5% of the peaks were in the TSS or intragenic regions.

Transcriptome profiling of *Zic2*$^{kd/kd}$ E8 embryos compared to *Zic2*$^{+/+}$ retrieved 1097 differentially expressed genes (DEG), 272 upregulated and 825 downregulated. A clear enrichment of the Wnt pathway was also observed by GO analysis, this data together with the ChIP-seq analysis demonstrates that Zic2 directly regulates the transcription of genes belonging to this pathway. Wnt pathway is known to be implicated in NC EMT. Wnt canonical signalling has been recently shown to be deactivated just before NCCs delamination (Rabadán et al., 2016).

The examination of Zic2 hypomorph mutants revealed defects in NC cells delamination. Many NCCs were accumulated in the dorsal neural tube as seen with GFP labelling together with the marker FoxD3. This phenotype is better visualized in E11.5 embryos, in which we observed that cells do not migrate in a stereotyped manner in the *Zic2*$^{kd/kd}$ [Tg(Zic2^{EGFP})] mutants compared to the

controls. In fact, cells remain near the dorsal mesenchyme. These results were in coincidence with experiments shown in Gerald Muça's thesis in which he performed the temporal downregulation of Zic2 in chicken embryos by using short hairpin RNAs. Thus, Zic2 downregulation causes defects in delamination. We hypothesized that these defects are due, at least in part, to the lack of deactivation of the Wnt Canonical Signalling pathway needed for EMT to take place and functional experiments have in fact confirmed this hypothesis. So we performed *in vivo* functional experiments. First, by GOF assays we showed that Zic2 represses the canonical Wnt pathway and then by LOF experiments observed that downregulation of Zic2 leads to de-repression of the Wnt canonical signalling pathway.

On the other hand, we wondered whether Zic2, in addition to block the Wnt signalling pathway, is able to induce delamination. GOF experiments indeed demonstrated that after Zic2 electroporation cells delaminate and remain accumulated in the dorsal mesenchyme. A similar phenotype was previously described in *Xenopus* embryos. In this animal model they observed accumulation of NCCs in the dorsal mesenchyme and because they interpret this as an increase in the number of melanocytes they propose that Zic2 induces melanocytic fate. However, we do not observe an increase in the number of MITF positive cells after Zic2 induction and therefore our results argue against this hypothesis rather pointing out a role for Zic2 in stopping proliferation and inducing delamination. Even further, we hypothesized that Zic2 is able to induce delamination thanks to its regulation of the TGF-β pathway, shown in the genomic analysis. In these analysis, we found that the genes Sall4, Foxh1 or Ski (Zhang et al., 2008) which are activators of the TGF-β pathway were downregulated in

the Zic2 mutants while Bambi, that encodes a protein that when eliminated allows TGF-β signaling, was upregulated. The analysis of Bambi downregulation show that this protein is able to induce the same effect in delamination as Zic2 induces in chicken embryos when it is overexpressed, but without affecting migration. Altogether, these experiments reveal that Zic2 is able to, on one hand, inhibit Wnt pathway to stop proliferation and switch to the Wnt PCP pathway, and in the other hand activate TGF-β pathway, necessary to induce NCCs delamination.

To go deeper in how Zic2 exerts Wnt inhibition, we investigated the molecule Draxin/Neucrin, which has been demonstrated to play critical roles in regulating the cranial NC cells EMT (Hutchins and Bronner, 2018). Draxin appears to act by sequestering LRP5/6, thereby inhibiting βcatenin accumulation and subsequent transcriptional activation, similarly to what the antagonists Dickkopf-related family proteins do. In fact, Draxin protein contains an N-terminal signal peptide for secretion and a highly conserved C-terminal 60–aminoacid CRD that has homology with the C-terminal cysteine-rich colipase fold domain of Dkk-1 (Hutchins and Bronner, 2018). Loss of Draxin results in defects in delamination and a failure to mesenchymalize and in an overactivation of the Wnt canonical signalling pathway (Hutchins and Bronner, 2018). Moreover, it has been shown that Draxin perturbation affects laminin organization and so impedes basement membrane remodelling during this process (Hutchins and Bronner, 2019). Previous microarrays data from the lab designed to find Zic2 targets in the chick spinal cord found Draxin as a putative candidate. Now we have confirmed that Zic2 is able to induce Draxin in chicken embryos inside the dorsal neural tube. In mouse embryos, we also see that the mRNA expression of Draxin at E8.5 partially coincides with Zic2 expression and we detect a significant reduction in

Zic2$^{kd/kd}$ mutants at E8.5- E9 but not earlier but we did not find significant changes in the RNA-seq performed at E8 with Zic2$^{kd/kd}$ mutants, coinciding with the observation that counts for *Draxin mRNA* in wildtype embryos are very low at E8. These resulIts have several potential explanations. A first option is that Draxin plays a significant role in neural crest cell delamination in chicken but not in mouse, or at least not in trunk NCCs, where it could be expressed from E8.5 to help to the specification of the spinal cord. A second, not exclusive, possibility is that Zic2 only regulates Draxin expression in the absence of Wnt signalling. In line with this last possibility, Murgan et al, 2015a & 2015b reports that in *C. elegans* Zic proteins may act as activators when TCF binds together with Zic to a genomic binding site for Zic, but as repressors when TCF goes together with βcatenin, so when Wnt canonical signaling pathway is active. In the case of Draxin, it would not be induced by Zic2 in NCCs because they are exposed to Wnt in the dorsal part of the tube. However, in cells that are far from Wnt influence Zic2 would be able to induce its expression.

The phenotype described for Draxin downregulation in chicken in Hutchins and Bronner, 2018 implies that cranial NCCs prematurely delaminate but without having completed EMT. This premature delamination causes a downregulation of Snail2 (Slug) and Sox9. On the other hand, GOF experiments trigger a decrease in delamination (Hutchins and Bronner, 2018). This phenotype is not totally coincident with the one elicited by Zic2, as downregulation of this TF does not cause a premature delamination as Draxin. Here, we have to consider the cranial vs trunk EMT and delamination. Whereas cranial NCCs need Wnt canonical signalling to delaminate, trunk NC have to inhibit this pathway transiently to be able to delaminate and then they reactivate it again when they

have migrated away from the neural tube (Rabadán et al., 2016). The ectopic induction of Draxin in the trunk NC after GOF of Zic2 could explain in part the increase in delamination. Although in cranial NCCs Draxin overexpression causes a decrease in delamination triggered by inhibition of Wnt signalling, as I have exposed before, trunk NC cells need this inhibition to delaminate. Thus, when we overexpress Zic2 ectopically, Draxin is upregulated, it inhibits Wnt canonical signalling and cells delaminate prematurely.

Zic2 downregulation phenotype could be partly explained by the regulation of other two proteins, Dapper homolog 1 and 2 (Dact1 and Dact2), that are downregulated in *Zic2*$^{kd/kd}$ embryos compared to the controls in our RNA-seq screenings at E8. These proteins have been implicated in the inhibition of Wnt canonical signalling in chicken trunk NCCs. They bind to Dishevelled, resulting in the accumulation of βcatenin into the nucleus where they sequester βcatenin in structures resembling NBs preventing it from acting as a TCF transcriptional co-activator (Rabadán et al., 2016). They have been also implicated in PCP/non-canonical Wnt signalling pathway (Kivimäe et al., 2011). Here we demonstrate that Zic2 inhibits the canonical Wnt signalling pathway in NCCs and a recent work from our lab (Morenilla-Palao et al, BioRxv) has demonstrated that Zic2 enables the accumulation of βcatenin in differentiated neurons at the same time that inhibits the activation of the Wnt canonical pathway. Interestingly, βcatenin has been shown to interact directly with the three murine DACT paralogues (Kivimäe et al., 2011; Wang et al., 2015).

Another observation to consider is that while Dact proteins influence the PCP pathway, Draxin is able to inhibit the Wnt canonical signalling but not to turn on the non-canonical PCP pathway. We have found several crucial genes

involved in this pathway in the RNA-seq at E8 such as Celsr3 (a.k.a Flamingo), Vangl2 and some Frizzled receptors. Thus, we propose that Zic2 might inhibit the canonical Wnt signalling pathway and induce a switch to activate a Wnt-dependent but non-canonical pathway.

Zic2 DNA binding profiles in development

The study of the Zic2 DNA binding profiles at E6 and at E8 could help us understand the different regulatory mechanisms that the cell presents when is pluripotent compared to when is multipotent. From the ChIP-seq analysis at E6 we retrieved that most peaks were in the TSS or intragenic regions (67,5%). Only a minority were located in intergenic regions (32,5%), contrasting with the previously reported scenario in an embryonic stem cell line in which only 21% of the Zic2-peaks were found in TSS or intragenic regions and more than 50% were in intergenic regions (Luo et al., 2015). Our results rather coincided with previous Zic2-ChIPseq analysis in Epi-like cells (Epi-SCs) differentiated in vitro (Matsuda et al., 2017). At E8 the number of Zic2 peaks is strongly reduced and most of them are found in promoter regions. These peaks located at promoter regions in E8 samples are also found in E6 samples, meaning that, although Zic2 binds to many places in the genome at early stages in a pluripotent cell, its binding eventually becomes restricted to promoter regions in multipotent cells.

Molecular mechanisms underlying Zic2 function in different contexts and implications for HPE

We have demonstrated that Zic2 is crucial for NC EMT in two species, mice and chicken. We propose that it works through inhibiting the Wnt Canonical Signalling to stop proliferation and likely initiate the PCP pathway to induce delamination at the time that activates the TGF-β pathway. In gastrulation, although we have not been able to find defects in EMT in *Zic2*$^{kd/kd}$ mutants, likely because there are still very few Zic2 positive cells and therefore mRNA changes are difficult to detect, it is possible that Zic2 is acting at the same level in this process. We have seen that Zic2 is expressed in endoderm and mesoderm, two layers that will form from cells that must undergo EMT to properly ingress through the PS. This process is occurring at E7.0 and unluckily, our *RNA*-seq data performed at E6, was not able to detect the regulatory changes exerted by Zic2. This TF is rapidly downregulated from the germ layers when they commence the proper allocation and starts again when the neural plate and neural plate border forms. Both processes imply EMT and delamination and are tightly regulated by the Wnt and TGF-β signalling. Although it has not been described whether the Wnt pathway must be downregulated for gastrulation EMT to proceed, as it happens in trunk NC EMT, it is likely that the mechanism is similar in gastrulation. The inhibition of Wnt canonical signalling pathway, has also been shown as crucial for correct specification of axial (notochord) versus lateral (somitic) mesoderm (Niehrs, 1999). The fact that both kumba mutants and the *Zic2*$^{kd/kd}$ hypomorph mutants have defects in the specification of the anterior notochord might be explained by a failure in the inhibition of Wnt canonical signalling due to the lack of Zic2. Thus,

Zic2 phenotypes related to HPE can be explained by the malfunction of the Wnt signalling pathway.

Although it has been demonstrated that Zic2 regulates Nodal targets, we do not detect these changes by RNA-seq at E8. We do not see either a peak in FoxA2 locus in the genome nor a change in the mRNA level comparing $Zic2^{kd/kd}$ and $Zic2^{+/+}$ at E8.0-E8.5, suggesting that Zic2 does not regulate this targets to helps in the EMT process.

In addition to this, there are other processes during the development of the nervous system in which Zic2 is highly expressed and that are also affected by Wnt or TGF-β pathways. So, it is also plausible that Zic2 plays a similar role in these other scenarios.

Finally, Zic2 is aberrantly expressed in several types of tumours such as meningiomas (Aruga et al., 2010), medulloblastomas (Pfister et al., 2007), small cell lung cancer (Sabater et al., 2008) and breast cancer types (Wang et al., 2009). There are several studies demonstrating a relationship between Zic2 and invasiveness of the tumour (Wang et al., 2018; Zhang et al., 2019; Lu et al., 2017) and it is known that the invasiveness of the tumour depends on the capacity of metastasis (Nieto et al., 2016), which involves a process of EMT, so it is likely that Zic2 could be regulating this process also in cancer cells.

CONCLUSIONS

1. Zic2 transiently detected in the three germ layers of the epiblast during gastrulation stages as well as in premigratory neural crest cells, which are all cells undergoing epithelial-to-mesenchymal transition.

2. Zic2 is essential for the formation of the notochord.

3. Zic2 is necessary and sufficient for neural crest cells delamination from the dorsal neural tube.

4. Zic2 binds to many more genomic sequences in gastrula cells than in neural crest cells and Zic2-binding sequences are often located into or near the TSS in both types of cells.

5. Zic2 directly regulates the expression of many genes related to the Wnt, cadherin and TGF-β signalling pathways.

6. Zic2 inhibits the Wnt canonical signalling pathway in premigratory neural crest cells and it is sufficient to induce the expression of the antagonist Wnt-canonical protein Draxin.

7. Downregulation of Bambi, a gene that represses the TGF-β, partially recapitulates the defects in delamination observed after Zic2 ectopic induction in NCCs.

8. In summary, our results demonstrate that Zic2 directly regulates many genes implicated in the Wnt, cadherin and TGF-β to control EMT processes in neural crest cells and suggest that it may also have an impact in these pathways in gastrula cells.

CONCLUSIONES

1. Zic2 se expresa transitoriamente en las tres capas germinales del epiblasto durante estadios de gastrulación, así como en células premigratorias de la cresta neural, que son las células que están experimentando una transición epitelio mesénquima.

2. Zic2 es esencial para la formación de la notocorda.

3. Zic2 es necesario y suficiente para la delaminación de las células de la cresta neural del tubo neural dorsal.

4. Zic2 se une a muchas más secuencias genómicas en células de gástrula que en células de la cresta neural y las secuencias de unión a Zic2 están a menudo localizadas en la región TSS o cerca de ella en ambos tipos de células.

5. Zic2 regula directamente la expresión de muchos genes relacionados con la vía de Wnt, las cadherinas o la vía de TGF-β.

6. Zic2 inhibe la vía canónica de Wnt in células premigratorias de la cresta neural y es suficiente para inducir la expresión de Draxin, un antagonista de esta vía.

7. La bajada de expresión de Bambi, un gen que reprime la vía de TGF-β, recapitula parcialmente los defectos en delaminación observados después de la inducción ectópica de Zic2 en las células de la cresta neural.

8. Resumiendo, nuestros resultados demuestran que Zic2 regula directamente muchos genes implicados en la vía de Wnt, cadherina y TGF-β para controlar procesos de transición epitelio mesénquima in células de la cresta neural y sugiere que puede regular estas vías de señalización en células de gástrula.

REFERENCES

Acloqué H, Adams MS, Fishwik K, Bronner-Fraser M, Nieto MA (2009), Epithelial-mesenchymal transitions: the importance of changing cell state in development and disease. J. Clin. Invest. 119:1438-1449.

Acloqué H, Ocaña O, Matheu A, Rizzoti K, Wise C, Lovell-Badge R, Nieto MA (2011), Developmental Cell 21:546–558.

Ali RG, Bellchambers HM, Arkell RM. (2012) Zinc fingers of the cerebellum (Zic): transcription factors and co-factors. Int. J. Biochem. Cell Biol. 44: 2065-2068.

Aragón E, Wang Q, Zou Y, Morgani SM, Ruiz L, Kaczmarska Z, Su J, Torner C, Tian L, Hu J, Shu W, Agrawal S, Gomes T, Márquez JA, Hadjantonakis AK, Macias MJ, Massagué J (2019). Structural basis for distinct roles of SMAD2 and SMAD3 in FOXH1 pioneer-directed TGF-β signaling. Genes Dev. 33(21-22):1506-1524.

Arkell RM, Fossat N and Tam PPL (2013). Wnt signalling in mouse gastrulation and anterior development: new players in the pathway and signal output. Current Opinion in Genetics & Development 23:454–460.

Aruga J (2004). The role of *Zic* genes in neural development. Mol. Cell. Neurosci. 26:205-221.

Aruga J, Inoue T, Hoshino J, Mikoshiba K. (2002a) Zic2 Controls Cerebellar Development in Cooperation with Zic1. The Journal of Neuroscience, 22(1):218–225.

Aruga J, Nozaki Y, Hatayama M, Odaka YS, Yokota N (2010). Expression of ZIC family genes in meningiomas and other brain tumors. BMC Cancer, 10:79.

Aruga J, Tohmonda T, Homma S, Mikoshiba K (2002b). Zic1 promotes the expansion of dorsal neural progenitors in spinal cord by inhibiting neuronal differentiation. Dev Biol 244(2):329-341.

Bajpai R, Chen DA, Rada-Iglesias A, Zhang J, Xiong Y, Helms J, Chang C-P, Zhao Y, Swigut T, Wysocka J (2010). CHD7 cooperates with PBAF to control multipotent neural crest formation. Nature 463:958–962.

Barrallo-Gimeno A, Nieto MA (2005) The Snail genes as inducers of cell movement and survival: implications in development and cancer. Development 132(14):3151-61.

Barratt and R. M. Arkell (2018) Chapter 14 *ZIC2* in Holoprosencephaly. From Aruga J. (ed) *Zic family*. Advances in Experimental Medicine and Biology 1046.

Barriga EH, Trainor PA, Bronner M, Mayor R, (2015). Animal models for studying neural crest development: is the mouse different? Development. 142(9):1555-60.

Basch ML, Bronner-Fraser M & García-Castro MI. (2006). Specification of the neural crest occurs during gastrulation and requires Pax7. Nature, 441, 218–222.

Bertrand V and Hobert O (2009). Linking asymmetric cell division to the terminal differentiation program of postmitotic neurons in *C. elegans*. Dev Cell 16(4):563-575.

Betancur P, Bronner-Fraser M, Sauka-Spengler T (2010) Assembling neural crest regulatory circuits into a gene regulatory network. Annu Rev Cell Dev Biol. 26:581-603.

Betters E, Charney RM, and García-Castro MI (2018). Early specification and development of rabbit neural crest cells. Developmental Biology,21, 316–320.

Brown Y, Kottman AH and Brown S (2003). Immunolocalization of Zic2 expression in the developing mouse forebrain. Gene expression patterns, 3,361-367.

Brown L and Brown S (2009). Zic2 is expressed in pluripotent cells in the blastocyst and adult brain expression overlaps with makers of neurogenesis. Gene Expr Patterns 9(1):43-9.

Buitrago-Delgado E, Nordin K, Rao A, Geary L, and LaBonne C (2015). Shared Pluripotency Programs Suggest Derivation of Vertebrate Neural Crest from Blastula Cells. Science 348(6241): 1332–1335.

Burstyn-Cohen T, Stanleigh J, Sela-Donenfeld D, Kalcheim C (2004). Canonical Wnt activity regulates trunk neural crest delamination linking BMP/noggin signalling with G1/S transition. Development, 131,5327–5339

Cano A, Pérez-Moreno MA, Rodrigo I, Locascio A, Blanco MJ, del Barrio MG, Portillo F, Nieto MA (2000). The transcription factor Snail controls epithelial–mesenchymal transitions by repressing E-cadherin expression. Nat Cell Biol. 2(2):76-83.

Chan WY, Tam PPL, (1988). A morphological and experimental study of the mesencephalic neural crest cells in the mouse embryo using wheat germ agglutinin-gold conjugate as the cell marker. Development 102, 427–442.

Cheung M, Chaboissier MC, Mynett A, Hirst E, Schedl A and Briscoe J (2005). The transcriptional control of trunk neural crest induction, survival, and delamination. Dev Cell 8: 179-192.

Chuai M, Hughes D and Weijer CJ (2012). Collective Epithelial and Mesenchymal Cell Migration During Gastrulation. Current Genomics 13: 267-277.

Clevers H, Nusse R, Wnt/beta-catenin signalling and disease (2012). Cell 149 1192–1205.

Coffman CR, Skoglund P, Harris WA. and Kintner CR (1993). Expression of an extracellular deletion of Xotch diverts cell fate in Xenopus embryos. Cell 73, 659-671.

del Barrio MG, and Nieto MA (2002). Overexpression of snail family members highlights their ability to promote chick neural crest formation. Development, 129, 1583–1593.

Devotta A, Hong CS, & Saint-Jeannet JP (2018). Dkk2 promotes neural crest specification by activating Wnt/β-catenin signalling in a GSK3β independent manner. eLife, 7, e34404.

Duband JL, Monier F, Delannet M, Newgreen D (1995). Epithelium-Mesenchyme Transition during Neural Crest Development. Acta Anat, 154:63-78.

Dykes IM, Szumska D, Kuncheria L, Puliyadi R, Chen C, Papanayotou C, Lockstone H, Dubourg C, David V, Schneider JE, Keane TM, Adams DJ, Brown SDM, Mercier S, Odent S, Collignon J and Bhattacharya S (2018). A Requirement for Zic2 in the Regulation of Nodal Expression Underlies the Establishment of Left-Sided Identity. Sci Rep. 11;8(1):10439.

Elms P, Siggers P, Napper D, Greenfield A, Arkell R (2003) Zic2 is required for neural crest formation and hindbrain patterning during mouse development. Dev Biol. 264(2):391-406.

Elms P, Scurry A, Davies J, Willoughby C, Hacker T, Bogani D, Arkell R (2004) Overlapping and distinct expression domains of Zic2 and Zic3 during mouse gastrulation. Gene Expression Patterns 4:505–511.

Endo Y, Osumi N, Wakamatsu Y (2002). Bimodal functions of Notch-mediated signalling are involved in neural crest formation during avian ectoderm development. Development 129:863-73.

Erickson CA, Duong TD and Tosney, KW (1992). Descriptive and experimental analysis of the dispersion of neural crest cells along the dorsolateral path and their entry into ectoderm in the chick embryo. Dev Biol 151: 251-272.

Escalante A, Murillo B, Morenilla-Palao C, Klar A, Herrera E (2013). Zic2-dependent axon midline avoidance controls the formation of major ipsilateral tracts in the CNS. Neuron 80(6):1392-406.

Gammill LS, Roffers-Agarwal (2010). Division of labor during trunk neural crest development. J.Dev Biol. 344(2):555-65.

Garcia-Castro MI, Marcelle C, & Bronner-Fraser M (2002). Ectodermal Wnt function as a neural crest inducer. Science, 297, 848–851.

Glavic A, Silva F, Aybar MJ, Bastidas F, Mayor R (2004). Interplay between Notch signalling and the homeoprotein Xiro1 is required for neural crest induction in *Xenopus* embryos. Development 131:347–-59.

Gouignard N, Andrieu C, Theveneau E (2018). Neural crest delamination and migration: Looking forward to the next 150 years. Genesis e23107.

Hall BK (2000). The neural crest as a fourth germ layer and vertebrates as quadroblastic not triploblastic. Evolution & Development,2,3–5.

Hall BK (2008). The neural crest and neural crest cells: discovery and significance for theories of embryonic organization; J. Biosci. 33 781–793.

Hall BK (2018). Germ layers, the neural crest and emergent organization in development and evolution. Genesis,56, e23103.

Hamburger and Hamilton (1951) A series of Normal Stages in the Development of the Chick Embryo. J. Morphol. 88:49-92.

Han W, Zhang C, Gao X, Wang H, Chen F, Cao F,Hu Y, Ma Y, Gu X, Ding H (2018). Clinicopathologic and Prognostic Significance of the Zinc Finger of the Cerebellum Family in Invasive Breast Cancer. Breast Cancer 21(1): 51-61.

Hatayama M, Aruga J (2010). Characterization of the tandem CWCH2 sequence motif: a hallmark of inter-zinc finger interactions. BMC Evolutionary Biology, 10:53

Henion PD, Weston JA (1997). Timing and pattern of cell fate restrictions in the neural crest lineage. Development 124:4351-9.

Herrera E, Brown L, Aruga J, Rachel RA, Dolen G, Mikoshiba K, Brown S, Mason CA (2003). Zic2 patterns binocular vision by specifying the uncrossed retinal projection. Cell. 114(5):545-57.

Houtmeyers R, Souopgui J, Tepjar S, Arkell R. (2013). The ZIC gene family encodes multi-functional proteins essential for patterning and morphogenesis. Cell. Mol. Life Sci. 70(20):3791-811.

Houtmeyers R, Tchouate Gainkam O, Glanville-Jones HA, Van den Bosch B, Chappell A, Barratt KS, Souopgui J, Tejpar S, Arkell RM (2016). *Zic2* mutation causes Holoprosencephaly via disruption of NODAL signalling. Hum Mol Genet. 25(18):3946-3959.

Ingo Burtscher and Heiko Lickert (2009). Foxa2 regulates polarity and epithelialization in the endoderm germ layer of the mouse embryo. Development 136, 1029-1038.

Inoue T, Ota M, Mikoshiba K, Aruga J. (2007) *Zic2* and *Zic3* synergistically control neurulation and segmentation of paraxial mesoderm in mouse embryo. Developmental Biology 306:669-684.

Ishiguro A, Hatayama M, Otsuka MI and Aruga J (2018). Link between the causative genes of holoprosencephaly: Zic2 directly regulates Tgif1 expression. Sci Rep.8(1):2140.

Jia L, Cheng L, Rapera J (2005). Slit/Robo signalling is necessary to confine early neural crest cells to the ventral migratory pathway in the trunk. Developmental Biology 282:411 – 421

Jones NC, Trainor PA (2005). Role of morphogens in neural crest cell determination. J. Neurobiol. 64:388–-404.

Johnston CJC, Smyth DJ, Dresser DW, Maizels RM (2016). TGF-β in tolerance, development and regulation of immunity. Cellular Immunology 299:14–22.

Kalcheim C (2015). Epithelial–Mesenchymal Transitions during Neural Crest and Somite Development. J. Clinical Medicine, 5, 1.

Kerosuo L and Bronner-Fraser M (2012). What is bad in cancer is good in the embryo: importance of EMT in neural crest development. Semin Cell Dev Biol. 23(3):320-32.

Keynes R, Cook G, Davies J, Lumsden A, Norris W, Stern C (1990). Segmentation and the development of the vertebrate nervous system. J Physiol 84(1):27-32.

Kivimäe S, Yong Yang XY and Cheyette BNR (2011). All Dact (Dapper/Frodo) scaffold proteins dimerize and exhibit conserved interactions with Vangl, Dvl, and serine/threonine kinases. Kivimäe et al. BMC Biochemistry 12:33.

Knecht AK, Bronner-Fraser M (2002). Induction of the neural crest: a multigene process. Nat. Rev. Genet. 3:453-61.

Kojima Y, Tam OH & Tam PP (2014). Timing of developmental events in the early mouse embryo. Seminars in Cell & Developmental Biology 34: 65–75.

Krispin S, Nitzan E, Kalcheim C (2010). The dorsal neural tube: a dynamic setting for cell fate decisions. Dev Neurobiol. 70(12):796-812.

Krull CE (2001). Segmental organization of neural crest migration. Mech Dev.105(1-2):37-45.

Kuriyama S and Mayor R (2008). Molecular analysis of neural crest migration. Philos. Trans. R. Soc. London Ser. B 363, 1349–1362.

Le Douarin NM, Kalcheim C, (1999). The Neural Crest. Cambridge University Press, Cambridge, UK.

LaBonne C & Bronner-Fraser M (1998) Neural crest induction in *Xenopus*: evidence for a two-signal model. Development. 125:2403-14

Light W, Vernon AE, Lasorella A, Iavarone A, LaBonne C (2005) *Xenopus* Id3 is required downstream of Myc for the formation of multipotent neural crest progenitor cells. Development. 132:1831–41.

Lister JA, Robertson CP, Lepage T, Johnson SL, Raible DW (1999). nacre encodes a zebrafish microphthalmia-related protein that regulates neural-crest-derived pigment cell fate. Development. 126:3757–-67.

Lister JA, Cooper C, Nguyen K, Modrell M, Grant K, Raible DW (2006). Zebrafish Foxd3 is required for development of a subset of neural crest derivatives. Dev Biol. 290(1):92-104.

Liu JA, Wu MH, Yan CH, Chau BK, So H, Ng A, Chan A, Cheah KS, Briscoe J and Cheung M (2013). Phosphorylation of Sox9 is required for neural crest delamination and is regulated downstream of BMP and canonical Wnt signalling. Proc Natl Acad Sci USA 110: 2882-2887.

Locascio A, Manzanares M, Blanco MJ & Nieto MA (2002). Modularity and reshuffling of snail and slug expression during vertebrate evolution. Proceedings of the National Academy of Sciences, 99,16841–16846.

Lolas M, Valenzuela PD, Tjian R, Liu Z, (2014). Charting Brachyury-mediated developmental pathways during early mouse embryogenesis, Proc Natl Acad Sci USA 111(12):4478–4483.

Lu SX, Zhang CZ, Luo RZ, Wang CH, Liu LL, Fu J, Zhang L, Wang H, Xie D, Yun JP (2017). Zic2 promotes tumor growth and metastasis via PAK4 in hepatocellular carcinoma. Cancer Lett. 402:71-80.

Luo Z, Gao X, Lin C, Smith ER, Marshall SA, Swanson SK, Florens L, Washburn MP, Shilatifard A (2015). Zic2 is an enhancer-binding factor required for embryonic stem cell specification. Mol Cell. 57(4):685-694.

Martínez-Morales PL, Diez del Corral R, Olivera-Martínez I, Quiroga AC, Das RM, Barbas JA, Storey KG and Morales AV (2011). FGF and retinoic acid activity gradients control the timing of neural crest cell emigration in the trunk. J. Cell Biol. 194(3):489–503.

Matsuda K, Mikami T, Oki S, Iida H, Andrabi M, Boss JM, Yamaguchi K, Shigenobu S, Kondoh H (2017). ChIP-seq analysis of genomic binding regions of five major transcription factors highlights a central role for ZIC2 in the mouse epiblast stem cell gene regulatory network. Development 144 (11):1948-1958.

Matsunaga E, Shiota K. Holoprosencephaly in human embryos: epidemiologic studies of 150 cases (1977) Teratology 16:261-272.

Mayor R and Theveneau E (2014). The role of the non-canonical Wnt–planar cell polarity pathway in neural crest migration. Biochem. J. 457, 19–26.

Mercier S, Dubourg C, Garcelon N, Campillo-Gimenez B, Gicquel I, Belleguic M, Ratié L, Pasquier L, Loget P, Bendavid c, Jaillard S, rochard L, Quélin C, Dupé V, David V, Odent S (2011). New findings for phenotype-genotype correlations in a large European series of holoprosencephaly cases. J Med Genet 48:752–760.

Monsoro-Burq AH, Fletcher RB, Harland RM (2003). Neural crest induction by paraxial mesoderm in Xenopus embryos requires FGF signals. Development. 130:3111-24.

Monsoro-Burq AH, Wang E, Harland R (2005). Msx1 and Pax3 cooperate to mediate FGF8 and WNT signals during *Xenopus* neural crest induction. Dev. Cell.; 8:167–-78.

Morales AV, Barbas JA, Nieto MA (2005). How to become neural crest: From segregation to delamination. Seminars in Cell & Developmental Biology 16:655–662.

Muenke M and Beachy PA (2000) Genetics of ventral forebrain development and holoprosencephaly. Current Opinion in Genetics & Development 10:262-269.

Murgan S and Bertrand V (2015a). How targets select activation or repression in response to Wnt. Worm 4(4):e1086869.

Murgan S, Kari W, Rothbächer U, Iché-Torres M, Mélénec P, Hobert O, Bertrand V (2015). Atypical Transcriptional Activation by TCF via a Zic Transcription Factor in C. elegans Neuronal Precursors. Dev Cell. 33(6):737-45.

Murillo B, Ruiz-Reig N, Herrera M, Fairén A, Herrera E (2015). Zic2 Controls the Migration of Specific Neuronal Populations in the Developing Forebrain. J Neurosci. 35(32):11266-80.

Murray SA, Gridley T (2006). Snail family genes are required for left-right asymmetry determination, but not neural crest formation, in mice. Proc Natl Acad Sci U S A 103:10300-10304.

Nagai T, Aruga J, Minowa O, Sugimoto T, Ohno Y, Noda T (2000). Zic2 regulates the kinetics of neurulation. PNAS 97(4):1618-23.

Nagy A, Gertsentein M, Vintersten K, Behringer R (2003). Manipulating the mouse embryo: a laboratory manual. 3rd edition. Cold Spring Harbor Laboratory Press, Cold Spring Harbor, New York. 2nd Chapter.

Nakata K, Nagai T, Aruga J, Mikoshiba K (1997). *Xenopus* Zic3, a primary regulator both in neural and neural crest development. Proc Natl Acad Sci USA 94:11980–11985.

Nakata K, Nagai T, Aruga J, Mikoshiba K (1998). *Xenopus* Zic family and its role in neural and neural crest development. Mech Dev. 75(1-2):43-51.

Nguyen VH, Schmid B, Trout J, Connors SA, Ekker M, Mullins MC (1998). Ventral and lateral regions of the zebrafish gastrula, including the neural crest progenitors, are established by a bmp2b/swirl pathway of genes. Dev. Biol. 199:93-110.

Nieto MA, Yun-Ju R, Huang, Jackson RA and Thiery JP (2016) EMT:2016, Cell 1, 21-45.

Niehrs C (1999). Head in the WNT: the molecular nature of Spemann's head organizer. Trends Genet. (8):314-9.

Nitzan E, Krispin S, Pfaltzgraff ER, Klar A, Labosky PA and Kalcheim C (2013). A dynamic code of dorsal neural tube genes regulates the segregation between neurogenic and melanogenic neural crest cells. Development 140: 2269-2279.

Patthey C, Edlund T, & Gunhaga L (2009). Wnt-regulated temporal control of BMP exposure directs the choice between neural plate border and epidermal fate. Development,136,73–83.

Patthey C, Gunhaga L & Edlund T (2008). Early development of the central and peripheral nervous systems is coordinated by Wnt and BMP signals. PLoS One,3, e1625.

Pfister S, Schlaeger C, Mendrzyk F, Wittmann A, Benner A, Kulozik A, Scheurlen W, Radlwimmer B, Lichter P (2007). Array-based profiling of reference-independent methylation status (aPRIMES) identifies frequent promoter methylation and consecutive downregulation of ZIC2 in pediatric medulloblastoma. Nucleic Acids Res.35(7):e51.

Pla P & Monsoro-Burq AH (2018). The neural border: Induction, specification and maturation of the territory that generates neural crest cells. Developmental Biology 444: S36–S46.

Pourebrahim R, Houtmeyers R, Ghogomu S, Janssens S, Thelie A, Tran HT, Langenberg T, Vleminckx K, Bellefroid E, Cassiman JJ, Tejpar S (2011). Transcription factor Zic2 inhibits Wnt/β-catenin protein signalling. J Biol Chem. 286(43):37732-40.

Prasad MS, Charney RB, García-Castro MI (2019). Specification and formation of the neural crest: Perspectives on lineage segregation. Genesis 57:e23276

Pshennikova ES, Voronina AS. (2019) Neural Crest-An Unusual Population of Embryonic Cells. Mol Biol 53(2):256-267.

Rabadán MA, Herrera A, Fanlo L, Usieto S, Carmona-Fontaine C, Barriga EH, Mayor R, Pons S and Martí E (2016) Delamination of neural crest cells requires transient and reversible Wnt inhibition mediated by Dact1/2. Development 143, 2194-2205.

Rada-Iglesias A, Bajpai R, Swigut T, Brugmann SA, Flynn RA, & Wysocka J (2011). A unique chromatin signature uncovers early developmental enhancers in humans. Nature, 470, 279–283.

Ragland, J. W., & Raible, D. W. (2004). Signals derived from the underlying mesoderm are dispensable for zebrafish neural crest induction. Developmental Biology, 276, 16–30.

Raible DW, Eisen JS (1994). Restriction of neural crest cell fate in the trunk of the embryonic zebrafish. Development 120:495-503.

Raible DW, Eisen JS (1996). Regulative interactions in zebrafish neural crest. Development 122:501–507.

Richardson J, Gauert A, Briones Montecinos L, Fanlo L, Alhashem ZM, Assar R, Marti E, Kabla A, Härtel S, Linker C (2016). Leader Cells Define Directionality of Trunk, but Not Cranial, Neural Crest Cell Migration Cell Rep. 15(9):2076-88.

Rogers CD, Jayasena CS, Nie S, Bronner ME (2012). Neural crest specification: tissues, signals, and transcription factors. Rev Dev Biol. 1:52-68.

Rogers C.D, Saxena A, and Bronner ME (2013). Sip1 mediates an E-cadherin-to-N-cadherin switch during cranial neural crest EMT. J Cell Biol 203: 835-847.

Rogers CD, Nie S, (2018) Specifying neural crest cells: From chromatin to morphogens and factors in between. Rev Dev Biol.3:e322.

Sabater L, Bataller L, Suárez-Calvet M, Saiz A, Dalmau J, Graus F (2008). ZIC antibodies in paraneoplastic cerebellar degeneration and small cell lung cancer. J Neuroimmunol.201-202:163-5.

Sauka-Spengler T, Bronner-Fraser M (2008). A gene regulatory network orchestrates neural crest formation. Nat. Rev. Mol. Cell Biol. 9:557–-68.

Sauka-Spengler T, Meulemans D, Jones M, Bronner-Fraser M (2007). Ancient evolutionary origin of the neural crest gene regulatory network. Dev. Cell.13:405–-20.

Scheibner K, Bakhti M, Bastidas-Ponce A and Lickert H (2019). Wnt signalling: implications in endoderm development and pancreas organogenesis. Current Opinion in Cell Biology 61:48–55.

Schille C, Bayerlová M, Bleckmann A and Schambony A (2016). Ror2 signalling is required for local upregulation of GDF6 and activation of BMP signalling at the neural plate border. Development 143, 3182-3194.

Schwarz Q, Maden CH, Vieira JM, Ruhrberg C. (2009) Neuropilin 1 signalling guides neural crest cells to coordinate pathway choice with cell specification. Proc Natl Acad Sci U S A.

Simões-Costa MS, McKeown SJ, Tan-Cabugao J, Sauka-Spengler T, & Bronner, M. E. (2012). Dynamic and differential regulation of stem cell factor FoxD3 in the neural crest is encrypted in the genome. PLoS Genetics, 8, e1003142.

Simões-Costa M, Stone M, & Bronner ME (2015). Axud1 integrates Wnt signalling and transcriptional inputs to drive neural crest formation. Developmental Cell, 34, 544–554.

Solomon BD, Lacbawan F, Mercier S et al (2010a) Mutations in ZIC2 in human holoprosencephaly:description of a novel ZIC2 specific phenotype and comprehensive analysis of 157 individuals. J Med Genet 47:513–524.

Solomon BD, Mercier S, Vélez JI et al (2010b). Analysis of genotype-phenotype correlations in human holoprosencephaly. Am J Med Genet C Semin Med Genet 154:133–141.

Steventon B, Araya C, Linker C, Kuriyama S, & Mayor R. (2009). Differential requirements of BMP and Wnt signalling during gastrulation and neurulation define two steps in neural crest induction. Development,136, 771–779.

Streit A and Stern CD (1999). Establishment and maintenance of the border of the neural plate in the chick: involvement of FGF and BMP activity. Mech. Dev. 82, 51-66.

Strobl-Mazzulla PH, Sauka-Spengler T, Bronner-Fraser M (2010). Histone demethylase JmjD2A regulates neural crest specification. Dev Cell, 19:460–468.

Stuhlmiller TJ, & García-Castro MI (2012). Current perspectives of the signalling pathways directing neural crest induction. Cellular and Molecular Life Sciences, 69, 3715–3737.

Sun Y, Liu X, Eaton EN, Lane WS, Lodish HF, Weinberg RA (2019). Interaction of the Ski oncoprotein with Smad3 regulates TGF-beta signaling. Mol Cell. (4):499-509.

Tam PP, Loebel DA and Tanaka SS (2006). Building the mouse gastrula: signals, asymmetry and lineages. Current Opinion in Genetics & Development, 16:419–425.

Tam PP, Loebel DA (2007). Gene function in mouse embryogenesis: get set for gastrulation. Nat Rev Genet. 8(5):368-81.

Taylor KM, LaBonne C (2007). Modulating the activity of neural crest regulatory factors. Curr Opin Genet Dev 17(4):326-31.

Teslaa JJ, Keller AN, Nyholm MK, Grinblat Y (2013). Zebrafish Zic2a and Zic2b regulate neural crest and craniofacial development. Dev Biol. 380(1):73-86.

Theveneau E, Marchant L, Kuriyama S, Gull M, Moepps B, Parsons M and Mayor R (2010). Collective chemotaxis requires contact-dependent cell polarity. Dev. Cell 19, 39–53.

Tribulo C, Aybar MJ, Nguyen VH, Mullins MC, Mayor R (2003). Regulation of Msx genes by a Bmp gradient is essential for neural crest specification. Development 130:6441-52.

Tuazon FB and Mullins MC (2015). Temporally coordinated signals progressively pattern the anteroposterior and dorsoventral body axes. Semin Cell Dev Biol. 42: 118–133.

Turner N and Grose R (2010). Fibroblast growth factor signalling: from development to cancer. Nature Reviews Cancer, 10(2), 116–129.

Upadhyay G, Yin Y, Yuan H, Li X, Derynck R, Glazer RI (2011). Stem cell antigen-1 enhances tumorigenicity by disruption of growth differentiation factor-10 (GDF10)-dependent TGF-beta signaling. Proc Natl Acad Sci U S A. 108(19):7820-5.

Vega-Lopez GA, Cerrizuela S, and Aybar MJ (2017). Trunk neural crest cells: formation, migration and beyond, Int J Dev Biol. 2017;61(1-2):5-15.

Wang YF, Yang HY, Shi XQ, Wang Y (2018). Upregulation of microRNA-129-5p inhibits cell invasion, migration and tumor angiogenesis by inhibiting ZIC2 via downregulation of the Hedgehog signaling pathway in cervical cancer. Cancer Biol Ther. 19(12):1162-1173.

Wang L and Chen YG (2016) Signalling Control of Differentiation of Embryonic Stem Cells toward Mesendoderm. J Mol Biol; 428(7):1409-22.

Warr N, Powles-Glover N, Chappell A, Robson J, Norris D, Arkell RM (2008) Zic2-associated holoprosencephaly is caused by a transient defect in the organizer region during gastrulation. Hum Mol Genet 17:2986–2996.

Weijer CJ (2009). Collective cell migration in development. Journal of Cell Science 122, 3215-3223.

Wilson PA, Lagna G, Suzuki A, Hemmati-Brivanlou A (1997). Concentration-dependent patterning of the *Xenopus* ectoderm by BMP4 and its signal transducer Smad1. Development 124:3177-84.

Wilson SI, Rydstrom A, Triborn T, Willert K, Nusse R, Jessell TM and Edlund T (2001). The status of Wnt signalling regulates neural and epidermal fates in the chick embryo. Nature 411, 325-330.

Xin N, Benchabane H, Tian A, Nguyen K, Klofas L, Ahmed Y (2011). Erect Wing facilitates context-dependent Wnt/Wingless signaling by recruiting the cell-specific Armadillo-TCF adaptor Earthbound to chromatin. Development Nov;138(22):4955-67.

Yardley N & García-Castro MI (2012). FGF signalling transforms nonneural ectoderm into neural crest. Developmental Biology, 372,166–177.

Yasumi T, Inoue M., Maruhashi M, Kamachi Y, Higashi Y, Kondoh H and Uchikawa M (2016). Regulation of trunk neural crest delamination by deltaEF1 and Sip1 in the chicken embryo. Dev Growth Differ 58: 205-214.

Zalc A, Rattenbach R, Auradé F, Cadot B and Relaix F (2015). Pax3 and Pax7 play essential safeguard functions against environmental stress induced birth defects. Developmental Cell, 33, 56–66.

Zhang P, Yang F, Luo Q, Yan D, Sun S (2019). miR-1284 Inhibits the Growth and Invasion of Breast Cancer Cells by Targeting ZIC2. Oncol Res. 27(2):253-260.

Zhang S, Su Y, Gao J, Zhang C and Tanaka H (2017). A potential inhibitory function of draxin in regulating mouse trunk neural crest migration. In Vitro Cell.Dev.Biol. Animal 53:43–53.

Zhang X, Zhang P, Shao M, Zang X, Zhang J, Mao F, Qian H, Xu W (2018). SALL4 activates TGFβ/SMAD signaling pathway to induce EMT and promote gastric cancer metastasis. Cancer Manag Res. 10:4459-4470.

Zohn IE, Li Y, Skolnik EY, Anderson KV, Han J and Niswander L (2006). p38 and a p38-Interacting Protein Are Critical for Downregulation of E-Cadherin during Mouse Gastrulation Cell 125, 957–969.

Zic2 regulates Nrp2 during neural crest cells migration

A. Giner de Gracia[1], G. Muça[1], A. Escalante Rodríguez[1], C. Morenilla-Palao[1] and E. Herrera [1]
[1]Instituto de Neurociencias UMH-CSIC, San Juan de Alicante, Spain

Summary: The transcription factor Zic2 (Zinc Finger Protein of the Cerebellum 2) plays an important role in early stages of neural development. Mutations in Zic2 cause holoprosencephaly, spina bifida and many other body malformations. It has been demonstrated that during development, Zic2 is essential for the formation of the neural crest (NC) but its precise role in this process has not been clearly described. The NC is a population of migratory cells with an extraordinary potential to differentiate and contribute to nearly every organ in the adult body. Through functional experiments *in vivo* we first demonstrate here a critical role for Zic2 in the migration of NC cells. Second, in an unbiased genome-wide screen, we identified the transmembrane protein Nrp2 as a potential effector for Zic2. Nrp2 is a receptor for some of the SEMA3 family ligands that has been previously described as a guidance molecule for NC cells. We confirmed that Zic2 and Nrp2 are highly co-expressed in premigratory NC cells and observed that downregulation of Zic2 leads to a significant reduction in the expression of Nrp2. All these findings together indicate that Zic2 controls the expression of Nrp2 and both molecules are essential for the proper formation of the NC.

Introduction

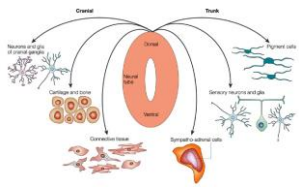

Fig 1: The neural crest is a transient structure composed by a population of precursor cells that generate a large range of derivatives including neurons, melanocytes, skeletal elements, and glia.
From Anne K. Knecht & Marianne Bronner-Fraser
Nature Reviews Genetics (2002)

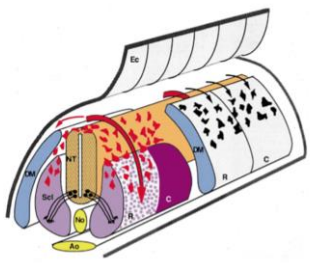

Fig 2: Avian and mammal neural crest cells travel on two distinct pathways after emigration from the neural tube. Schematic diagram of a longitudinal view of the trunk region of an avian embryo. Some trunk neural crest cells (red) emerge from the dorsal neural tube and travel ventromedially, through the rostral, but not caudal, somitic sclerotome. Other neural crest cells (black) migrate dorsolaterally in a uniform manner between the somites and ovelying ectoderm. DM, dermomyotome; Scl, sclerotome; No, notochord; Ao, aorta; Ec, ectoderm; NT, neural tube; R, rostral ; C, caudal.
From *C.E. Krull, Mechanisms of Development* (2001)

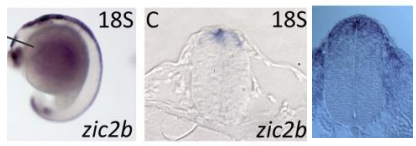

Fig 3: Zic2 is expressed in the neural tube of zebrafish and in mouse embryos during the timing of neural crest cells migration. From J. TeSlaa et al *Developmental Biology* (2013) (zebrafish) and P. Elms et al. *Developmental Biology* 264 (2003) (mouse)

Results

Zic2 is expressed in premigratory neural crest cells

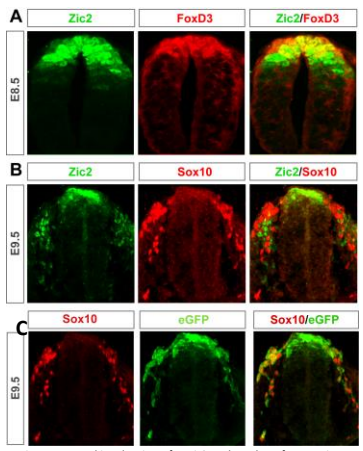

Fig 4. Immunohistochemistry for Zic2 and markers for premigratory neural crest cells (FoxD3) at E8.5 (A) or postmigratory neural crest cells (Sox10) at E9.5 (B) in transverse sections from the neural tube. Immunohistochemistry for GFP and Sox10 in Zic2^{eGFP} reporter mice at e9.5.

Zic2 $^{kd/kd}$ embryos have defects in neural crest cells migration

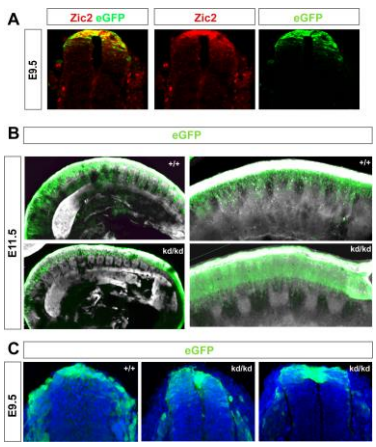

Fig 5. Zic2^{eGFP} reporter mice recapitulate the expression of Zic2 in neural crest cells (A). Expression of eGFP in Zic2$^{kd/kd}$ mouse embryos in whole mount view (B) and in sections (C)

Ectopic expression of Zic2 alters the migration of neural crest cells

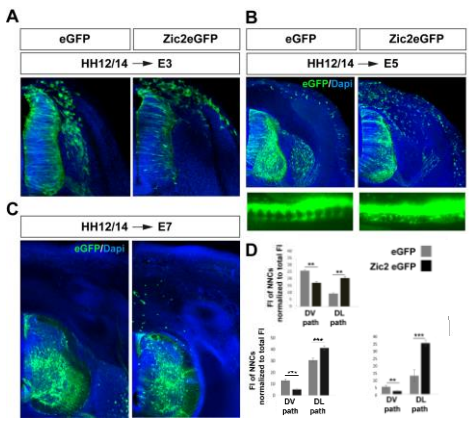

Fig 6. Ectopic expression of Zic2 in HH12/14 (E2) chick embryos at E3 (A), E5 (B) and E7 (C). Quantification of the number of GFP cells entering in the dorsolateral or the ventromedial pathways at the different stages (D).

Nrp2 mRNA is upregulated in Zic2 GOF experiments

Gene	GFP	Zic2	log2(FC)	p_value	References
Nrp2	0.859735	5.71501	2.73279	5.00E-05	
Zic2	51.0492	582.127	3.51137	5.00E-05	Herrera et al (2003) *Cell*
EphB1	8.61956	17.3343	1.00795	0.0002	García-Frigola et al (2008) *Development*
Isl2	7.65628	2.79327	-1.45469	0.0139	Pak et al (2004) *Cell*
Brn3a	44.8554	21.3029	-1.07423	0.00185	Quina et al (2005) *The Journal of Neuroscience*

Fig 7: RNA-Seq comparison between RGC expressing GFP or Zic2GFP reveal Nrp2 as a likely candidate to be regulated by Zic2

Nrp2 expression is reduced in Zic2$^{kd/kd}$ embryos

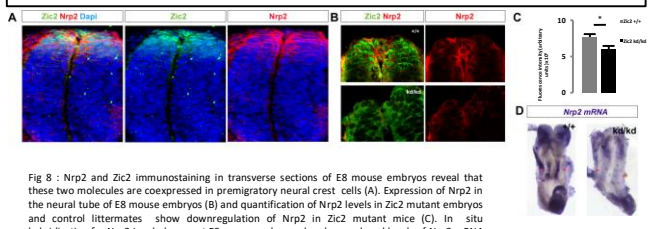

Fig 8 : Nrp2 and Zic2 immunostaining in transverse sections of E8 mouse embryos reveal that these two molecules are coexpressed in premigratory neural crest cells (A). Expression of Nrp2 in the neural tube of E8 mouse embryos (B) and quantification of Nrp2 levels in Zic2 mutant embryos and control littermates show downregulation of Nrp2 in Zic2 mutant mice (C). In situ hybridization for Nrp2 in whole mount E8 mouse embryos also show reduced levels of *Nrp2 mRNA* in Zic2 mutant mice (D).

Conclusions

- **Zic2 is expressed in premigratory neural crest cells**
- **Both Zic2 LOF and GOF affect neural crest cells migration**
- **Nrp2 and Zic2 are coexpressed in the neural tube (E8.0)**
- **Zic2 is sufficient to induce Nrp2 expression**
- **Zic2 is required for the expression of Nrp2 in neural crest cells**

Zic2 regulates Draxin to promote Neural Crest cells delamination

A. Giner de Gracia[1], G. Muça[1], A. Escalante Rodríguez[1], C. Morenilla-Palao[1] and E. Herrera [1]
[1]Instituto de Neurociencias UMH-CSIC, San Juan de Alicante, Spain

Summary: Neural Crest Cells (NCC) are pluripotent cells that originate in the dorsal neuroephitelium of the neural tube and travel all over the embryo to contribute to the formation of many organs. The zinc finger transcription factor Zic2 participates in several steps of development, including neural crest formation, but its precise role in this process has not been clearly stated. Here, we show that Zic2 is expressed in premigratory but not in migrating NCC and its downregulation leads to an accumulation of NCC at the dorsal tip of the neural tube and a concomitant decrease in the number of migrating NCCs. Conversely, Zic2 gain of function experiments produces preccocius NCC exit. In an unbiased gene-wide screen designed to search for Zic2 targets, we identified the secreted molecule Draxin/Neucrin, an antagonist of the Wnt canonical signaling pathway essential to regulate the onset of NCC delamination and functional experiments in mouse and chick confirm that Zic2 regulates Draxin/Neucrin expression to allow NCCs egression from the neural tube. All these observations together, point to Zic2 as a critical player on NCC delamination by inducing the expression of Draxin/Neucrin.

Introduction

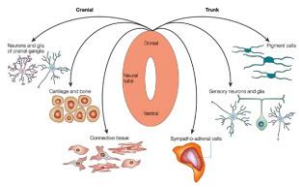

The neural crest is a transient structure composed by a population of precursor cells that generate a large range of derivatives including neurons, melanocytes, skeletal elements, and glia. Knecht & Bronner-Fraser. *Nature Reviews Genetics* (2002).

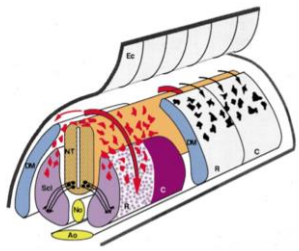

Avian and mammal neural crest cells travel on two distinct pathways after emigration from the neural tube. Schematic diagram of a longitudinal view of the trunk region of an avian embryo. Some trunk neural crest cells (red) emerge from the dorsal neural tube and travel ventromedially, through the rostral, but not caudal, somitic sclerotome. Other neural crest cells (black) migrate dorsolaterally between the somites and ovelying ectoderm. DM, dermomyotome; Scl, sclerotome; No, notochord; Ao, aorta; Ec, ectoderm; NT, neural tube; R, rostral ; C, caudal. *C.E. Krull, Mech. of Devlop.* (2001).

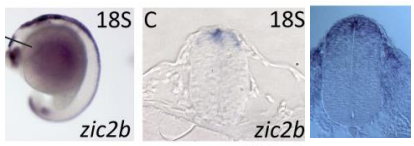

Zic2 is expressed in the neural tube of zebrafish and in mouse embryos during the timing of neural crest cells migration. TeSla et al *Developmental Biology* (2013) (zebrafish) and Elms et al. *Developmental Biology* 264 (2003) (mouse).

Results

Zic2 is expressed in premigratory neural crest cells (NCCs)

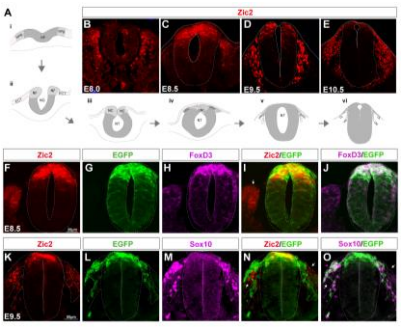

Fig 1. (A-E) Immunohistochemistry for Zic2 at different stages of NC development (F-O) triple immunohistochemistry for Zic2, GFP and markers for premigratory neural crest cells (FoxD3) at E8.5 (F-J) or migratory neural crest cells (Sox10) at E9.5 (K-O) in transverse sections from the neural tube of Zic2 reporter mice [Tg(Zic2^{eGFP})].

Zic2 is required for NCCs delamination

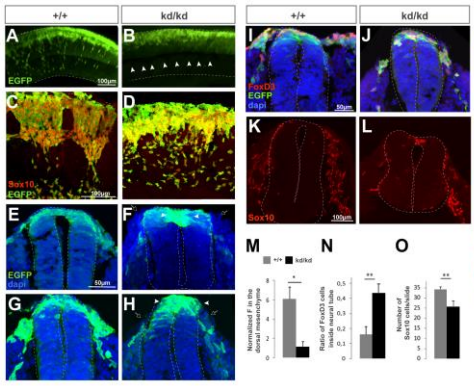

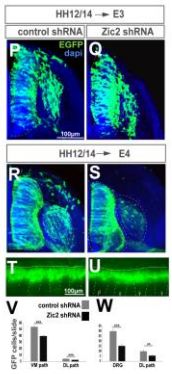

Fig 2. (A-D) Wholemount E9.0 and E11.5 Tg(Zic2^{eGFP})::Zic2$^{kd/kd}$ embryos and control littermates. (E-H) Transverse sections through E8.5 (upper panels) and E9.5 (bottom panels) Tg(Zic2^{eGFP})::Zic2$^{kd/kd}$ embryos and control littermates. (I, J) Immunostaining against FoxD3 in transverse sections of E8.5 Tg(Zic2^{eGFP})::Zic2$^{kd/kd}$ embryos and control littermates. (K, L) Immunostaining against Sox10 in transverse sections of E10.5 Tg(Zic2^{eGFP})::Zic2$^{kd/kd}$ embryos and control littermates. (M-O) Graphs show the quantification of the different mouse experiments in this figure. (P-S) Transverse sections of E3 and E4 chick embryos electroporated at HH12/14 with control shRNA or Zic2shRNAs plus EGFP encoding plasmids. At both stages the number of migrating NCC is reduced in embryos with downregulated expression of Zic2. (T,U) Dorsal view of wholemount E4 chick embryos electroporated at HH12/14 with control shRNA or Zic2shRNAs plus eGFP encoding plasmids. Empty arrows point to the segments where eGFP should be migrating as in control embryos. (V,W) Graphs represent fluorescence intensity across the dorsolateral (DL) path or in the dorsal root ganglia (DRG) region normalized to total fluorescence in transverse sections of E3 (V) and E4 (W) chick embryos electroporated at HH12/14 with control shRNA or Zic2shRNAs plus eGFP encoding plasmids

Zic2 overexpression produces precocious NCCs delamination

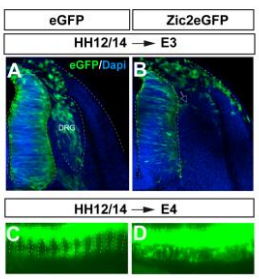

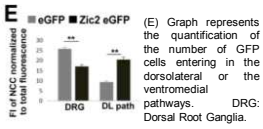

Fig 3: (A, B) Transverse sections of E3 chick embryos electroporated at HH12/14 with plasmids encoding Zic2 and eGFP or eGFP plasmids plus an empty vector. (C, D) Dorsal view of wholemount E4 chick embryos of the same conditions. Note that cells don't follow a segmental way of migration in Zic2 GOF in D.

(E) Graph represents the quantification of the number of GFP cells entering in the dorsolateral or the ventromedial pathways. DRG: Dorsal Root Ganglia.

Zic2 regulates the expression of Draxin and Draxin LOF partially reproduces the Zic2 LOF phenotype

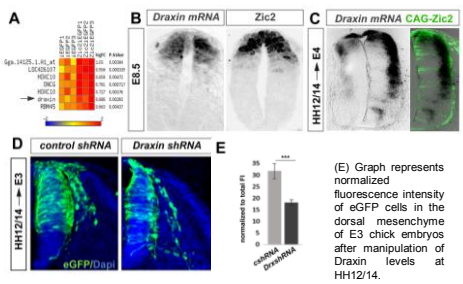

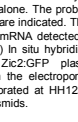

(E) Graph represents normalized fluorescence intensity of eGFP cells in the dorsal mesenchyme of E3 chick embryos after manipulation of Draxin levels at HH12/14.

Fig 4: (A) DNA microarray hit map generated from embryos electroporated with Zic2 and eGFP encoding plasmids or eGFP alone. The probe-set ID, gene symbol, fold change and P values for each transcript are indicated. The color scale bar indicates up-regulation in red (B) Draxin/Neucrin mRNA detected by in situ hybridization in sections from E8.5 mouse embryos. (C) In situ hybridization in sections from E4 chick embryos electroporated with Zic2:GFP plasmids shows an strong upregulation of Draxin mRNA levels in the electroporated side. (D) Transverse sections of E3 chick embryos electroporated at HH12/14 with control shRNA or Draxin shRNAs plus eGFP encoding plasmids.

Zic2 deactivates the canonical Wnt signalling pathway

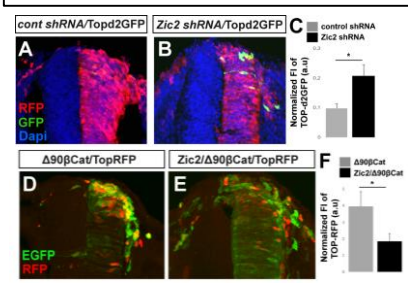

Fig 5: (A,B) Transverse sections of E3 chick embryos electroporated at HH12/14 with a shRNA for Zic2 or a control shRNA plus a non-stable TopGFP. (C) Quantification of GFP normalized by RFP. (D,E) Transverse sections of E3 chick embryos electroporated at HH12/14 with a non-degradable form of βcatenin (Δ90βcat) plus TopRFP plus empty plasmid or with a non-degradable form of βcatenin (Δ90βcat) plus TopRFP plus *Zic2* encoding plasmid. (F) Quantification of RFP normalized by GFP.

Conclusions

- **Zic2 is expressed in premigratory neural crest cells**
- **Both Zic2 LOF and GOF affect NCC delamination**
- **Draxin and Zic2 are co-expressed in the dorsal neural tube during NCC migration stages**
- **Zic2 is sufficient to induce Draxin expression**
- **Draxin LOF partially recapitulates Zic2 LOF phenotype**
- **Zic2 deactivates the canonical Wnt signalling pathway**

Deregulation of the Wnt and TGF-β signaling pathways underlies Zic2-associated holoprosencephaly

A. Giner de Gracia[1], C. Morenilla-Palao[1], MT. López-Cascales[1], G. Muça[1] and E. Herrera[1]
[1]Instituto de Neurociencias UMH-CSIC, San Juan de Alicante, Spain

Summary: The transcription factor Zic2 is one of the genes most commonly mutated in patients with holoprosencephaly (HPE), and in mice Zic2 mutations recapitulate the HPE phenotype. It has been shown that Zic2 transcripts are expressed during early stages of development including gastrulation and neurulation, two processes that imply an epithelial to mesenchymal transition (EMT) step and involve both the Wnt and BMP/TGFβ pathways. Despite intense research trying to unveil Zic2 functions during these early stages of development, little is still known about the precise function or the molecular program controlled by this transcription factor. Here, we describe for the first time the spatiotemporal expression of Zic2 during mouse gastrulation and neurulation. This detailed characterization of Zic2 expression in the early embryo reveals that it is not specific of a particular germ layer (ectoderm, mesoderm and endoderm) but it is transiently and dynamically detected in those layers undergoing EMT. Later, Zic2 is expressed in premigratory Neural Crest (NC) cells and it is then downregulated as soon as these cells leave the neural tube. Then, by performing Zic2 ChIP-seq and RNA-seq assays in E6.0-6.5 and E8.0-8.5 embryos we unveiled the Zic2-binding regions across the genome and define the set of genes regulated by Zic2 during these stages that include many genes related to the Wnt and the BMP/TGFβ pathways. Functional experiments in mouse and chicken then demonstrate that Zic2 inhibits the Wnt canonical signalling pathway in NC cells and induces delamination.

Introduction

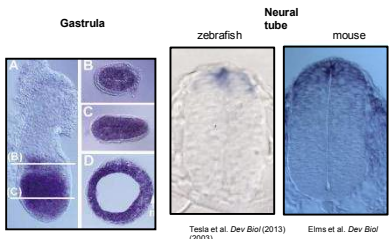

Elms et al. *Gene expression patters* (2004)
Tesla et al. *Dev Biol* (2013) (2003)
Elms et al. *Dev Biol*

***Zic2 mRNA* expression during gastrulation and neurulation**

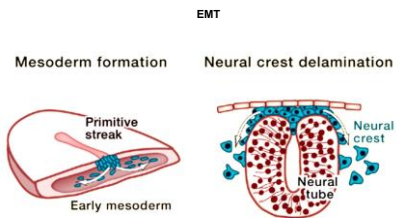

Embryonic processes involving EMT. Modified from Thiery et al. *Cell* (2009)

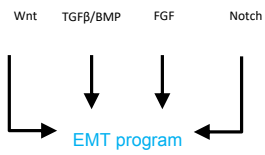

Pathways involved in EMT during early embryogenesis. Modified from Acloque et al. *J Clin Invest.* (2009)

Results

Zic2 is transiently expressed in gastrula cells

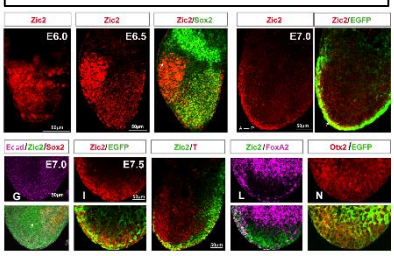

Fig. 1. Expression of Zic2 in the mouse epiblast during gastrulation. (A,B,D,H) Immunohistochemistry for *Zic2* at different stages from E6.0 to E7.5. (C) Double immunohistochemistry for Zic2/Sox2 at E6.5 (E,I). Double immunohistochemistry for Zic2/EGFP at E7.0 (E) and at E7.5 (I). (F,G) Triple immunohistochemistry for E-cadherin, Zic2 and Sox2. Note that big Zic2$^+$/Sox2$^-$ cells are negative for E-cadherin (arrows in G). (J-L) Double immunohistochemistry for Zic2 and markers for mesoderm (T/Brachyury) at E7.5 and endoderm (FoxA2) at E7.5. (M,N) Double immunohistochemistry for EGFP and the marker for neuroectoderm Otx2 at E7.5.

Zic2 function impacts gene expression at E8.0 but not at E6.0

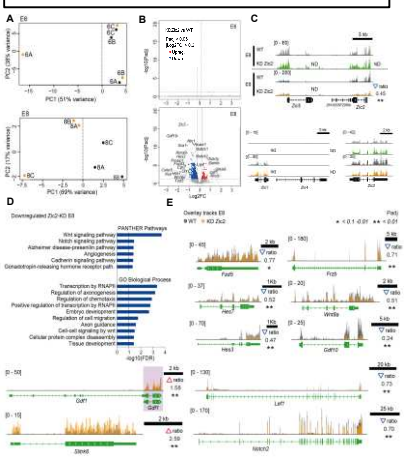

Fig. 4. WT and Zic2 mutant transcriptome analysis at E6 and E8. (A) Principal component analysis (PCA) of *Zic2$^{kd/kd}$* (KD Zic2) samples and *Zic2$^{+/+}$* (WT) at E6.0 and E8.0. (B) Volcano plot showing the significance value of differential expression genes after DESeq2 analysis in RNAseq at E6.0 and E8.0 samples. (C) Transcriptomic profiles of Zic2 family of genes at E6.0 and E8.0. (D) Gene ontology analysis of genes downregulated in the Zic2 mutants. (E) Transcriptomic profiles of genes related to the Wnt, Notch and TGFβ signaling pathways.

Zic2 is expressed in premigratory NCCs

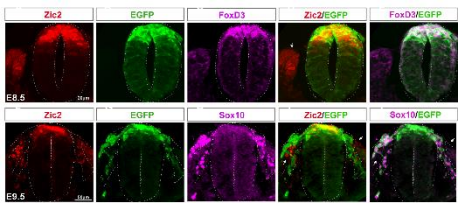

Fig. 2. Expression of Zic2 in premigratory NC cells. Triple immunohistochemistry for Zic2, GFP and markers for premigratory neural crest cells (FoxD3) (A-E) or migratory neural crest cells (Sox10) (F-J) in transverse sections from the neural tube of Zic2 reporter mice [Tg(Zic2EGFP)].

Zic2 regulates the expression of many genes associated to the Wnt and TGFβ pathways

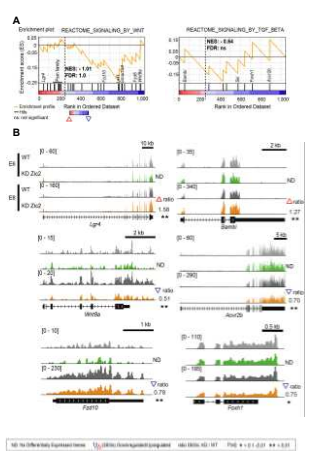

Fig. 5. Zic2 impacts on the Wnt and TGFβ pathways at E8.0.

(A) Gene Set Enrichment Analysis (GSEA) of the Wnt and TGFβ signalling pathways. On the x-axis, the mouse genes are ranked from the most up-regulated (left end) to the most down-regulated (right end) at E8.0. The "barcode" indicates the position of the genes from the biological pathway. The y-axis shows a running enrichment score (ES), which goes up when genes are encountered in the pathway and goes down otherwise leading to an assessment of the distribution within the set of all genes. The normalized enrichment score (NES) is inferred from permutations (1000) of the gene set and the false discovery rate (FDR).

(B) Transcriptomic profiles of genes in *Zic2$^{kd/kd}$* compared to *Zic2$^{+/+}$* at E6.0 and E8.0.

Zic2 binds prominently to gene promoters in NCCs

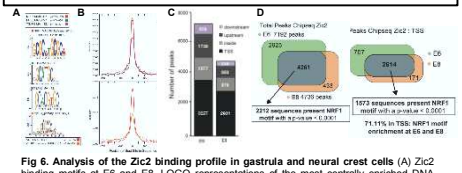

Fig 6. Analysis of the Zic2 binding profile in gastrula and neural crest cells (A) Zic2 binding motifs at E6 and E8. LOGO representations of the most centrally enriched DNA motifs (right). (B)Comparative CentriMo probability plot, that identifies the region of maximum central enrichment in a set of ChIP-seq peak regions at E6 (upper panel) and E8 (lower panel) and displays the positional distributions of predicted sites. (C) Peak distribution inside the genome of E6.0-6.5 samples (left) and E8.0-8.5 samples (right). (D) Distribution of NRF1 motif inside the TSS E6.0-E8.0 common peaks.

Zic2 is required for NCCs delamination

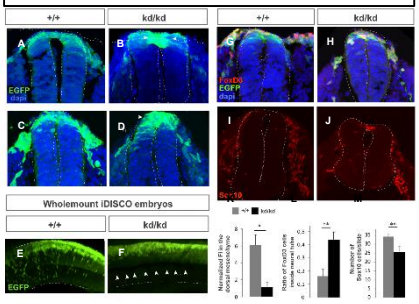

Fig. 3. Zic2 loss-of-function experiments in mouse. (A-D) Transverse sections through E8.5 (upper panels) and E9.5 (bottom panels) embryos. (E,F) Wholemount E9.0 Tg(Zic2^{eGFP})::Zic2$^{kd/kd}$ embryos and control littermates. (G,H) Immunostaining against FoxD3 in transverse sections of E8.5 embryos. (I,J) Immunostaining against Sox10 in transverse sections of E10.5 embryos. (K-M) Quantification of GFP, FoxD3 and Sox10 cells in Zic2 mutant embryos.

Zic2 deactivates the Wnt canonical pathway

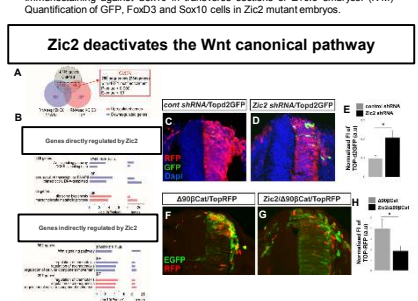

Fig 7. Wnt pathway activity after manipulation of Zic2 levels. (A)Venny diagram of RNA and ChIP-seq at E8.0-8.5. (B)Gene Ontology of direct (upper panel) and indirect (lower panel) targets of Zic2. (C,D)Transverse sections of E3 chick embryos electroporated at HH12/14 with a shRNA for Zic2 or a control shRNA plus a non-stable TopGFP to monitor canonical Wnt signalling activity. (E)Quantification of Wnt activity of C,D experiments. (F,G)Experiments of electroporation with a non-degradable form of βcatenin (Δ90βcat) and TopRFP to induce Wnt signaling, plus an empty plasmid or a Zic2 encoding plasmid. (H)Quantification of Wnt activity in Zic2 GOF.

Zic2 induces an accumulation of NCCs in the dorsal mesenchyme

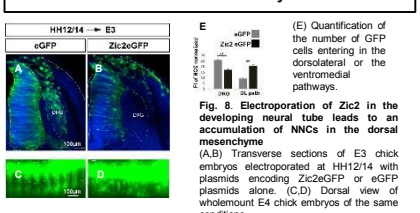

(E) Quantification of the number of GFP cells entering in the dorsolateral or the ventromedial pathways.

Fig. 8. Electroporation of Zic2 in the developing neural tube leads to an accumulation of NNCs in the dorsal mesenchyme
(A,B) Transverse sections of E3 chick embryos electroporated at HH12/14 with plasmids encoding Zic2eGFP or eGFP plasmids alone. (C,D) Dorsal view of wholemount E4 chick embryos of the same conditions.

Conclusions

- **Zic2 is expressed transiently in gastrula and premigratory neural crest cells at the time they undergo epithelial-to-mesenchymal transition.**
- **Zic2 is necessary for neural crest cells delamination from the neural tube.**
- **Zic2 binding profile changes from pluripotent (gastrula) to multipotent (neural crest) cells being more restricted to gene promoters at late stages.**
- **Zic2 directly regulates the expression of many genes related to the Wnt pathway and affects some genes associated to the Notch and TGF-β signaling pathways.**
- **Zic2 deactivates the canonical Wnt pathway.**
- **Zic2 gof experiments suggest that Zic2 induces neural crest cells delamination.**

ENCODS 2017

European Neuroscience Conference for Doctoral Students

This to certify that

Aida Giner

has participated as member of
the organizing commitee in the
European Neuroscience Conference
for Doctoral Students 2017

held at Benidorm, Spain

the 4th, 5th and 6th of May

The ENCODS 2017 organizing comittee